

Lawrence Berkeley National Laboratory

Recent Work

Title

Chemical Sciences Division Annual 1990

Permalink

<https://escholarship.org/uc/item/6qj4z4vc>

Author

Maio, L.

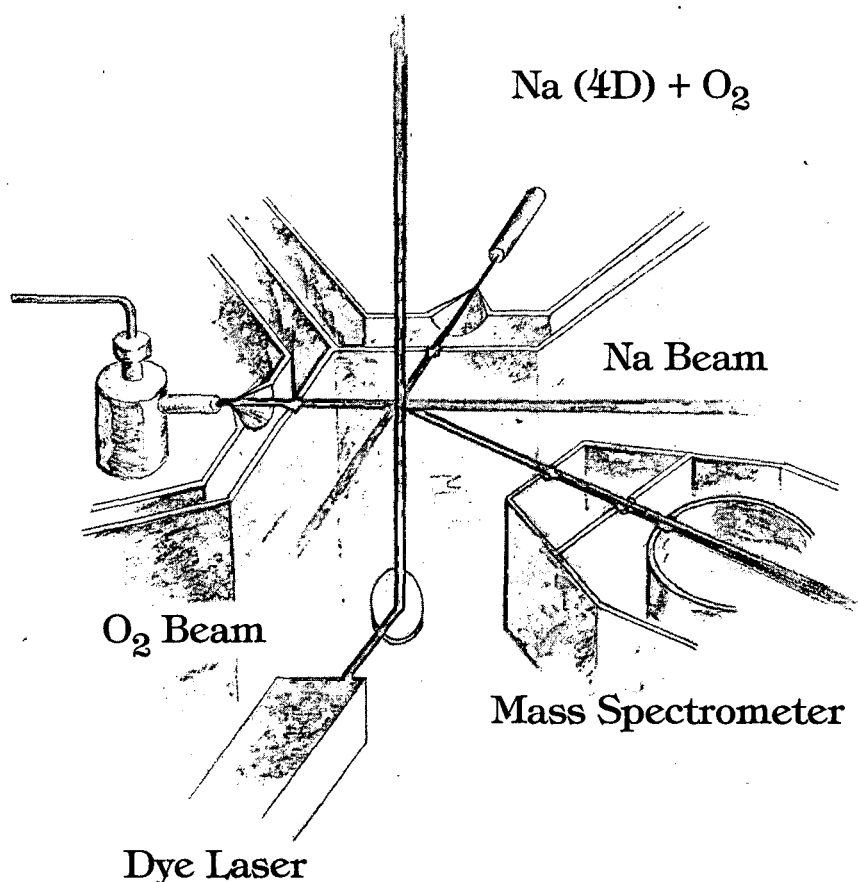
Publication Date

1991-08-01

CHEMICAL SCIENCES DIVISION

Annual Report 1990

August 1991



Lawrence Berkeley Laboratory
University of California
Berkeley, California 94720

LOAN COPY
Circulates
for 4 weeks
Bldg. 50 Library.
Copy 2
LBL-30460

DISCLAIMER

This document was prepared as an account of work sponsored by the United States Government. Neither the United States Government nor any agency thereof, nor The Regents of the University of California, nor any of their employees, makes any warranty, express or implied, or assumes any legal liability or responsibility for the accuracy, completeness, or usefulness of any information, apparatus, product, or process disclosed, or represents that its use would not infringe privately owned rights. Reference herein to any specific commercial product, process, or service by its trade name, trademark, manufacturer, or otherwise, does not necessarily constitute or imply its endorsement, recommendation, or favoring by the United States Government or any agency thereof, or The Regents of the University of California. The views and opinions of authors expressed herein do not necessarily state or reflect those of the United States Government or any agency thereof or The Regents of the University of California and shall not be used for advertising or product endorsement purposes.

Available to DOE and DOE Contractors
from the Office of Scientific and Technical Information
P.O. Box 62, Oak Ridge, TN 37831
Prices available from (615) 576-8401, FTS 626-8401

Available to the public from the
National Technical Information Service
U.S. Department of Commerce
5285 Port Royal Road, Springfield, VA 22161

Lawrence Berkeley Laboratory is an equal opportunity employer.

DISCLAIMER

This document was prepared as an account of work sponsored by the United States Government. While this document is believed to contain correct information, neither the United States Government nor any agency thereof, nor the Regents of the University of California, nor any of their employees, makes any warranty, express or implied, or assumes any legal responsibility for the accuracy, completeness, or usefulness of any information, apparatus, product, or process disclosed, or represents that its use would not infringe privately owned rights. Reference herein to any specific commercial product, process, or service by its trade name, trademark, manufacturer, or otherwise, does not necessarily constitute or imply its endorsement, recommendation, or favoring by the United States Government or any agency thereof, or the Regents of the University of California. The views and opinions of authors expressed herein do not necessarily state or reflect those of the United States Government or any agency thereof or the Regents of the University of California.

CHEMICAL SCIENCES DIVISION

Annual Report 1990

August 1991

Lawrence Berkeley Laboratory
University of California
Berkeley, California 94720

Contents

REMARKS BY THE DIVISION DIRECTOR

<i>Norman E. Phillips</i>	v
---------------------------------	---

CHEMICAL SCIENCES

Fundamental Interactions

Photochemical and Radiation Sciences

Photochemistry of Materials in the Stratosphere

<i>Harold S. Johnston, Investigator</i>	1
---	---

Chemical Physics

Energy Transfer and Structural Studies of Molecules on Surfaces

<i>Charles B. Harris, Investigator</i>	3
--	---

Crossed Molecular Beams

<i>Yuan T. Lee, Investigator</i>	6
--	---

Molecular Interactions

<i>William A. Lester, Jr., Investigator</i>	13
---	----

Theory of Atomic and Molecular Collision Processes

<i>William H. Miller, Investigator</i>	16
--	----

Selective Photochemistry

<i>C. Bradley Moore, Investigator</i>	20
---	----

Photodissociation of Free Radicals

<i>Daniel M. Neumark, Investigator</i>	23
--	----

Physical Chemistry with Emphasis on Thermodynamic Properties

<i>Kenneth S. Pitzer, Investigator</i>	24
--	----

Chemical Physics at High Photon Energies

<i>David A. Shirley, Investigator</i>	27
---	----

Atomic Physics

High-Energy Atomic Physics

<i>Harvey Gould, Investigator</i>	34
---	----

Atomic Physics

<i>Michael H. Prior, Investigator</i>	36
---	----

Processes and Techniques

Chemical Energy

High-Energy Oxidizers and Delocalized-Electron Solids

<i>Neil Bartlett, Investigator</i>	39
--	----

Catalytic Hydrogenation of CO	
<i>Alexis T. Bell, Investigator</i>	42
Transition Metal–Catalyzed Conversion of CO, NO, H ₂ , and Organic Molecules to Fuels and Petrochemicals	
<i>Robert G. Bergman, Investigator</i>	46
Formation of Oxyacids of Sulfur from SO ₂	
<i>Robert E. Connick, Investigator</i>	50
Potentially Catalytic and Conducting Polyorganometallics	
<i>K. Peter C. Vollhardt, Investigator</i>	51
Heavy-Element Chemistry	
Actinide Chemistry	
<i>Norman M. Edelstein, Richard A. Andersen, Kenneth N. Raymond, and Andrew Streitwieser, Jr., Investigators</i>	57
Chemical Engineering Sciences	
Molecular Thermodynamics for Phase Equilibria in Mixtures	
<i>John M. Prausnitz, Investigator</i>	69
WORK FOR OTHERS	
United States Office of Naval Research	
Superconductivity	
<i>Vladimir Z. Kresin, Investigator</i>	75
APPENDICES	
Appendix A: Division Personnel	77
Appendix B: Division Committees	81
Appendix C: List of Divisional Seminars	82
Appendix D: Index of Investigators	84

REMARKS BY THE DIVISION DIRECTOR

In 1990 the Materials and Chemical Sciences Division experienced a dramatic organizational change. On October 1 that Division was separated into two parts: the Materials Sciences Division (MSD), under Daniel S. Chemla, who was recruited from AT&T Bell Laboratories to be Division Director; and the Chemical Sciences Division (CSD), for which I continued as Director. The separation was along funding lines — the Chemical Sciences Division includes the programs funded by the DOE Chemical Sciences Division that had been in MCSD. (Using the DOE titles, these are the programs in Photochemical and Radiation Sciences, Chemical Physics, Atomic Physics, Chemical Energy, Chemical Engineering Science, and Heavy Element Chemistry.) The splitting of MCSD into two Divisions was intended, in part, to reflect the growing demands on the Division Director's time that are presented by the Combustion Dynamics Initiative [CDI, as it was renamed from Combustion Dynamics Facility (CDF) during the year]. The following remarks will address only the Chemical Sciences Division and its activities.

At the outset the two Divisions continued to share the same administrative support personnel below the Division Administrator level, but it was recognized that that arrangement might not continue. Linda Maio became the Division Administrator for CSD, and Meredith Montgomery took that position in MSD. Rolf Muller continued as Associate Division Director for CSD. (Rolf retired from the Laboratory early in calendar year 1991.)

Planning for the CDI advanced substantially during the year. A major workshop to review the proposed scientific program and research facilities was held in April. The Attendance was excellent — 78 scientists from outside of LBL/UCB, 18 scientists from Sandia National Laboratories, and 37 local scientists. That meeting led to the preparation of the "CDF Scientific Program Summary." (The name change had not yet been made.) In October the Technical, Cost, Schedule, and Management Review (TCSM) or, as it is commonly called, the "Temple Review" (after Dr. Ed Temple, who has conducted these reviews for the DOE for many years), was held. The CDI came through with flying colors. A panel of DOE officials and six outside scientific and technical experts judged the proposed scientific program and the facilities to be, respectively, excellent, and feasible and appropriate. They did recommend strengthening of the scientific collaboration between the two laboratories and some increases in the experimental facilities budget, both of which were subsequently incorporated into the plans.

The last few months of 1990 saw the Division feverishly preparing for the Tiger Team visit that was expected for mid-February of 1991. Phil Ross and Linda

Maio worked as a team planning and implementing the preparations for both the Chemical Sciences Division and the Materials Sciences Division. They spent most of the fall and winter on these activities, and both Divisions are greatly indebted to them for their efforts and for their success. The "Tigers" were to be a group of 60 inspectors assembled by DOE, experts on environment, health, and safety problems, who would conduct an intensive search for shortcomings in these areas over a six-week period. The difficulty in preparing for the Tigers was compounded by the recognition, very late in the preparations, that they would also visit LBL laboratories on the campus. Nevertheless substantial improvements were made. In general the Division and LBL as a whole did a very creditable job in improving conditions in these areas and displayed a positive and constructive attitude that turned out to be important in itself.

Awards and honors received by CSD investigators in 1990 include:

- Neil Bartlett received a Dr. *honoris causa* degree from the University of Nantes and was admitted Associé Etranger, Academie des Sciences, Institut de France.
- Robert Bergman received the 1990 Edgar Fahs Smith Award from the Philadelphia Section of the American Chemical Society and the 1990 Remsen Award from the Maryland Section of the American Chemical Society.
- Yuan T. Lee received a Dr. *honoris causa* degree from Arizona State University.
- William Miller received the 1990 Irving Langmuir award in Chemical Physics.
- Daniel Neumark received a Camille and Henry Dreyfus Teacher-Scholar Award.
- J.M. Prausnitz received the Solvay Prize for innovative chemical engineering, and the Corcoran Award of the American Society for Engineering Education.
- K.P.C. Vollhardt received the 1990 Otto Bayer Prize and was announced as the recipient of the American Chemical Society's 1991 Arthur C. Cope Scholar Award.

Norman E. Phillips
Division Director
Chemical Sciences Division



FUNDAMENTAL INTERACTIONS

PHOTOCHEMICAL AND RADIATION SCIENCES

Photochemistry of Materials in the Stratosphere*

Harold S. Johnston, Investigator

INTRODUCTION

This research is concerned with global change in the atmosphere, including theoretical and experimental gas-phase photochemistry. The experimental work was completed and concluded by June 30, 1991, but there will remain about six journal articles to be written and submitted for publication. The theoretical work involves photochemical modeling in collaboration with Lawrence Livermore National Laboratory (LLNL) and as an advisor to the Upper Atmosphere Research Program, Atmospheric Effects of Stratospheric Aircraft, of the National Aeronautics and Space Administration (NASA). The value of the Principal Investigator as advisor to this program is complete financial and scientific independence from NASA, long-term knowledge of the relations between supersonic aircraft and stratospheric ozone, and a record of scientific environmental work.

1. Topical Review of Stratospheric Aircraft and Global Ozone (Publication 5)

H.S. Johnston

The history of stratospheric aircraft and its calculated effect on ozone is reviewed for the period 1971-90, including the present problem.

(1) *The problem.* Using the most recent photochemical data, basing aircraft fuel usage on Boeing-proposed fleet size, and basing nitric oxide emissions on Pratt and Whitney emission measurements, the LLNL two-dimensional atmospheric model calculates that nitrogen oxides from Mach 2 to 3 stratospheric aircraft cruising at 20 km would reduce global ozone by about 15%, a value

greater than the scenarios for chlorofluorocarbons (CFCs) in which CFC emissions are assumed to remain constant from 1990 onward.

(2) *Possible solutions to the problem.* The calculation in (1) above is based on an aircraft cruise emission index of 39.5 grams of nitric oxide per kg of fuel consumed in the stratosphere and flying at 20 km altitude. (a) Use of "advanced emission reduction technology" to design and build a new type of aircraft engine promises greatly to reduce NO_x emissions. (b) LLNL model calculations find that for a given injection of nitrogen oxides, the calculated effect on total ozone is a strong function of altitude, and lower-Mach-number supersonic aircraft flying well below 20 km give much less calculated ozone reductions. (c) The models do not include the recently discovered heterogeneous chemistry associated with the Antarctic ozone hole, but inclusion of this feature in the models may decrease or increase the calculated ozone reductions.

(3) *Some problems with these possible solutions.* (a) Engineers at both Pratt and Whitney and General Electric "have identified combustor concepts that they believe have the potential to achieve a cruise NO_x emission index of 5 to 10... it would be a high risk development program with potential barriers to success being premixing duct flashback and auto ignition..." (b) Calculated ozone changes for stratospheric aircraft flying between 15 and 20 km are extremely sensitive to assigned eddy diffusion functions in some two-dimensional models, and the vertical grid height of many models is 3 km, which is much too coarse at these altitudes. Current models are not good enough to support a policy decision as to where between 14 and 19 km it is safe to emit large amounts of NO_x. There is need to carry out major model developments and calibrations specifically devoted to the aircraft problems.

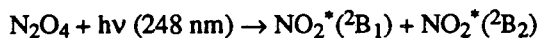
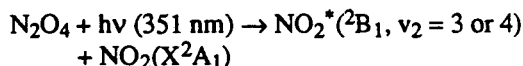
2. NO₂ Fluorescence Following N₂O₄ Photolysis (Publications 6 and 8)

W.N. Sisk, C.E. Miller, and H.S. Johnston

A supersonic jet of N₂O₄ has been photolyzed at three wavelengths: 193, 248, and 351 nm. The resultant fluorescence of NO₂ has been dispersed, and the energy distribution of fluorescent NO₂ has been determined by the photolysis-induced fluorescence (PIF) scheme. The spread of the energy distribution increased with increasing

*This work was supported by the Director, Office of Energy Research, Office of Basic Energy Sciences, Chemical Sciences Division, of the U.S. Department of Energy under Contract No. DE-AC03-76SF00098.

photolysis energy. These results have been compared to Kawasaki's time-of-flight translational energy distributions at 193 and 248 nm. From these complementary measurements, we conclude that the most probable N_2O_4 photodissociation channels are



3. Work in Progress

Energy-Transfer Rates Obtained by High-Speed Fluorescence Measurements

When nitrogen dioxide is excited by a visible dye-laser pulse, the internal energy distribution of the excited state has about the same width as the rotational-energy spread of the ground-state molecules. Upon collision with NO_2 or with foreign gases, the distribution of internal energy changes. The collision-dependent internal-energy distributions are evaluated by the method derived in recent years here to study photolysis-induced fluorescence.

Two-Product Channels from the Photolysis of the Nitrate Free Radical (obtained in collaboration with Professor Y.T. Lee)

In 1979, this project published the quantum yields in the photolysis of the nitrate free radical: $NO_3 + hv \rightarrow NO_2 + O$ and $NO + O_2$. It was desirable to re-investigate this important atmospheric reaction under collision-free conditions with a molecular-beam system. Preliminary results tend to confirm the older measurements, and the new methods promise to give additional information about NO_3 .

Atmospheric Model Calculations

With the strong connections established between this project and the Atmospheric Sciences group at Lawrence Livermore National Laboratory, extensive further calculations are planned concerning global budgets of ozone, oxides of nitrogen, chlorine compounds, heterogeneous chemistry in the stratosphere, the effects of stratospheric aircraft, and related problems.

1990 PUBLICATIONS AND REPORTS

Refereed Journals

1. H. Johnston, "Evaluation of Excess Carbon 14 and Strontium 90 Data for Suitability to Test Two-Dimensional Stratospheric Models," *J. Geophys. Res.* **94**, 18485 (1989); LBL-25677.
2. H. Johnston, D. Kinnison, and D. Wuebbles,[†] "Nitrogen Oxides from High Altitude Aircraft: An Update of Potential Effects on Ozone," *J. Geophys. Res.* **94**, 16351 (1989); LBL-26206.
3. K.O. Patten, Jr., J.D. Burley, and H.S. Johnston, "Radiative Lifetimes of Nitrogen Dioxide for Excitation Wavelengths from 400 to 750 nm," *J. Phys. Chem.* **94**, 7960 (1990); LBL-28435.
4. B. Kim, B.L. Hammond, W.A. Lester, Jr., and H.S. Johnston, "Ab Initio Study of the Vibrational Spectra of NO_3 ," *Chem. Phys. Lett.* **168**, 131 (1990); LBL-28434.

Other Publications

5. H.S. Johnston, "Topical Review of Stratospheric Aircraft and Global Ozone," NASA Reference Publication 1247, September 1990; LBL-28226.

LBL Reports

6. W.N. Sisk (Ph.D. Thesis), "Nitrogen Dioxide Fluorescence Following Photolysis in a Supersonic Jet," LBL-29112.
7. B. Kim (Ph.D. Thesis), " NO_3 , the Study of Molecular Properties and Photodissociation by Ab Initio Method, Spectroscopy, and Translational Spectroscopy," LBL-29688.
8. W.N. Sisk, C. E. Miller, and H. S. Johnston, " NO_2 Fluorescence Following N_2O_4 Photolysis," submitted to *J. Phys. Chem.*

Invited Talks

9. H.S. Johnston, "Global Ozone Balance and Currently Proposed Supersonic Aircraft," Welch Foundation Lecture, University of Houston, Baylor University, and Texas Christian University, September 1990; American Chemical Society National Meeting, Washington, DC, August 1990.

[†]Permanent address: Lawrence Livermore National Laboratory, Livermore, CA 94550.

CHEMICAL PHYSICS

Energy Transfer and Structural Studies of Molecules on Surfaces*

Charles B. Harris, Investigator

INTRODUCTION

The goal of this research is to study the dynamics of excited electronic states on surfaces, at interfaces, and in condensed phases, and to develop new laser techniques for studying these dynamics. The research program is both theoretical and experimental in character, and includes nonlinear optical and ultrafast laser techniques in addition to a variety of standard surface-science tools for characterizing surfaces and adsorbate-surface interactions. Recent work has centered on the development of new techniques for studying the dynamics of electrons at interfaces on femtosecond time scales, carrier diffusion in semiconductors, and photodissociation of transition metal carbonyls in solution. The results of this program have a direct bearing on high-speed technological devices and materials, and on other problems of general interest such as the dynamics of electrical transmission in conductors on ultrafast time scales and the optical properties of thin films.

1. Ultrafast Studies of Chemical Reactions in Liquids: Validity of Gas-Phase Vibrational Relaxation Models and Density Dependence of Bound Electronic-State Lifetimes (Publications 1, 2, 3, and 6)

M.E. Paige and C.B. Harris

The dynamics of the I_2 geminate recombination reaction in liquid Xe are monitored with transient picosecond absorption spectroscopy as a function of solvent density and temperature. Specifically, the I_2 X state vibrational relaxation and the nonradiative electronic curve crossing from the deeply bound A' and A states to the X state are measured over a Xe density range that spans the

entire liquid-phase region of the phase diagram. The density dependence of the X-state vibrational relaxation is shown to be consistent with the isolated binary collision (IBC) model of vibrational relaxation through a procedure that, unlike previous studies of IBC theory, is performed by ascertaining whether vibrational energy vs time plots at different solvent density can be overlapped by a linear scaling of the time axis. The consistency with IBC theory demonstrated in this system is surprising because of the low I_2 vibrational frequency (170–214 cm^{-1}) and the large-amplitude oscillations involved in the relaxation process. Contrary to theoretical predictions of the A'/A-state lifetime based on Langevin modeling in the high-density Kramers' limit, the A'/A state lifetime shows very little dependence on solvent density, although both viscosity and activation barrier increase substantially with solvent density. This finding suggests that a non-Markovian description of the solvent frictional effects and a model of nonadiabatic curve crossing must be included in order to correctly calculate the excited-state lifetime.

2. Energy Dissipation in Chemical Reactions on Ultrafast Timescales (Publications 4 and 5)

D.J. Russell, M.E. Paige, and C.B. Harris

A series of picosecond experiments and computer simulations are presented that test collisional and hydrodynamic models for vibrational relaxation in liquids. The relationships between isolated binary collision (IBC) models and stochastic dynamics are presented. The appropriateness of IBC theory in describing vibrational relaxation in liquids is also discussed.

3. Work in Progress

Image potential states on clean and adsorbate-covered metal surfaces were investigated using two-photon photoemission and the single-electron counting apparatus. Image potential states are 'Rydberg'-like states resulting from the Coulombic attraction between an electron outside

*This work was supported by the Director, Office of Energy Research, Office of Basic Energy Sciences, Chemical Sciences Division, of the U.S. Department of Energy under Contract No. DE-AC03-76SF00098.

a metal surface and the induced positive charge on the surface. The binding energies of the $N = 1$ and $N = 2$ states for Ag(111) and the $N = 1$ state for Cu(111) were measured to be 0.77 eV, 0.24 eV, and 0.86 eV, respectively, in good agreement with previously published reports. This technique gave superior energy resolution to earlier work, with the peak width of 35 meV for a ultraviolet(UV)-visible(VIS) peak and 50 meV for a UV-UV peak for the $N = 1$ state of Ag(111). The widths of the peaks are greater than the predicted theoretical energy resolution of the instrument, setting a lower limit on the lifetime of the state at 10 femtoseconds.

The effect of adsorbates on the image potential state was studied by dosing xenon or cyclohexane onto a Ag(111) surface. With both adsorbates the image state peak persisted, though with much smaller intensity. For a monolayer coverage of Xe, the binding energy of the image state peak was found to decrease by 10 meV, suggesting dielectric screening of the image charge due to the absorbed Xe. Other workers have determined the energy position of the π^* orbital of molecular adsorbates on a metal surface using inverse photoemission. Some of the same systems use two-photon photoemission. Dosing carbon monoxide onto Pt(111) or benzene onto Ag(111) leads to the disappearance of the image potential state. At this time no evidence of peaks due to the excited molecular orbital have been observed.

Time-resolved photoluminescence measurements of homogeneous $\text{CdS}_x\text{Se}_{1-x}$ semiconductors were performed in the past year. The lifetime of the carriers was determined by time-resolved single-photon counting. Alloy samples with compositions $x = 0, 0.25, 0.5, 0.75,$ and 1 were studied. For a sample with particular value of x , the decays at various emission wavelengths were measured. The observed wavelength dependence of the lifetimes yields information on the dynamics of electron-hole-pair relaxation within a given alloy material. Furthermore, the influence of fluctuations in the local chemical potential due to the compositional disorder are of interest. By studying the luminescence of materials over the full range of $0 < x < 1$, this disorder effect can be probed. The samples studied exhibit fast lifetimes at room temperature, within a couple hundred picoseconds at all wavelengths examined. The forms of the decays display varying degrees of nonexponential character. Fits to various theories will be performed in order to model the functional form of the data.

The dynamics and chemistry caused by metal-metal bond cleavage in $\text{Fe}_3(\text{CO})_{12}$ were studied using visible pump-probe spectroscopy. The photochemistry of this compound was found to involve two reaction pathways. First, the compound could isomerize to a coordinatively unsaturated species, and then with a time constant of 150 ps, this isomer can return back to the ground state. Alternatively, the compound can fragment to mono- and di-

iron species. The rate of this fragmentation was found to depend on the excess energy in the molecule.

1990 PUBLICATIONS AND REPORTS

Refereed Journals

1. M.E. Paige and C.B. Harris, "Level Crossing in Liquids Involving Intermolecular Electronic to Vibrational Energy Transfer," *J. Chem. Phys.*, Notes **93**, 1481 (1990); LBL-28553.†‡
2. M.E. Paige and C.B. Harris, "A Generic Test of Gas Phase Isolated Binary Collision Theories for Vibrational Relaxation at Liquid State Densities Based on the Rescaling Properties of Collision Frequencies," *J. Chem. Phys.*, Communication **93**, 3712 (1990); LBL-28906.†

LBL Reports

3. M.E. Paige and C.B. Harris, "Ultrafast Studies of Chemical Reactions in Liquids: I. Validity of Gas Phase Vibrational Relaxation Models, and II. Density Dependence of Bound Electronic State Lifetimes," *Chem. Phys.* (special issue, in press); LBL-29164.†‡¶
4. D.J. Russell, M.E. Paige, and C.B. Harris, "Energy Dissipation in Chemical Reactions on Ultrafast Timescales," in *Proc. Rate Processes in Dissipative Systems: 50 Years after Kramers* (in press); LBL-29735.†¶
5. D.J. Russell (Ph.D. Thesis), "Vibrational Relaxation in Liquids: Comparison Between Gas Phase and Liquid Phase Theories," LBL-30000.†¶
6. M.E. Paige (Ph.D. Thesis), "Density Effects on the Molecular Dynamics of the I_2 Geminate Recombination Reaction in Liquid Xe," LBL-28970.†‡

Invited Talks

7. C.B. Harris, "Probing Chemical Reactions in Liquids on the Femtosecond Timescale," Pittsburgh Spectroscopy Conference, Pittsburgh, PA, March 5-9, 1990.
8. C.B. Harris, "Chemical Reaction in Liquids on Ultrafast Timescales: Experiments Designed to Critically Test Theoretical Models," ACS National Meeting on "Classical and Quantal Simulations for Reactive and Solvation Dynamics and their Critical Experimental Tests," Boston, MA, April 23-27, 1990.
9. C.B. Harris, "Reactions in the Condensed Phase on the Femtosecond Timescale," Gordon Conference on the Chemistry of Energetic Materials, New Hampton School, NH, June 25-29, 1990.
10. C.B. Harris, "Femtosecond Studies of Chemical Reactions in Liquids," Gordon Conference on Radiation Chemistry, Newport, RI, July 8-13, 1990.
11. C.B. Harris, "Condensed Phase Reactions Using Femtosecond Laser Spectroscopy," Center for the Study of

Fast Transient Processes, ARO program review, Mount St. Mary's College, August 12-14, 1990.

12. C.B. Harris, "Energy Dissipation in Chemical Reactions on Ultrafast Timescales," Conference on Rate Processes in Dissipative Systems: 50 Years after Kramers, Evangelische Akademie Tutzing/Germany, September 10-13, 1990.

†National Science Foundation Program using DOE equipment.

‡Office of Naval Research Program using DOE equipment.

|| Office of Army Research Program using DOE equipment.

¶Calculations performed at the San Diego Supercomputer Center.

Crossed Molecular Beams*

Yuan T. Lee, Investigator

INTRODUCTION

The major thrust of this research project is to elucidate detailed dynamics of simple elementary reactions that are theoretically important and to unravel the mechanism of complex chemical reactions or photochemical processes that play important roles in many macroscopic processes. Molecular beams of reactants are used to study individual reactive encounters between molecules or to monitor photodissociation events in a collision-free environment. Most of the information is derived from measurement of the product fragment energy, angular, and state distributions. Recent activities are centered on the mechanisms of elementary chemical reactions involving oxygen atoms with unsaturated hydrocarbons, the dynamics of endothermic substitution reactions, the dependence of the chemical reactivity of electronically excited atoms on the alignment of excited orbitals, the primary photochemical processes of polyatomic molecules, intramolecular energy transfer of chemically activated and locally excited molecules, the energetics of free radicals that are important to combustion processes, the infrared-absorption spectra of carbonium ions and hydrated hydronium ions, and the bond-selective photodissociation through electronic excitation.

1. Tunable Far-Infrared Laser Spectroscopy of Ultracold Free Radicals (Publication 6)

R.C. Cohen, K.L. Busarow, C.A. Schmuttenmaer, Y.T. Lee, and R.J. Saykally

We report a new high-resolution spectroscopic technique designed for the study of short-lived radicals and clusters containing free radicals. Excimer laser photolysis of a suitable precursor during the initial stages of a planar supersonic expansion is used to generate ultracold free radicals that are subsequently probed by a tunable far-infrared laser. A detection limit of 10^8 molecules/cm³ for light hydrides is demonstrated, and prospects for two to three orders of magnitude improvement are discussed.

2. Vibrational Spectroscopy of the Hydrated Hydronium Cluster Ions $H_3O^+(H_2O)_n$ ($N = 1,2,3$) (Publication 7)

L.I. Yeh, M. Okumura, J.D. Myers, J.M. Price, and Y.T. Lee

The gas-phase infrared spectra of the hydrated hydronium cluster ions $H_3O^+(H_2O)_n$ ($N = 1,2,3$) have been observed from 3550 to 3800 cm⁻¹. The new spectroscopic method developed for this study is a two-color laser scheme consisting of a tunable cw infrared laser with 0.5 cm⁻¹ resolution used to excite the O-H stretching vibrations and a cw CO₂ laser that dissociates the vibrationally excited cluster ion through a multiphoton process. The apparatus is a tandem mass spectrometer with a radio-frequency ion trap that utilizes the following scheme: the cluster ion to be studied is first mass selected; spectroscopic interrogation then occurs in the radio-frequency ion trap; finally, a fragment ion is selected and detected using ion-counting techniques. The vibrational spectra obtained in this manner are compared with one taken previously using a weakly bound H₂ "messenger." A spectrum of H₇O₃⁺ taken using a neon messenger is also presented. *Ab initio* structure and frequency predictions by Remington and Schaefer are compared with the experimental results.

3. Photodissociation of Vinyl Bromide and the Heat of Formation of the Vinyl Radical (Publication 8)

A.M. Wodtke, E.J. Hintsä, J. Somorjai, and Y.T. Lee

We have performed measurements of the translational-energy distributions and anisotropy parameters of the photodissociation products of vinyl bromide at 193 nm. Br-atom and HBr elimination were observed with a branching ratio of 1.28 ± 0.05 between the two channels. Both processes occurred with a large release of translational energy, an average of about 2.0 eV for the Br-atom channel and somewhat less for HBr elimination. The maximum release of translational energy for Br + C₂H₃ formation led to an upper limit of 77 ± 3 kcal/mol to D₀(C₂H₃-Br), from which an upper limit to the heat of formation of the vinyl radical, 71 ± 3 kcal/mol, was derived. This result was used to re-examine crossed-molecular-beams data relevant to the determination of the heat of formation of the vinyl radical. A metastable state of C₂H₃ observed in the photodissociation of vinyl bromide was interpreted as the formation of C₂H₃(\bar{A}^2A).

*This work was supported by the Director, Office of Energy Research, Office of Basic Energy Sciences, Chemical Sciences Division, of the U.S. Department of Energy under Contract No. DE-AC03-76SF00098.

4. Electronic Structure and Chemical Bonding of the First-Row Transition-Metal Dichlorides, MnCl_2 , NiCl_2 , and ZnCl_2 : A High-Resolution Photoelectron Spectroscopic Study (Publication 17)

L.-S. Wang, B. Niu, Y.T. Lee, and D.A. Shirley

High-resolution HeI (584 Å) photoelectron spectra of ZnCl_2 , MnCl_2 , and NiCl_2 were measured using a high-temperature supersonic molecular-beam source. In ZnCl_2 , vibrational structures were resolved, and spectroscopic constants were derived for the observed molecular ion states. A single ν_1 vibrational progression was observed for the $\text{C}^2\Sigma_g^+$ state of ZnCl_2^+ . A Franck-Condon factor calculation allowed us to obtain a Zn-Cl equilibrium bond-length increase of 0.095(5) Å and a ν_1 vibrational frequency of 290(8) cm^{-1} . For the open-shell molecules, MnCl_2 and NiCl_2 , no vibrational structure could be resolved because of their very low bending frequencies. Transitions from the ligand orbital and metal d-orbital ionizations were clearly resolved, with those of the d orbitals having considerably narrower band widths. Even though many final states are expected for ionization of the open-shell d orbitals, only a few states were observed. This was explained in MnCl_2 by the one-electron spin-selection rule: $S_f = S_i \pm 1/2$. Besides the spin-selection rule, a propensity toward high spin was proposed to account for the spectrum of NiCl_2 . From the metal d-orbital and ligand orbital splittings, the degree of covalent bonding was inferred to be in the order of: $\text{MnCl}_2 > \text{NiCl}_2 > \text{ZnCl}_2$.

5. Orbital Alignment Dependence and Angular Distributions of Ions from the Reaction of $\text{Ba}(^1S, ^1P)$ with Cl_2 (Publication 19)

A.G. Suits, H. Hou, and Y.T. Lee

We report crossed-molecular-beam studies of positive ions produced in the reaction of ground-state and electronically excited barium atoms with Cl_2 at collision energies of 0.75 and 3.0 eV. At 0.75 eV, angular distributions for BaCl^+ from the exothermic chemi-ion channel were largely backscattered relative to the barium beam. For $\text{Ba}(^1P)$, the cross section for BaCl^+ formation was much lower at both collision energies studied. At 3.0 eV, the product Ba^+ was observed, and the yield increased 20-fold on electronic excitation. In addition, the Ba^+ intensity was further enhanced twofold when the barium p orbital was aligned along the relative velocity vector over that seen with the p orbital perpendicular to the relative velocity vector.

6. Crossed-Molecular-Beams Study of the Reaction $\text{D} + \text{H}_2 \rightarrow \text{DH} + \text{H}$ at Collision Energies of 0.53 and 1.01 eV (Publication 21)

R.E. Continetti, B.A. Balko, and Y.T. Lee

This paper reports the first product differential cross-section (DCS) measurements for the $\text{D} + \text{H}_2 \rightarrow \text{DH} + \text{H}$ reaction as a function of laboratory (lab) scattering angle with sufficient resolution to resolve product DH vibrational states. Using a D-atom beam produced by the photodissociation of DI at 248 nm, product velocity and angular distributions were measured at 12 lab angles at a nominal collision energy of 0.53 eV and at 22 lab angles at a nominal collision energy of 1.01 eV with a crossed-molecular-beams apparatus. After correction of the raw-product time-of-flight (TOF) spectra for modulated background, a comparison with recent exact quantum-mechanical scattering calculations was made using a Monte Carlo simulation of the experimental conditions. The simulation showed that although the theoretical predictions agree qualitatively with the measurements, some significant discrepancies exist. Using the Monte Carlo simulations, a best-fit set of $\text{DH}(v,j)$ DCSs that showed good agreement with the measurements was found. At the detailed level of the state-to-state DCS, significant differences were observed between theory and experiment for rotationally excited $\text{DH}(v,j)$ products. The discrepancies observed suggest that some regions of the current *ab initio* H_3 potential-energy surfaces, particularly the bending potential at high energies, may need further examination.

7. Vibrational Spectroscopy of the Ammoniated Ammonium Ions $\text{NH}_4^+(\text{NH}_3)_n$ (for $n = 1-10$) (Publication 23)

J.M. Price, M.W. Crofton, and Y.T. Lee

The gas-phase vibration-internal rotation spectra of mass-selected ammoniated ammonium ions $\text{NH}_4^+(\text{NH}_3)_n$ (for $n = 1$ to 10) have been observed from 2600 cm^{-1} to 4000 cm^{-1} . The spectra show vibrational features that have been assigned to modes involving both the ion core species, NH_4^+ , and the first-shell NH_3 solvent molecules. Nearly free internal rotation of the solvent molecules about their local C_3 axes in the first solvation shell has been observed in the smaller clusters ($n = 1$ to 6). For the largest clusters studied ($n = 7$ to 10), the spectra converge, with little difference between clusters differing by one solvent molecule. For these clusters, the spectrum in the 3200-3500 cm^{-1} region is quite similar to that of liquid ammonia,

and the entire region of 2600–3500 cm^{-1} also bears considerable resemblance to the spectra of ammonium salts dissolved in liquid ammonia under some chemical conditions. This indicates the onset of a liquid-like environment for the ion core and first-shell solvent molecules in clusters as small as $\text{NH}_4^+(\text{NH}_3)_8$.

8. Reaction of Ba Atoms with NO_2 , O_3 and Cl_2 : Dynamic Consequences of the Divalent Nature of Barium (Publication 24)

H.F. Davis, A.G. Suits, H. Hou, and Y.T. Lee

The role of the divalent nature of barium atoms in chemical reactivity was explored using crossed molecular beams. Angular and velocity distributions of products from reactions of $\text{Ba}(^1\text{S})$ with NO_2 and O_3 indicate the existence of long-lived collision intermediates despite very large reaction exothermicities. The existence of these intermediates results from barriers to transfer of the second electron necessary to form ground-state products. Although BaO was the dominant product in both reactions, two previously unknown channels were observed: $\text{Ba} + \text{NO}_2 \rightarrow \text{BaON} + \text{O}$ and $\text{Ba} + \text{O}_3 \rightarrow \text{BaO}_2 + \text{O}$. We obtained bond-dissociation energies of $D_0(\text{Ba-ON}) = 65 \pm 20$ kcal/mole and $D_0(\text{Ba-O}_2) = 120 \pm 20$ kcal/mole for these molecules. The dependence of the cross sections for the ion channels $\text{Ba}(^1\text{P}) + \text{Cl}_2 \rightarrow \text{Ba}^+ + \text{Cl}_2$ and $\text{Ba}(^1\text{P}) + \text{Cl}_2 \rightarrow \text{BaCl}^+ + \text{Cl}^-$ on $\text{Ba}(^1\text{P})$ orbital alignment and collision energy was used to probe the course of the reaction through intersections between the ionic and covalent potential-energy surfaces.

9. Molecular-Beam Studies and Hot-Atom Chemistry (Publication 25)

R.E. Continetti and Y.T. Lee

A review of recent applications of crossed-molecular-beams studies to the study of hot-atom chemical reactions is given. Studies of the endoergic bromine-substitution reactions $\text{Br} + \text{R-Cl} \rightarrow \text{RBr} + \text{Cl}$ have shown that the transient addition complex formed exhibits limited energy randomization. State-resolved scattering experiments on the $\text{D} + \text{H}_2 \rightarrow \text{DH} + \text{H}$ reaction using a D-atom beam produced by excimer-laser photolysis are also reviewed. These studies, in conjunction with detailed theoretical predictions now available, have shown where further theoretical work on the potential-energy surface that governs this fundamental elementary reaction may be required. Future directions for the study of hot-atom chemical reactions are also discussed.

10. Photoelectron Spectroscopy and Electronic Structure of Clusters of the Group V Elements. I. Dimers (Publication 26)

L.-S. Wang, Y.T. Lee, D.A. Shirley, K. Balasubramanian, and P. Feng

The HeI (584 Å) high-resolution photoelectron spectra of As_2^+ , Sb_2^+ , and Bi_2^+ have been obtained with a high-temperature molecular-beam source. A pure As_2 beam was produced by evaporating Cu_3As . Sb_2 was generated as a mixture with only the atoms from the pure element. Vibrational structure was well resolved for the As_2^+ spectrum. Spectroscopic constants were derived and reported for the related ionic states. In addition, we have carried out relativistic complete-active-space self-consistent field followed by multi-reference single + double configuration-interaction calculations on these dimers, both for the neutral ground states and for the related ionic states. The agreements between the calculated and experimentally derived spectroscopic constants were fairly good, although the calculations tended to consistently underestimate the strength of the bonding in these heavy homonuclear diatomics.

11. Photoelectron Spectroscopy and Electronic Structure of Clusters of the Group V Elements. II. Tetramers: Strong Jahn-Teller Coupling in the Tetrahedral ^2E Ground States of P_4^+ , As_4^+ , and Sb_4^+ (Publication 27)

L.-S. Wang, B. Niu, Y.T. Lee, D.A. Shirley, E. Ghelichkhani, and E.R. Grant

High-resolution HeI (548 Å) photoelectron spectra have been obtained for the tetrameric clusters of the group V elements: P_4 , As_4 , and Sb_4 . The spectra establish that the ground ^2E states of tetrahedral P_4^+ , As_4^+ , and Sb_4^+ are unstable with respect to distortion in the $\nu_2(\text{e})$ vibrational coordinate. The $\text{E} \otimes \text{e}$ Jahn-Teller problem has been treated in detail, yielding simulated spectra to compare with experimental ones. Vibronic calculations, extended to second order (quadratic coupling) for P_4^+ , account for vibrational structure that is partially resolved in its photoelectron spectrum. A Jahn-Teller stabilization energy of 0.65 eV is derived for P_4^+ , which can be characterized in its ground vibronic state as being highly distorted, and highly fluxional. Linear-only Jahn-Teller coupling calculations performed for As_4^+ and Sb_4^+ show good qualitative agreement with experimental spectra, yielding stabilization energies of 0.84 eV and 1.4 eV, respectively.

12. Photoelectron Spectroscopy and Electronic Structure of Clusters of the Group V Elements. III. Tetramers: The 2T_2 and 2A_1 Excited States of P_4^+ , As_4^+ , and Sb_4^+ (Publication 28)

L.-S. Wang, B. Niu, Y.T. Lee, D.A. Shirley, E. Ghelichkhani, and E.R. Grant

Methods employing high-resolution HeI (584 Å) photoelectron spectroscopy have been applied to the tetrameric clusters of the group V elements, to resolve details of vibronic and spin-orbit structure in the first three electronic states of P_4^+ , As_4^+ , and Sb_4^+ . Measured spacings of distinct vibrational progressions in the ν_1 mode for the 2A_1 states of P_4^+ and As_4^+ yield vibrational frequencies of 577 (5) cm^{-1} for P_4^+ and 350 (6) cm^{-1} for As_4^+ . Franck-Condon factor calculations suggest bond changes for the ions in the 2A_1 states of 0.054 (3) Å for P_4^+ and 0.060 (3) Å for As_4^+ . Strong Jahn-Teller distortions in the $\nu_2(e)$ vibrational mode dominate the structure of the 2E ground states of the tetrameric ions. Both Jahn-Teller and spin-orbit effects appear in the spectra of the 2T_2 states of the tetrameric ions, with the spin-orbit effect being dominant in Sb_4^+ and the Jahn-Teller effect dominant in P_4^+ . Vibrational structure is resolved in the P_4^+ spectrum, and the $\nu_3(t_2)$ mode is found to be the one principally active in the Jahn-Teller coupling. A classical metal-droplet model is found to fit well with trends in the IPs of the clusters as a function of size.

13. Production and Photodissociation of CCl_3 Radicals in a Molecular Beam (Publication 29)

E.J. Hints, X. Zhao, W.M. Jackson, W.B. Miller, A.M. Wodtke, and Y.T. Lee

We have produced a pulsed supersonic beam of CCl_3 radicals by photolyzing CCl_4 at 193 nm inside a teflon nozzle. The radicals were thermalized by a buffer gas, then expanded out the end of the nozzle. Cold CCl_3 radicals were photodissociated at 308 nm, and the product velocity distributions were measured by time-resolved mass spectrometry. Only one primary reaction was observed, $CCl_3 \rightarrow CCl_2 + Cl$ with an average kinetic energy release of 13 kcal/mol. Some of the CCl_2 absorbed a second photon to produce $CCl + Cl$.

14. IR Spectroscopy of Hydrogen-Bonded Charged Clusters (Publication 30)

M.W. Crofton, J.M. Price, and Y.T. Lee

New experiments describing the infrared vibrational predissociation spectra of a number of mass-selected ionic cluster systems have been obtained and analyzed in the 2600 to 4000 cm^{-1} region. The species studied include the hydrated hydronium ions, $H_3O^+(H_2O)$, and ammoniated ammonium ions, $NH_4^+(NH_3)_n(H_2O)_m$ ($n + m = 4$). In each case, the spectra reveal well-resolved structures that can be assigned to transitions arising from the vibrational motions of both the ion core of the clusters and the surrounding neutral solvent molecules.

For a given ionic cluster, these transitions show systematic frequency shifts with increasing solvation (increasing values of n or m). These shifts and the appearance or disappearance of core vibrational features have been used to determine the number of ligands involved in the first solvation shell about the ions and possibly the number of solvent molecules required for the onset of a liquid-like environment about the core.

Information has also been gained about solvent-solvent interaction in these systems. For the ionic clusters involving the ammonium ion as the core, structures were observed that can be assigned to transitions arising from the internal rotation of the ligands in the first solvation shell of the cluster about their hydrogen bonds to the ion core. It has been found that this rotation is essentially free, with a very low barrier to the motion (10 cm^{-1}) for the ammoniated ammonium $n = 1$ cluster. This rotation occurs only when the rotating first-shell ligand is not involved in hydrogen bonding with a ligand in the second solvation shell that quenches the free rotation.

15. Work in Progress:

In order to make a rigorous comparison with theoretical calculations, a "complete" experiment on $D + H_2 \rightarrow DH + H$ is now under way. In this crossed-molecular-beams experiment, not only will initial translation energies and initial quantum states of reagents be specified, but also angular distributions of every vibrational-rotational state of DH products will be measured using the state-specific laser-detection scheme.

This experiment will allow us to observe the consequences of the dynamic resonances directly. Other reactive-scattering experiments under investigation are those involving ozone, methyl radical, and various metal atoms.

In the primary photodissociation studies, the dynamics and energetics of photodissociation of NO_3 is our main focus. The branching ratios between $\text{NO} + \text{O}_2$ and $\text{NO}_2 + \text{O}$ channels as a function of excitation wavelength and the heat of formation of NO_3 will be determined. The photodissociation of polyatomic radicals and the primary dissociation processes of small hydrocarbons and chlorinated hydrocarbons are also under investigation.

The work on IR vibrational spectroscopy of solvated ions is now focused on the solvation of carbonium ions by hydrocarbons and H_2 .

The other work that is now under investigation is the pair-interaction potential between two Hg atoms from the measurement of elastic differential cross sections.

1990 PUBLICATIONS AND REPORTS

Refereed Journals

- X. Zhao, R.E. Continetti, A. Yokoyama, E.J. Hints, and Y.T. Lee, "Dissociation of Cyclohexene and 1,4-Cyclohexadiene in a Molecular Beam," *J. Chem. Phys.* **91**, 4118-4127 (1989); LBL-26333.
- A.M. Schmoltner, P.M. Chu, and Y.T. Lee, "Crossed Molecular Beam Study of the Reaction $\text{O}(^3\text{P}) + \text{C}_2\text{H}_2$," *J. Chem. Phys.* **91**, 5365-5373 (1989); LBL-27287.
- T. Trickl, E. Cromwell, Y.T. Lee, and A.H. Kung, "State-Selective Ionization of Nitrogen in the $X^2E_g^+ v_+ = 0$ and $v_+ = 1$ States by Two-Colour (1+1) Photon Excitation Near Threshold," *J. Chem. Phys.* **91**, 6006-6012 (1989); LBL-27186.
- A.M. Schmoltner, P.M. Chu, R.J. Brudzynski, and Y.T. Lee, "Crossed Molecular Beam Study of the Reaction $\text{O}(^3\text{P}) + \text{C}_2\text{H}_4$," *J. Chem. Phys.* **91**, 6926-6936 (1989); LBL-27577.
- A.M. Wodtke, E.J. Hints, J. Somorjai, and Y.T. Lee, "Photodissociation of Vinyl Bromide and the Heat of Formation of the Vinyl Radical," *Israel J. Chem.* **29**, 383-391 (1989); LBL-26710.
- R.C. Cohen, K.L. Busarow, C.A. Schmuttenmaer, Y.T. Lee, and R.J. Saykally, "Tunable Far Infrared Spectroscopy of Ultracold Free Radicals," *Chem. Phys. Lett.* **164**, 321-324 (1989); LBL-27939.
- L.I. Yeh, M. Okumura, J.D. Myers, J.M. Price, and Y.T. Lee, "Vibrational Spectroscopy of the Hydrated Hydronium Cluster Ions, $\text{H}_3\text{O}^+(\text{H}_2\text{O})_n$ ($n = 1, 2, 3$)," *J. Chem. Phys.* **91**, 7319-7330 (1989); LBL-26708.
- A.M. Wodtke, E.J. Hints, J. Somorjai, and Y.T. Lee, "Photodissociation of Vinyl Bromide and the Heat of Formation of the Vinyl Radical," *Israel J. Chem.* **29**, 383-391 (1989); LBL-26710.
- R.C. Cohen, K.L. Busarow, Y.T. Lee, and R.J. Saykally, "Tunable Far Infrared Laser Spectroscopy of Van der Waals Bonds: The Intermolecular Stretching Vibration and Effective Radial Potentials for $\text{Ar}-\text{H}_2\text{O}$," *J. Chem. Phys.* **92**, 169-177 (1990); LBL-27537.
- G.N. Robinson, R.E. Continetti, and Y.T. Lee, "The Translational Energy Dependence of the $\text{F} + \text{C}_2\text{H}_4 \rightarrow \text{H} + \text{C}_2\text{H}_3\text{F}$ Reaction Threshold," *J. Chem. Phys.* **92**, 275-284 (1990); LBL-27629.
- L.-S. Wang, B. Niu, Y.T. Lee, D.A. Shirley, and K. Balasubramanian, "Photoelectron Spectroscopy and Electronic Structure of Heavy Group IV-VI Diatomics," *J. Chem. Phys.* **92**, 899-908 (1990); LBL-27699.
- E.J. Hints, X. Zhao, and Y.T. Lee, "Photodissociation of 2-Bromoethanol and 2-Chloroethanol at 193 nm," *J. Chem. Phys.* **92**, 2280-2286 (1990); LBL-27737.
- E.F. Cromwell, D.-J. Liu, M.J.J. Vrakking, A.H. Kung, and Y.T. Lee, "Dynamics of H_2 Elimination from 1,4-Cyclohexadiene," *J. Chem. Phys.* **92**, 3230-3231 (1990); LBL-28068.
- A. Yokoyama, X. Zhao, E.J. Hints, R.E. Continetti, and Y.T. Lee, "Molecular Beam Studies of the Photodissociation of Benzene at 193 and 248 nm," *J. Chem. Phys.* **92**, 4222-4233 (1990); LBL-27736.
- M. Okumura, L.I. Yeh, J.D. Myers, and Y.T. Lee, "Infrared Spectra of the Solvated Hydronium Ion: Vibrational Predissociation Spectroscopy of Mass-Selected $\text{H}_3\text{O}^+(\text{H}_2\text{O})_n(\text{H}_2)_m$," *J. Phys. Chem.* **94**, 3416-3427 (1990); LBL-26833.
- L.-S. Wang, J.E. Reutt-Robey, B. Niu, Y.T. Lee, and D.A. Shirley, "High Temperature and High Resolution UV Photoelectron Spectroscopy Using Supersonic Molecular Beams," *J. Electron Spectrosc. Rel. Phenom.* **51**, 513-526 (1990); LBL-27583.
- L.-S. Wang, B. Niu, Y.T. Lee, and D.A. Shirley, "Electronic Structure and Chemical Bonding of the First Row Transition Metal Dichlorides, MnCl_2 , NiCl_2 , and ZnCl_2 : A High Resolution Photoelectron Spectroscopic Study," *J. Chem. Phys.* **93**, 957-966 (1990); LBL-27925.
- Z.Z. Yang, L.S. Wang, Y.T. Lee, D.A. Shirley, S.Y. Huang, and W.A. Lester, Jr., "Molecular Beam Photoelectron Spectroscopy of Allene," *J. Phys. Chem.* **171**, 9-13 (1990); LBL-27633.
- A.G. Suits, H. Hou, and Y.T. Lee, "Orbital Alignment Dependence and Angular Distributions of Ions from the Reaction of $\text{Ba}(^1\text{S}, ^1\text{P})$ with Cl_2 ," *J. Phys. Chem.* **94**, 5672-5674 (1990); LBL-29121.
- L.-S. Wang, B. Niu, Y.T. Lee, and D.A. Shirley, "High Resolution Photoelectron Spectroscopy of Clusters of Group V Elements," *Physica Scripta* **41**, 867-869 (1990); LBL-27584.
- R.E. Continetti, B.A. Balko, and Y.T. Lee, "Crossed Molecular Beams Study of the Reaction $\text{D} + \text{H}_2 \rightarrow \text{DH} + \text{H}$ at Collision Energies of 0.53 and 1.01 eV," *J. Chem. Phys.* **93**, 5719-5740 (1990); LBL-28926.

Other Publications

22. R.E. Continetti, B.A. Balko, and Y.T. Lee, "Molecular Beam Studies of Hot Atom Chemical Reactions: Reactive Scattering of Energetic Deuterium Atoms," International Symposium on Near-Future Chemistry in Nuclear Energy Field, February 15-16, 1989, Japan Atomic Energy Research Institute, Ibaraki-Ken, Japan, 1989, pp. 14-24; LBL-26762.
23. R.E. Continetti and Y.T. Lee, "Molecular Beam Studies and Hot Atom Chemistry," in *Handbook of Hot Atom Chemistry*, J.P. Adloff, P.O. Gaspar, A.G. Maddock, M. Immamura, T. Matsuura, H. Sano, and K. Yoshihara, eds., Kodansha Ltd. Publishers, Tokyo, Japan, 1990; LBL-29314.
34. M.S. Helfand (Ph.D. Thesis), "Photodissociation Studies of the Chlorotoluenes at 193 nm and 248 nm," LBL-28127.
35. S.L. Laursen (Ph.D. Thesis), "Matrix Photochemistry of Small Molecules: Influencing Reaction Dynamics on Electronically Excited Hypersurfaces," LBL-28512.
36. L.-S. Wang (Ph.D. Thesis), "High Resolution Photoelectron Spectroscopy of Metal Clusters and High Temperature Species," LBL-28606.

LBL Reports

24. J.M. Price, M.W. Crofton, and Y. T. Lee, "Vibrational Spectroscopy of the Ammoniated Ammonium Ions, $\text{NH}_4^+(\text{NH}_3)_n$ ($n = 1-10$)," J. Phys. Chem. (in press); LBL-29016.
25. H.F. Davis, A.G. Suits, H. Hou, and Y.T. Lee, "Reaction of Ba Atoms with NO_2 , O_3 , and Cl_2 : Dynamic Consequences of the Divalent Nature of Barium," submitted to Ber. Bunsenges. Phys. Chem.; LBL-29122.
26. L.-S. Wang, Y.T. Lee, D.A. Shirley, K. Balasubramanian, and P. Feng, "Photoelectron Spectroscopy and Electronic Structure of Cluster of the Group V Elements. I. Dimers," submitted to J. Chem. Phys.; LBL-28871.
27. L.-S. Wang, B. Niu, Y.T. Lee, D.A. Shirley, E. Ghelichkhani, and E.R. Grant, "Photoelectron Spectroscopy and Electronic Structure of Clusters of the Group V Elements. II. Tetramers: Strong Jahn-Teller Coupling in the Tetrahedral 2E Ground States of P_4^+ , As_4^+ and Sb_4^+ ," submitted to J. Chem. Phys.; LBL-28872.
28. L.-S. Wang, B. Niu, Y.T. Lee, D.A. Shirley, E. Ghelichkhani, and E.R. Grant, "Photoelectron Spectroscopy and Electronic Structure of Clusters of the Group V Elements. III. Tetramers: The 2T_2 and 2A_1 Excited States of P_4^+ , As_4^+ and Sb_4^+ ," submitted to J. Chem. Phys.; LBL-28873.
29. E.J. Hintsa, X. Zhao, W.M. Jackson, W.B. Miller, A.M. Wodtke, and Y.T. Lee, "Production and Photodissociation of CCl_3 Radicals in a Molecular Beam," J. Phys. Chem. (in press); LBL-29640.
30. M.W. Crofton, J.M. Price, and Y.T. Lee, "IR Spectroscopy of Hydrogen Bonded Charged Clusters," in *Clusters of Atoms and Molecules*, H. Haberland, Ed., Springer-Verlag, Berlin (in press); LBL-29681.
31. E.J. Hintsa (Ph.D. Thesis), "Molecular Beam Photodissociation Studies of Polyatomic Molecules and Radicals," LBL-26904.
32. A.-M. Schmoltner (Ph.D. Thesis), "Molecular Beam Studies of Oxygen Atom Reactions with Unsaturated Hydrocarbons," LBL-27916.
33. R.E. Continetti (Ph.D. Thesis), "Vibrational State-Resolved Differential Cross Sections for the $\text{D} + \text{H}_2 \rightarrow \text{DH} + \text{H}$ Reaction," LBL-28126.
37. Y.T. Lee, "Combustion of Fossil Fuel in Modern Society," Sir Run Run Shaw Distinguished Lecture, Shaw College, Chinese University of Hong Kong, October 11, 1989.
38. Y.T. Lee, "IR Spectroscopy of Ammoniated Ammonium Ions," Department of Chemistry, Brookhaven National Laboratory, Upton, NY, November 6, 1989.
39. Y.T. Lee, "Chemical Laser and Laser Chemistry," Haworth Distinguished Lecture, Brookhaven National Laboratory, Upton, NY, November 8, 1989.
40. Y.T. Lee, "Combustion of Fossil Fuel in Human Society," Kaoshiung Technical College, Kaoshiung, Republic of China, December 13, 1989.
41. Y.T. Lee, "Reaction of Ground and Electronically Excited Ba Atoms with Simple Molecules," Annual Meeting, Chinese Chemical Society (Taipei), Fujen University, Taipei, Republic of China, December 16, 1989.
42. Y.T. Lee, "Photodissociation of Chloroethanol and Bromoethanol," Joint Workshop on Molecular Dynamics, Institute for Molecular Sciences (Japan) and Institute of Atomic and Molecular Sciences (Taiwan), Taipei, Republic of China, December 19, 1989.
43. Y.T. Lee, "Infrared Absorption Spectroscopy of Solvated Ions in the Gas Phase," Western Spectroscopy Association Thirty-seventh Annual Conference, Asilomar Conference Grounds, Pacific Grove, CA, January 25, 1990.
44. Y.T. Lee, "Combustion of Fossil Fuels in the Human Society," Pomona College, Claremont, CA, February 20, 1990.
45. Y.T. Lee, "Chemical Lasers and Laser Chemistry," Pomona College, Claremont, CA, February 21, 1990.
46. Y.T. Lee, "IR Spectroscopy of Solvated Ions," Pomona College, Claremont, CA, February 22, 1990.
47. Y.T. Lee, "Concerted Unimolecular Dissociation of Organic Molecules," Pomona College, Claremont, CA, February 23, 1990.
48. Y.T. Lee, "Observation of Rotational Structure in the Vibrational Predissociation Spectrum of H_5^+ ," High Energy Density Materials Contractors Conference, Long Beach, CA, February 26, 1990.
49. Y.T. Lee, "Investigation of the Solvation of Ions Using Infrared Absorption Spectroscopy: $\text{NH}_2^+(\text{NH}_3)_n$ ($n = 1-10$)," International Seminar on Photochemical Dynamics, REFOST, Hamamatsu, Japan, March 26-28, 1990.
50. Y.T. Lee, "Reaction Dynamics and Combustion Chemistry," Sandia National Laboratory, Albuquerque, NM, March 30, 1990.

Invited Talks

51. Y.T. Lee, "Application of IRFEL and ALS Undulator Beam Line in Chemical Dynamics Research," Spring Meeting of the American Physical Society Meeting, Washington, DC, April 16-17, 1990.
52. Y.T. Lee, "Elementary Reactions and Primary Dissociation Processes Relevant to Combustion," American Chemical Society National Meeting, Kinetics and The Environment, Boston, MA, April 25, 1990.
53. Y.T. Lee, "Molecular Beam Chemical Kinetics," Department of Chemistry, University of California, Davis, May 3, 1990.
54. Y.T. Lee, "Molecular Collisions and Chemical Reactions," Distinguished Visiting Professor Lecture Series, San Francisco State University, San Francisco, CA, May 3, 1990.
55. Y.T. Lee, "Chemical Laser and Laser Chemistry," Fundacion Ramon Areces, Madrid, Spain, May 22, 1990.
56. Y.T. Lee, "Reaction of Ba Atoms with NO₂, O₃, and Cl₂: Dynamic Consequences of the Divalent Nature of Barium," Assembly of the Deutsche Bunsen-Gesellschaft, Tübingen, Germany, May 24-26, 1990.
57. Y.T. Lee, "Infrared Absorption Spectroscopy of Solvated Ions in the Gas Phase," Physikalisches Chemisches Kolloquium, ETH (Eidgenössische Technische Hochschule), Laboratorium für Physikalische Chemie, Zurich, Switzerland, May 29, 1990.
58. Y.T. Lee, "How to Set-Off a H₂ Helicopter," Symposium Celebrating Peter Toennies' 60th Birthday, Max-Planck-Institut, Göttingen, Germany, June 1, 1990.
59. Y.T. Lee, "Molecular Beam Studies of Reaction Dynamics," 1990 Combustion Research Contractor's Meeting, Granlibakken, Lake Tahoe, CA, June 6-8, 1990.
60. Y.T. Lee, "Recent Advances in Molecular Beam Chemistry," 3rd SCBA International Symposium, Hong Kong, June 24, 1990.
61. Y.T. Lee, "A Scientist's View on Recent Changes in China," New Asia College, Chinese University of Hong Kong, Hong Kong, June 26, 1990.
62. Y.T. Lee, "Primary Dissociation of NO₃," Institute of Atomic and Molecular Sciences, Academia Sinica, Taipei, Republic of China, June 29, 1990.
63. Y.T. Lee, "Molecular Beam Chemistry," Molecular Science Research Center, Battelle Northwest Laboratory, Richland, WA, August 13, 1990.
64. Y.T. Lee, "Electron Transfers in Chemical Reactions," Department of Chemistry, University of California at Berkeley, August 28, 1990.
65. Y.T. Lee, "Dynamics of Elementary Chemical Reactions," McDowell Lecture, Department of Chemistry, University of British Columbia, Vancouver, BC, September 18, 1990.
66. Y.T. Lee, "Photofragmentation Translational Spectroscopy," Department of Chemistry, University of British Columbia, Vancouver, BC, September 19, 1990.
67. Y.T. Lee, "IR Vibrational Spectroscopy of Solvated Ions," International Mass Spectroscopy Conference, Asilomar Conference Grounds, Pacific Grove, CA, September 24, 1990.

Molecular Interactions*

William A. Lester, Jr., Investigator

INTRODUCTION

This research program is directed at extending fundamental knowledge of atoms and molecules, including their electronic structure, mutual interaction, collision dynamics, and interaction with radiation. The approach combines the use of *ab initio* methods—multiconfiguration Hartree-Fock (MCHF), configuration interaction (CI), and the recently developed quantum Monte Carlo (QMC)—to describe electronic structure, intermolecular interactions, and other properties, with various methods for characterizing inelastic and reactive collision processes and photodissociation dynamics.

1. Theoretical Study of the O(³P) + Allene Reaction (Publication 1)

B.L. Hammond,[†] S.-Y. Huang,[‡] W.A. Lester, Jr., and M. Dupuis^{||}

Ab initio complete active-space SCF calculations have been performed to determine the structures and energetics of the electrophilic addition of O(³P) to allene (propadiene). The long-established channel for this reaction has been O-atom attack of the central carbon atom (CCA). However, recent experimental studies by Y.T. Lee and coworkers have suggested that terminal carbon attack (TCA) is a significant process. In this study the classical barrier height for the CCA channel was found to be only 1.8 kcal/mol lower than that for the TCA channel. In addition, the triplet diradical species and the experimentally observed product of the TCA channel, allenylloxy radical, are characterized. Allenylloxy radical is predicted to have low-lying near-IR and UV transitions to electronic excited states 0.525 and 3.70 eV above the ground state. Similar transitions for the

analogous vinoxy radical have previously been predicted theoretically¹ and confirmed experimentally.²

[†]Present address: IBM Research Division, Almaden Research Center, San Jose, CA.

[‡]Present address: Four Dimensions, Hayward, CA.

^{||}Permanent address: IBM Research Laboratory, Kingston, NY.

1. M. Dupuis, J.J. Wendoloski, T. Takada, and W.A. Lester, Jr., *J. Chem. Phys.* **76**, 481 (1982); M. Dupuis, J.J. Wendoloski, and W.A. Lester, Jr., *J. Chem. Phys.* **76**, 488 (1982).

2. H.E. Hunziker, K. Kleinermanns, H. Knepe, A.C. Luntz, and H.R. Wendt, Abstract to 15th International Conference on Free Radicals (June 1981).

2. The Calculation of Excited States with Quantum Monte Carlo. II. Vibrational Excited States (Publication 3)

B. Bernu,[†] D.M. Ceperley,[‡] and W.A. Lester, Jr.

Using a new Monte Carlo method¹ for computing properties of excited quantum states, correlation function quantum Monte Carlo, we have calculated the lowest ten vibrational excited-state energies of H₂O and H₂CO in the Born-Oppenheimer approximation. The statistical errors for H₂O are 0.1 cm⁻¹ for the ground state and 15 cm⁻¹ for the tenth excited state, while for H₂CO they are 2 cm⁻¹ for the ground state and 30 cm⁻¹ for the eighth excited state. The method is a generalization of the transient-estimate method used for fermion Green's function Monte Carlo and of subspace projection methods used for computing eigenstates of matrices. The time-dependent autocorrelation function of a vector of trial functions is calculated for a random walk generated by the imaginary-time Schrödinger equation, and estimates of energy levels are determined by the eigenvalues of the matrix of correlation functions. This method is especially useful for treating states with the same symmetry as it automatically keeps higher states orthogonal to lower states. The estimated energy converges to the exact eigenvalue with a rate that decreases with increasing excitation energy, thus limiting the method to relatively low-lying states. The method is zero variance in the sense that as better trial functions are introduced, the statistical error decreases to zero. The method has a nontrivial bias.

[†]Permanent address: Laboratoire de Physique Theorique des Liquides, Université Pierre et Marie Curie, Tour 16, Paris Cedex, France.

[‡]Permanent address: National Center for Supercomputing Applications and Department of Physics, Loomis Laboratory of Physics, University of Illinois, Champaign, IL.

1. D.M. Ceperley and B. Bernu, *J. Chem. Phys.* **89**, 6316 (1988).

*This work was supported by the Director, Office of Energy Research, Office of Basic Energy Sciences, Chemical Sciences Division, of the U.S. Department of Energy under Contract No. DE-AC03-76SF00098.

3. *Ab Initio* Study of the Vibrational Spectra of NO₃ (Publication 4)

B. Kim, B.L. Hammond,[†] W.A. Lester, Jr., and H.S. Johnston

The vibrational spectra and geometry of the NO₃ molecule are studied using *ab initio* SCF and CASSCF methods. For all levels of theory and basis set, the highest symmetry found is C_{2v}. The computed vibrational levels agree well with recent experimental results.

[†]Present address: IBM Research Division, Almaden Research Center, San Jose, CA.

4. Theoretical Study of the Interaction of Ionized Transition Metals (Cr, Mn, Fe, Co, Ni, Cu) with Argon (Publication 5)

B.L. Hammond,[†] W.A. Lester, Jr., M. Braga,[‡] and C.A. Taft^{||}

Ab Initio Hartree-Fock effective-core-potential calculations have been performed to determine binding-energy trends of the transition-metal-argon diatomic positive ions. The interaction in these systems is governed mainly by charge-induced dipole forces, with the metal carrying the charge. It is found that all the species are bound and that the binding energy is strongly dependent on the electronic state of the transition-metal ion. A configuration-interaction prediction of the binding energy is also presented for the Cu⁺Ar system. The importance of the electron correlation in these systems is discussed.

[†]Present address: IBM Research Division, Almaden Research Center, San Jose, CA.

[‡]Permanent address: Departamento de Quimica Fundamental, Universidade Federal de Pernambuco, Brazil.

^{||}Permanent address: Centro Brasileiro de Pesquisas Fisicas, Rio de Janeiro, Brazil.

5. Quantum Monte Carlo for Electronic Structure of Atoms and Molecules (Publication 6)

W.A. Lester, Jr. and B.L. Hammond[†]

Quantum Monte Carlo (QMC) is a method that has only slowly come into acceptance as an *ab initio* quantum

chemistry technique over the last 15 years. However, because of the speed of new supercomputers and the simple manner in which QMC can be vectorized and parallelized in programs of usually only a few thousand lines, QMC has become the focus of increased interest. Originally used to treat bosons, QMC has been extended to fermion systems, including the electron gas, many-body hydrogen, and small molecules. The QMC method is simple in concept and implementation, and it is exact because the Schrödinger equation is solved without the independent-particle approximation or basis sets. But such "pure" forms of QMC are inefficient, and today's QMC implementations combine knowledge of the wavefunction gained from modest SCF or MCSCF trial functions with the exact QMC formalism. Such methods can speed computations by imposing certain, demonstrably small, approximations, as in fixed-node QMC, or can be retained in an exact form with greater cost, as in the full Green's function-released node QMC method.

The interaction between standard molecular-orbital (MO) methods and QMC is a symbiotic one: MO methods provide compact importance sampling functions to QMC, and QMC can provide answers to problems where the correlation energy is poorly described by an MO description. Also, QMC and the use of Monte Carlo to integrate expectation-value expressions containing arbitrary trial functions, often called variational Monte Carlo (VMC), have breathed new life into the investigation of explicitly correlated wave functions.

In this article we present the development and applications of QMC in computational quantum chemistry.

[†]Present address: IBM Research Division, Almaden Research Center, San Jose, CA.

6. Work in Progress

Studies are under way to extend the damped-core quantum Monte Carlo (DCQMC) method to transition metals. DCQMC is an all-electron method that reduces the computational effort associated with core electrons by treating them at the variational MC level and reserving the full QMC approach for valence electrons. Because of the difficulty of other methods to quantitatively describe properties of transition-metal systems and the good description of dynamic correlations made possible with QMC, this is an effort of high interest.

Refereed Journals

1. B.L. Hammond, S.-Y. Huang, W.A. Lester, Jr., and M. Dupuis, "Theoretical Study of the $O(^3P) +$ Allene Reaction," *J. Phys. Chem.* **54**, 7969 (1990); LBL-28656.
2. Z.Z. Yang, L.S. Wang, Y.T. Lee, D.A. Shirley, S.-Y. Huang, and W.A. Lester, Jr., "Molecular Beam Photoelectron Spectroscopy of Allene," *Chem. Phys. Lett.* **171**, 9 (1990); LBL-27633.
3. B. Bernu, D.M. Ceperley, and W.A. Lester, Jr., "The Calculation of Excited States with Quantum Monte Carlo. II. Vibrational Excited States," *J. Chem. Phys.* **93**, 552 (1990); LBL-30155.
4. B. Kim, B.L. Hammond, W.A. Lester, Jr., and H.S. Johnston, "Ab Initio Study of the Vibrational Spectra of NO_3 ," *Chem. Phys. Lett.* **168**, 131 (1990); LBL-28434.
5. B.L. Hammond, W.A. Lester, Jr., M. Braga, and C.A. Taft, "Theoretical Study of the Interaction of Ionized Transition Metals (Cr, Mn, Fe, Co, Ni, Cu) with Argon," *Phys. Rev. B* **41**, 10 447 (1990); LBL-28454.
6. W.A. Lester, Jr., and B.L. Hammond, "Quantum Monte Carlo for the Electronic Structure of Atoms and Molecules," *Ann. Rev. Phys. Chem.* **41**, 283 (1990); LBL-28715.
7. W.A. Lester, Jr., "Supercomputing and Research in Theoretical Chemistry," in *Energy Sciences Supercomputing 1990*, p. 34; UCRL-53916.

LBL Reports

8. B.N. Barnett (Ph.D. Thesis), "Quantum Monte Carlo for Atoms and Molecules," LBL-28994.
9. A.C. Pavao, M. Braga, C.A. Taft, B.L. Hammond, and W.A. Lester, Jr., "Theoretical Study of the CO Interaction with 3d-Metal Surfaces," accepted by *Phys. Rev. B*; LBL-29601.
10. P. Pernot, W.A. Lester, Jr., and C. Cerjan, "Quantum Time-Dependent Treatment of Molecular Collisions: Scattering of He by $H_2(B^1\Sigma_v^+)$," submitted to *Comp. Phys. Commu.*; LBL-28590.
11. P. Pernot and W.A. Lester, Jr., "Multidimensional Wave-Packet Analysis: Splitting Method for Time-Resolved

Invited Talks

12. B.L. Hammond and W.A. Lester, Jr., "Recent Developments in Quantum Monte Carlo," Thirtieth Anniversary 1990 Sanibel Symposia, St. Augustine, FL, March 17-24, 1990; LBL-28815.
13. J.C. Andrews, V.Z. Kresin, and W.A. Lester, Jr., "Chemical Reaction as a Quantum Transition: Product Energy Distributions for $OH + D \rightarrow OD + H$," West Coast Theoretical Chemistry Conference, Salt Lake City, UT, March 23-25, 1990; LBL-28813.
14. M.M. Soto and W.A. Lester, Jr., "Quantum Monte Carlo for Electronic Structure: Beyond the Fixed-Node Approximation," West Coast Theoretical Chemistry Conference, Salt Lake City, UT, March 23-25, 1990; LBL-28814.
15. B.L. Hammond, S.-Y. Huang, W.A. Lester, Jr., and M. Dupuis, "Theoretical Study of the $O(^3P) +$ Allene Reaction," 17th Annual NOBCCHE National Meeting, San Diego, CA, April 9-14, 1990; LBL-28816abs.
16. W.A. Lester, Jr., "Theoretical Studies of Molecular Interactions," 1990 Combustion Contractors Meeting, Lake Tahoe, CA, June 5-8, 1990; LBL-28817.
17. W.A. Lester, Jr., "Quantum Monte Carlo and Chemistry," Pennsylvania State University, University Park, PA, March 27, 1990.
18. W.A. Lester, Jr., "Quantum Monte Carlo for Molecules," University of Pittsburgh, Pittsburgh, PA, March 28, 1990.
19. W.A. Lester, Jr., "Quantum Time-Dependent Study of the Scattering of He by $H_2(B)$," Argonne National Laboratory, Argonne, IL, March 29-30, 1990.
20. W.A. Lester, Jr., "Theoretical Study of the $O(^3P) +$ Allene Reaction," 17th Annual Meeting of the National Organization of Black Chemists and Chemical Engineers, San Diego, CA, April 9-14, 1990.
21. W.A. Lester, Jr., "Theoretical Chemistry: The New Wave," Spelman College, Atlanta, GA, April 27, 1990.
22. W.A. Lester, Jr., "Introduction to QMC for Molecules," and "Status of QMC," CECAM Workshop Workshop on Quantum Monte Carlo, Paris, France, June 11-22, 1990.

Theory of Atomic and Molecular Collision Processes*

William H. Miller, Investigator

INTRODUCTION

This research is primarily involved with the development and application of theoretical methods and models for describing atomic and molecular collision processes and chemical reaction dynamics. Specific topics of interest have included the theory of inelastic and reactive scattering, collision processes involving electronically excited atoms or molecules, collisional ionization phenomena, statistical theories of chemical reactions, scattering of atoms and molecules from surfaces, and the interactions of molecular systems with high-power laser radiation.

Most recently, research has focused on the development of theoretical methods for a first-principles treatment of dynamics in *polyatomic* molecular systems. The goal is to develop approaches that can utilize *ab initio* quantum-chemical calculations of the potential-energy surface (in the Born-Oppenheimer approximation) as direct input into the dynamical treatment, and thus, to as great an extent as possible, have a truly predictive theory.

The potential application of these methods is almost without limit. In this group, hydrogen-atom transfer processes have been studied in a variety of systems. Other research groups have used these approaches to describe a variety of reactions that are relevant to the primary steps in combustion.

1. Photodissociation and Continuum Resonance Raman Cross Sections, and General Franck-Condon Intensities, from S-Matrix Kohn Scattering Calculations, with Application to the Photoelectron Spectrum of $\text{H}_2\text{F}^- + h\nu \rightarrow \text{H}_2 + \text{F}, \text{HF} + \text{H} + e^-$ (Publication 1)[†]

J.Z.H. Zhang[‡] and W.H. Miller

It is shown how the S-matrix version of the Kohn variational method for quantum scattering can be readily adapted to compute matrix elements involving the

scattering wavefunctions and also matrix elements of the scattering Green's function. The former of these quantities is what is involved in computing photodissociation cross sections, photodetachment intensities from a bound negative to a neutral scattering state, or the intensity of any Franck-Condon transition from a bound state to a scattering state. The latter quantity (i.e., a matrix element of the scattering Green's function between two bound states) gives the resonance Raman cross section for the case that the intermediate state in Raman process is a scattering state. Once the basic S-matrix Kohn scattering calculation has been performed, it is shown that little additional effort is required to determine these quantities. Application of this methodology is made to determine the electron energy distribution for photodetachment of H_2F^- to $\text{F} + \text{H}_2$, $\text{HF} + \text{H}$. Resonance structure in the $J = 0$ reaction probabilities is seen to appear in the electron energy distribution.

[†]Calculations were performed on the Berkeley Theoretical Chemistry computing facility, supported in part by the National Science Foundation Grant No. CHE-8920690.

[‡]Present address: Department of Chemistry, New York University, New York, NY 10003.

2. An Empirical Valence-Bond Model for Constructing Global Potential-Energy Surfaces for Chemical Reactions of Polyatomic Molecular Systems (Publication 7)[†]

Y.-T. Chang and W.H. Miller

An empirical valence bond (EVB) model is proposed for constructing *reactive* potential-energy surfaces of polyatomic molecular systems. Specifically, it is shown how the exchange potential $V_{12}(\mathbf{q})$ of the EVB model can be chosen so that the EVB potential $V(\mathbf{q}) \equiv 1/2[V_{11}(\mathbf{q}) + V_{22}(\mathbf{q})] - \sqrt{\{1/2[V_{11}(\mathbf{q}) - V_{22}(\mathbf{q})]\}^2 + V_{12}(\mathbf{q})^2}$ exactly reproduces the transition-state geometry, energy, and force-constant matrix obtained by an independent *ab initio* calculation. [Here \mathbf{q} denotes all the $3N-6$ nuclear coordinates of the N-atom system, and V_{11} and V_{22} are empirical diabatic (i.e., nonreactive) potential functions that describe the reactant and product regions of the potential surface, respectively.] Application of the overall prescription to a variety of two-dimensional test potential surfaces shows that this version of the EVB model provides an excellent description of reactive potential surfaces for a wide variety of situations.

[†]Calculations were performed on the Berkeley Theoretical Chemistry computing facility, supported in part by the National Science Foundation Grant No. CHE-8920690.

*This work was supported by the Director, Office of Energy Research, Office of Basic Energy Sciences, Chemical Sciences Division, of the U.S. Department of Energy under Contract No. DE-AC03-76SF00098.

3. *Ab Initio* Calculation of Anharmonic Constants for a Transition State, with Application to Semiclassical Transition State Tunneling Probabilities (Publication 10)[†]

W.H. Miller, R. Hernandez, N.C. Handy,[‡] D. Jayatilaka,[‡] and A. Willetts[‡]

“Good” (i.e., conserved) action variables exist in the vicinity of a *saddle point* (i.e., transition state) of a potential-energy surface in complete analogy to those related to a *minimum* on the surface. Transition-state theory tunneling (or transmission) probabilities can be expressed semiclassically in terms of these “good” action variables, including the effects of nonseparable coupling of all degrees of freedom with each other. This paper shows how *ab initio* quantum-chemistry methods recently developed for calculating anharmonic constants about a potential minimum (i.e., for ordinary vibrational-energy levels) can be readily adapted to obtain those related to a transition state, thus providing a rigorous and practical way to apply this nonseparable transition-state theory. Application is made to the transition state for the reaction $D_2CO \rightarrow D_2CO$.

[†]Calculations were performed on the Berkeley Theoretical Chemistry computing facility, supported in part by the National Science Foundation Grant No. CHE-8920690.

[‡]Present address: University Chemical Laboratory, Lensfield Road, Cambridge, CB21EW, UK.

4. A Transition State Theory–Based Statistical Distribution of Unimolecular Decay Rates, with Application to Unimolecular Decomposition of Formaldehyde (Publication 11)[†]

W.H. Miller, R. Hernandez, C.B. Moore, and W.F. Polik[‡]

A statistical distribution of state-specific unimolecular decay rates is derived (within the framework of random matrix theory) that is determined completely by the transition-state properties of the potential-energy surface. It includes the standard χ -square distributions as a special case. Model calculations are presented to show the extent to which it can differ from the χ -square distribution, and specific application is made to the state-specific unimolecular decay rate data for $D_2CO \rightarrow D_2CO$.

[†]Calculations were performed on the Berkeley Theoretical Chemistry computing facility, supported in part by the National Science Foundation Grant No. CHE-8920690.

[‡]Present address: Department of Chemistry, Hope College, Holland, MI 49423.

5. A New Perspective on Quantum Mechanical Transition-State Theory (Publication 13)[†]

G.A. Voth,[‡] D. Chandler, and W.H. Miller

In this article, some new ideas will be discussed regarding a quantum mechanical transition-state theory that is useful for calculating the rate constants of reactive processes in complicated physical systems. Our procedure is based on an evaluation of the equilibrium statistics of the centroids of imaginary-time quantum paths (and hence no real-time quantum dynamics). The connection between the present theory and the semiclassical instanton theory will also be outlined.

[†]Calculations were performed on the Berkeley Theoretical Chemistry computing facility, supported in part by the National Science Foundation Grant No. CHE-8920690.

[‡]Present address: Department of Chemistry, University of Pennsylvania, Philadelphia, PA 19104.

6. How to Observe the Elusive Resonances in H or $D + H_2 \rightarrow H_2$ or $HD + H$ Reactive Scattering (Publication 14)[†]

W.H. Miller and J.Z.H. Zhang[‡]

Short-lived collision complexes in H or $D + H_2$ ($v = j = 0$) $\rightarrow H_2$ or HD ($v'j'$) + H reactive scattering give rise to broad resonance structure. Though this structure is not observable in the energy dependence of the *integral* cross section, it is readily seen in the energy dependence in the *differential* cross section $\sigma(\theta, E)$, as a peak along a line in the E - θ plane. The equation of this resonance line is $E = E_r[J(\theta)]$, where $E_r(J)$ is the resonance energy as a function of total angular momentum J (i.e., the rotational quantum number of the complex) and $J(\theta)$ is the inverse function of $\theta(J)$, the effective classical deflection function for the transition. Observation of this resonance structure requires cross-section to individual final (v', j') states; it is quenched by summing over j' . It is even more enhanced in cross sections to specific final m' states with $m' \neq 0$ (m' is the helicity of the final state, the projection of the final diatomic molecule rotational angular momentum onto the final relative translational velocity vector). The results reported are all from rigorous three-dimensional quantum-mechanical reactive-scattering calculations for these cross sections.

[†]Calculations were performed on the Berkeley Theoretical Chemistry computing facility, supported in part by the National Science Foundation Grant No. CHE-8920690.

[‡]Present address: Department of Chemistry, New York University, New York, NY 10003.

7. Some New Approaches to Semiclassical and Quantum Transition-State Theory (Publication 15)[†]

W.H. Miller

Semiclassical and quantum-mechanical transition-state theory is reviewed and two new approaches described. One is a general implementation of a semiclassical rate expression¹ that involves the 'good' action-angle variables associated with the saddle point (i.e., transition state) of a potential-energy surface. The other is an evaluation of a formally exact quantum expression for the rate² in terms of Siegert eigenvalues associated with the transition state. Siegert eigenvalues are usually associated with scattering resonances, so their identification with the saddle point of a potential surface, and the expression for the reaction rate in terms of them, is quite an unexpected and novel development.

[†]Calculations were performed on the Berkeley Theoretical Chemistry computing facility, supported in part by the National Science Foundation Grant No. CHE-8920690.

1. Miller, Faraday Disc. Chem. Soc. 62, 40 (1977).
2. Miller, Schwartz, and Tromp, J. Chem. Phys. 79, 4889 (1983).

8. Work in Progress

The *empirical valence bond* model that we have recently devised is proving to be extremely useful for modeling reactive potential-energy surfaces for polyatomic reaction systems. It is currently being used to model potentials for the formic acid dimer, formaldehyde, and fluoroformaldehyde. Classical trajectory methods, including a semiclassical treatment of hydrogen tunneling, is being used to carry out reaction-dynamics simulations in these systems.

1990 PUBLICATIONS AND REPORTS

Refereed Journals

1. J.Z.H. Zhang and W.H. Miller, "Photodissociation and Continuum Resonance Raman Cross Sections, and General Franck-Condon Intensities, from S-Matrix Kohn Scattering Calculations, with Application to the Photoelectron Spectrum of $\text{H}_2\text{F}^- + h\nu \rightarrow \text{H}_2 + \text{F}, \text{HF} + \text{H} + \text{e}^-$," J. Chem. Phys. 92, 1811 (1990).
2. W.F. Polik, D.R. Guyer, W.H. Miller, and C.B. Moore, "Eigenstate-resolved Unimolecular Reaction Dynamics: Ergodic Character of S_0 Formaldehyde at the Dissociation Threshold," J. Chem. Phys. 92, 3471 (1990).
3. J.Z.H. Zhang and W.H. Miller, "Quasi-Adiabatic Basis Functions for the S-Matrix Kohn Variational Approach to

Quantum Reactive Scattering," J. Phys. Chem. 94, 7785 (1990).

4. S.M. Auerbach, J.Z.H. Zhang, and W.H. Miller, "Comparison of Quantum Scattering Calculations for the $\text{H} + \text{H}_2$ Reaction using the LSTH and DMBE Potentials," J. Chem. Soc. Faraday Trans. 86, 1701 (1990).
5. M. Moreno and W.H. Miller, "On The Tautomerization Reaction 2-Pyridone \rightleftharpoons 2-Hydroxypyridine: An *Ab Initio* Study," Chem. Phys. Lett. 171, 475 (1990).
6. W.H. Miller, "Quantum Mechanical Reactive Scattering Theory for Simple Chemical Reactions: Recent Developments in Methodology and Applications," AIP Conf. Proc. 205, *The Physics of Electronic and Atomic Collisions*, 1990, pp. 442-450.
7. Y.-T. Chang and W.H. Miller, "An Empirical Valence Bond Model for Constructing Global Potential Energy Surfaces for Chemical Reactions of Polyatomic Molecular Systems," J. Phys. Chem. 94, 5884 (1990).
8. W.H. Miller, "Recent Advances in Quantum Mechanical Reactive Scattering Theory, Including Comparison of Recent Experiments with Rigorous Calculations of State-to-State Cross Sections for the $\text{H/D} + \text{H}_2 \rightarrow \text{H}_2/\text{HD} + \text{H}$ Reactions," Anni. Rev. Phys. Chem. 41, 245-281 (1990).
9. R.E. Continetti, J.Z.H. Zhang, and W.H. Miller, "Resonance Structure in the Energy-Dependence of State-to-State Differential Scattering Cross Sections for the $\text{D} + \text{H}_2(\nu, j) \rightarrow \text{HD}(\nu', j') + \text{H}$ Reaction," J. Chem. Phys. 93, 5356 (1990).
10. W.H. Miller, R. Hernandez, N.C. Handy, D. Jayatilaka, and A. Willetts, "*Ab Initio* Calculation of Anharmonic Constants for a Transition State, with Application to Semiclassical Transition State Tunneling Probabilities," Chem. Phys. Lett. 172, 62 (1990).
11. W.H. Miller, R. Hernandez, C.B. Moore, and W.F. Polik, "A Transition State Theory-Based Statistical Distribution of Unimolecular Decay Rates, with Application to Unimolecular Decomposition of Formaldehyde," J. Chem. Phys. 93, 5657 (1990).
12. J.Z.H. Zhang, D.L. Yeager, and W.H. Miller, "3D Quantum Scattering Calculations of the Reaction $\text{He} + \text{H}_2^+ \rightarrow \text{HeH}^+ + \text{H}$ for Total Angular Momentum $J = 0$," Chem. Phys. Lett. 173, 489 (1990).

Other Publications

13. G.A. Voth, D. Chandler, and W.H. Miller, "A New Perspective on Quantum Mechanical Transition State Theory," in *Quantum Simulations of Condensed Matter Phenomena*, J.D. Doll and J.E. Gubernatis, eds., World Scientific Press, 1990, pp. 391-400.

LBL Reports

14. W.H. Miller and J.Z.H. Zhang, "How to Observe the Elusive Resonances in H or $\text{D} + \text{H}_2 \rightarrow \text{H}_2$ or $\text{HD} + \text{H}$ Reactive Scattering," J. Phys. Chem. (in press); LBL-29939.
15. W.H. Miller, "Some New Approaches to Semiclassical and

- Quantum Transition State Theory," Ber. Bunsenges. Phys. Chem. (in press); LBL-29938.
16. D.L. Yeager and W.H. Miller, "Complex Log-Derivative Method for Non-Reactive Coupled-Channel Scattering Calculations," J. Phys. Chem. (in press).

Invited Talks

17. W.H. Miller, "S-Matrix Version of the Kohn Variational Principle: Recent Developments in Methodology and Applications," Workshop on the Quantum Theory of Reactive Scattering, University of Cambridge, UK, March 25-27, 1990.
18. W.H. Miller, "Chemical Reaction Dynamics in Simple and Complex System," Awards Symposium, ACS National Meeting, Boston, MA, April 22-27, 1990.
19. W.H. Miller, "Latest Developments in Quantum Mechanical Reactive Scattering Theory and its Application," Symposium on Large Amplitude Motions in Vibrationally Excited Molecules, ACS National Meeting, Boston, MA, April 22-27, 1990.
20. W.H. Miller, "Some New Theoretical Methods for Reaction Dynamics in Polyatomic Systems: an Empirical Valence Bond Potential Surface and a Semiclassical Tunneling Model for Trajectory Simulations," Symposium on Classical and Quantal Simulations for Reactive and Solvation Dynamics and Their Critical Experimental Tests, ACS National Meeting, Boston, MA, April 22-27, 1990.
21. W.H. Miller, "A Transition State Theory for the Probability Distribution of State-Specific Unimolecular Rate Constants," Second World Association of Theoretical Organic Chemists World Congress, Toronto, Ontario, July 8-14, 1990.
22. W.H. Miller, "Quantum Mechanical Reactive Scattering: Its Recent Developments and Applications to Simple Chemical Reactions," Frontiers of Theoretical Chemistry Symposium, 73rd Canadian Chemical Congress, Halifax, Nova Scotia, July 15-20, 1990.
23. W.H. Miller, "Recent Developments in Quantum Mechanical Reactive Scattering Theory and its Application," Parallel Computing for Chemical Reactivity, Perugia, Italy, August 31-September 1, 1990.
24. W.H. Miller, "Quantum Theory of Reactive Scattering," 8th European Conference on Dynamics of Molecular Collisions, Bernkastel-Kues, Germany, September 10-14, 1990.
25. W.H. Miller, "Some New Aspects of Quantum Transition State Theory," NATO Advanced Research Workshop: Rate Processes in Dissipative Systems—50 Years After Kramers, Tutzing, Germany, September 10-13, 1990.

Selective Photochemistry*

C. Bradley Moore, Investigator

INTRODUCTION

The fundamental goals of this program are to understand the photophysics and photochemistry that occur following selective excitation of molecules and during the reactions of free radicals. Of particular interest are the chemical reactions of specifically excited states and the dynamics of energy transfer, both within a molecule and to surrounding molecules.

Molecules produced in bound excited singlet states may fragment following the conversion of electronic excitation energy into vibrational energy. Intersystem crossing to triplet states is often in competition with internal conversion to singlet states. In this work the dynamics of intersystem crossing and reaction of the triplet state are studied for both unimolecular and bimolecular systems.

For low levels of vibrational excitation in small molecules, individual quantum states may be excited, enabling the measurement of reaction and energy-transfer rate constants for each quantum state. For larger or more highly excited molecules, it is usually not possible to excite single eigenstates. Instead, a number of eigenstates are excited simultaneously, and a redistribution of the initial vibrational excitation occurs. This process, known as intramolecular vibrational-energy redistribution (IVR), is extremely rapid and severely limits the realization of truly mode-specific unimolecular reactions. Advances in mode-specific chemistry will come from a more complete understanding of the IVR process and the parameters that control its efficiency. By being able to predict the rates of IVR and the path of vibrational-energy flow through a molecule, experiments can be designed utilizing molecular systems that maximize the possibilities for mode-specific effects. Studies designed to elucidate the coupling mechanisms and dominant pathways for IVR are currently under way on a number of model systems. High-resolution measurements as a function of energy reveal the dynamics of passage through the transition state.

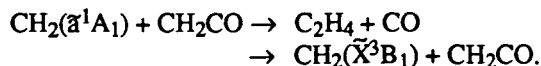
The rates and mechanisms of free-radical reactions, such as are important in combustion, are often best studied by flash kinetic spectroscopy using lasers for thermal heating, for photolyzing, and for spectroscopic probing.

Reactions can be studied as a function of individual quantum states. A fundamental understanding of the rate constants and product distributions for these reactions is sought to serve as a basis for modeling combustion processes.

1. The Yield of CO in the Reaction: $\text{CH}_2(\tilde{a}^1\text{A}_1) + \text{CH}_2\text{CO}$ (Publication 7)

E.R. Lovejoy, R.A. Alvarez, and C.B. Moore

In collisions between singlet methylene and ketene, two processes result in destruction of singlet methylene:



The yield of CO from $\text{CH}_2(\tilde{a}^1\text{A}_1) + \text{CH}_2\text{CO}$ has been measured by monitoring the transient IR absorption of carbon monoxide following pulsed laser photolysis of ketene ($\text{CH}_2\text{CO} + h\nu(308 \text{ nm}) \rightarrow \text{CH}_2(\tilde{a}^1\text{A}_1) + \text{CO}$). Analysis of the prompt CO production as a function of $\text{CH}_2(\tilde{a}^1\text{A}_1)$ scavenger concentration [(i-C₄H₈) and (N₂)] gives a CO yield of 0.63 ± 0.13 . This suggests that collision-induced intersystem crossing, $\text{CH}_2(\tilde{a}^1\text{A}_1) + \text{CH}_2\text{CO} \rightarrow \text{CH}_2(\tilde{\text{X}}^3\text{B}_1) + \text{CH}_2\text{CO}$, is important in this reaction.

2. Determination of the Singlet/Triplet Branching Ratio in the Photodissociation of Ketene (Publication 8)

S.K. Kim, Y.S. Choi, C.D. Pibel, Q.-K. Zheng, and C.B. Moore

The rotational distributions of CO products from the dissociation of ketene at photolysis energies 10 cm⁻¹ below, 56, 110, 200, 325, 425, 1107, 1435, 1720, and 2500 cm⁻¹ above the singlet threshold (30,116.2 cm⁻¹), are measured in a supersonic free jet of ketene. The CO ($\nu'' = 0$) rotational distributions at 56, 110, 200, 325, and 425 cm⁻¹ are bimodal (Figure 2-1). The peaks at low J's, which are due to CO from the singlet channel, show that the product rotational distribution of CO product from ketene dissociation on the singlet surface is well described by phase-space theory (PST). For CO ($\nu'' = 0$) rotational distributions at higher excess energies (1107, 1435, 1720,

*This work was supported by the Director, Office of Energy Research, Office of Basic Energy Sciences, Chemical Sciences Division, of the U.S. Department of Energy under Contract No. DE-AC03-76SF00098.

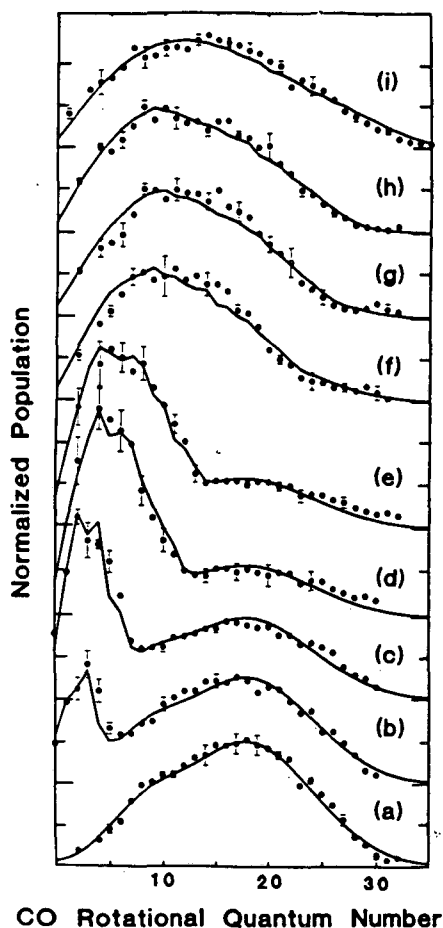


Figure 2-1. The rotational distributions of CO ($v'' = 0$) products from ketene dissociations at photolysis energies below and above the singlet threshold energy ($30,116.2 \text{ cm}^{-1}$). (a): The CO rotational distribution and the fit using two Gaussians at 10 cm^{-1} below the singlet threshold. The followings are the excess energies above the singlet threshold of the photolysis energies and the singlet yields corresponding to the best fits for (b)-(i): (b): 56 cm^{-1} , 0.15; (c): 110 cm^{-1} , 0.34; (d): 325 cm^{-1} , 0.60; (e): 425 cm^{-1} , 0.62; (f): 1107 cm^{-1} , 0.65; (g): 1435 cm^{-1} , 0.70; (h): 1720 cm^{-1} , 0.80; (i): 2500 cm^{-1} , 0.75. (XBL 918-1706)

and 2500 cm^{-1}), the singlet and triplet contributions are not clearly resolved, and the singlet/triplet branching ratios are estimated by assuming that PST accurately predicts the CO rotational distribution from the singlet channel and that the distribution from the triplet channel changes little from that at 10 cm^{-1} below the singlet threshold. The singlet yield shows a rapid increase in the low excess energy region ($0\text{--}300 \text{ cm}^{-1}$), and a slower increase above. The singlet and triplet rate constants are derived from the directly measured total rate constants using the singlet yields. The triplet rate constant increases monotonically with increasing photolysis energy through the singlet threshold region. The singlet

rate constant is accurately established in the threshold region and is found to increase much less rapidly than predicted by phase-space theory. At 2500 cm^{-1} excess energy, the CO ($v'' = 1$) rotational distribution is obtained, and the ratio of CO ($v'' = 1$) to CO ($v'' = 0$) products for the singlet channel is measured to be 0.045 ± 0.017 . This ratio is close to the variational RRKM calculation, 0.038, and the separate statistical ensembles (SSE) prediction, 0.041, but much greater than the PST prediction, 0.016.

3. Work in Progress

Energy transfer and chemical reaction rates are being studied for triplet CH_2 radicals. A diode-laser infrared flash kinetic spectrometer is being used to study the reaction with O_2 in order to identify product states and intermediates. Reaction rates for radical-radical reactions are being measured. Spectroscopy of radical-radical and radical-molecule reaction complexes is planned.

Unimolecular reaction dynamics are being studied by photofragment spectroscopy. Fragmentation on the triplet potential-energy surface of ketene is being studied by detection of CO fragments using a tunable photolysis laser below the threshold for singlet fragmentation. The yield and rates for carbon-atom exchange are studied by photolysis of $^{13}\text{CH}_2\text{CO}$. Rates are measured as a function of photolysis energy with cm^{-1} resolution.

Infrared and ultraviolet spectra of intermediates in organometallic photochemistry in gas and liquid phase are being studied jointly with R.G. Bergman. Emphasis is on CH activation chemistry. Studies of CH activation systems in liquid Kr and Xe are proceeding well.

1990 PUBLICATIONS AND REPORTS

Refereed Journals

1. I-C. Chen and C.B. Moore, "Photofragmentation of Ketene to $\text{CH}_2(\tilde{X}^3\text{B}_1) + \text{CO}$: I. Barrier Height And Dissociation Rate Constant," *J. Chem. Phys.* **94**, 263 (1990); LBL-26906.
2. I-C. Chen and C.B. Moore, "Photofragmentation of Ketene to $\text{CH}_2(\tilde{X}^3\text{B}_1) + \text{CO}$: II. Rotational State Distributions of Product CO," *J. Chem. Phys.* **94**, 269 (1990); LBL-26908.
3. T.J. Butenhoff, R.S. Chuck, H.-H. Limbach, and C.B. Moore, "The Near-Infrared Photochemistry of Porphine Imbedded in a n-Hexane Matrix," *Spectrochim. Acta A*, **46A**, 151 (1990); LBL-28352.
4. T.J. Butenhoff, R.S. Chuck, H.-H. Limbach, and C.B. Moore, "Vibrational Photochemistry of Porphine Imbedded in a n-Hexane- d_{14} Shpol'skii Matrix," *J. Phys. Chem. K.S. Pitzer 75th Birthday issue* **93**, 7847 (1990); LBL-28360.
5. C.B. Moore, Q.-K. Zheng, Y.S. Choi, W.H. Green, S.K. Kim, A.J. Mahoney, W.H. Miller, C.D. Pibel, W.F. Polik,

- and P. Teal, "The High Resolution Spectroscopy of Dissociating Molecules," *Philos. Trans. R. Soc. London A* **332**, 109 (1990); LBL-29756.
6. W.H. Miller, R. Hernandez, C.B. Moore, and W.F. Polik, "A Transition State Theory-Based Statistical Distribution of Unimolecular Decay Rates, with Application to Unimolecular Decomposition of Formaldehyde," *J. Chem. Phys.* **93**, 5657 (1990); LBL-29163.
 7. E.R. Lovejoy, R.A. Alvarez, and C.B. Moore, "The Yield of CO in the Reaction: $\text{CH}_2(\tilde{a}^1\text{A}_1) + \text{CH}_2\text{CO}$," *Chem. Phys. Lett.* **174**, 519 (1990); LBL-29433.
 13. I.C. Chen, W.H. Green, Jr., S.K. Kim, A.J. Mahoney, C.B. Moore, and Q.-K. Zheng, "Chemical Models for State-to-State Unimolecular Reactions," American Chemical Society, Division of Physical Chemistry Spring Meeting, Symposium on Chemical Dynamics, April 24, 1990.
 14. Y.S. Choi, D.R. Guyer, W.H. Miller, C.B. Moore, and W.F. Polik, "Vibrational States of Dissociating Molecules," American Chemical Society, Division of Physical Chemistry Spring Meeting, Symposium on Large Amplitude Motions in Vibrationally Excited Molecules, April 26, 1990.

LBL Reports

8. S.K. Kim, Y.S. Choi, C.D. Pibel, Q.-K. Zheng, and C.B. Moore, "Determination of the Singlet/Triplet Branching Ratio in the Photodissociation of Ketene," *J. Chem. Phys.* (in press); LBL-29754.

Invited Talks

9. C.B. Moore, "The High Resolution Spectroscopy of Dissociating Molecules," The Royal Society Discussion Meeting *Intramolecular Motion and Chemical Reactions*, London, February 14, 1990.
10. C.B. Moore, "Dynamical Control of Unimolecular Reactions," CIBA Foundation Discussion Meeting *Regularity and Chaos in Intramolecular Motions*, London, England, February 16, 1990.
11. C.B. Moore, "Probing the Transition State in Unimolecular Reactions—Rate Constants and Photofragmentation Dynamics," Cambridge University, Cambridge, England, February 19, 1990.
12. C.B. Moore, "Quantum Chaos in Dissociating Molecules," Los Alamos National Laboratory, Chemical and Laser Sciences Division, Los Alamos, NM, April 12, 1990.
15. C.B. Moore, "Photochemical Reaction Dynamics," 1990 DOE-BES Combustion Research Contractors Meeting, Granlibakken Conference Center, Tahoe City, CA, June 7, 1990.
16. C.B. Moore, "Gaseous Photochemistry," Second US/USSR Workshop on Linear and Nonlinear Laser Interactions and Molecular Dynamics, *Molecular Dynamics and Relaxation Processes*, Leningrad, USSR, June 19, 1990.
17. C.B. Moore, "Your College of Chemistry: Retrospective and Perspective," College of Chemistry, University of California at Berkeley, August 29, 1990.
18. C.B. Moore, "State-Resolved Study of the Dynamics of Free Radical Formation," International Conference on Free Radicals, Susono, Shizuoka, Japan, September 4, 1990.
19. C.B. Moore, "The Dynamics of Chemical Bond Breaking," Institute for Molecular Science, Okazaki, Japan, September 5, 1990.
20. C.B. Moore, "Laser Studies of Photodissociation Dynamics," NEC Fundamental Research Laboratories, Tsukuba, Japan, September 6, 1990.
21. C.B. Moore, "The Dynamics of Chemical Bond Breaking," Center for Computational Quantum Chemistry, The University of Georgia, Athens, GA, October 3, 1990.
22. C.B. Moore, "Molecular Energy Flow," Combustion Dynamics Workshop, LBL, October 16, 1990.

Photodissociation of Free Radicals*

Daniel M. Neumark, Investigator

INTRODUCTION

The photodissociation of polyatomic free radicals will be studied in order to characterize the spectroscopy and dissociation dynamics of the dissociative electronic states in these species. For each radical, the dissociative electronic states will be mapped out by measuring the photodissociation cross section as a function of wavelength. This will be followed by photodissociation dynamics experiments in which the photofragment energy and angular distributions are measured, yielding, among other things, bond-dissociation energies in the radical.

While many photodissociation studies of stable neutral molecules have been performed, the extension of the methods used in these experiments to reactive free radicals has been difficult. Our experiment makes use of a unique radical production and photofragment detection scheme. A fast, mass-selected beam of internally cold radicals is generated by negative-ion photodetachment. The radicals are dissociated with a second laser, and the fast photofragments are detected with high efficiency by a two-particle position- and time-sensing detector.

1. Photodissociation of N_3 and NCO (Publication 1)

R.E. Continetti, R.B. Metz, D.R. Cyr, and D.M. Neumark

Photodissociation cross sections for the N_3 and (just recently) NCO radicals have been obtained by measuring the total off-axis photofragment signal in our instrument as

a function of the wavelength of the photodissociation laser. These species were generated by photodetachment of N_3^- and NCO^- . N_3 was chosen as a test system because it has a known rotationally resolved absorption band that lies around 2 eV above the spin-allowed $N(2D) + N_2$ dissociation channel. Our experiment shows that excitation of this band indeed leads to dissociation. The observed rotational structure in our spectra shows that we can achieve rotational temperatures in the fast radical beam of less than 50 K. In the case of NCO, our results show that the diffuse bands near 294 nm seen in absorption many years ago are transitions to dissociating states of NCO and are not diffused solely by spectral congestion, as has been suggested by other investigators. This result has important implications for the heat of formation of NCO.

2. Work in Progress

The position- and time-sensing detector to be used in the photodissociation dynamics experiments has been designed and is currently under construction. This detector will measure the distance between the two photofragments and the delay between their arrival times. From these observations, the center-of-mass kinetic-energy release and scattering angle can be determined for each photodissociation event.

1990 PUBLICATIONS AND REPORTS

Refereed Journals

1. R.E. Continetti, R.B. Metz, D.R. Cyr, and D.M. Neumark, "Photodissociation of N_3 and NCO," *Chem. Phys. Lett.* (in press).

*This work was supported by the Director, Office of Energy Research, Office of Basic Energy Sciences, Chemical Sciences Division, of the U.S. Department of Energy under Contract No. DE-AC03-76SF00098.

Physical Chemistry with Emphasis on Thermodynamic Properties*

Kenneth S. Pitzer, Investigator

INTRODUCTION

The purpose of this program is the discovery and development of methods of calculation of thermodynamic and related properties of important chemical systems by the use of quantum and statistical mechanics together with experimental measurements for key systems. Current emphasis is on fluid systems that include ionic components in novel ranges of conditions, including near-critical and supercritical temperatures and compositions extending from pure water or other polar solvent to pure fused salt. A very recent study concerned a novel ionic system with a critical point near room temperature where it was possible to measure with high precision the near-critical properties including the critical exponent β . Recent theoretical advances include treatments of the dielectric constant of H_2O , the thermodynamics of ionic solutions in H_2O above its critical temperature, and the critical properties of pure ionic fluids such as NaCl. Earlier advances yielded improved equations for electrolyte solutions that are now being applied to a wide variety of systems of industrial or geological interest, including geothermal brines. Other recent research involved the relativistic quantum chemistry of molecules containing very heavy atoms.

1. Near-Critical Coexistence Curve and Critical Exponent of an Ionic Fluid (Publication 6)

R.R. Singh and K.S. Pitzer

The coexistence curve of an ionic liquid-liquid system has been obtained very close to the critical point by measuring the refractive indices of the two phases in equilibrium. The effective exponent β_e remains close to the classical value of 0.5 to $t = 1 - (T/T_c) = 0.0005$ or closer to T_c (see Figure 1-1). The data are, however, not inconsistent with a limiting exponent of 0.326 provided the Wegner correction terms are very large. This behavior is qualitatively consistent with available theory and other experimental knowledge, but further theory and experiments are needed before comparisons can be made.

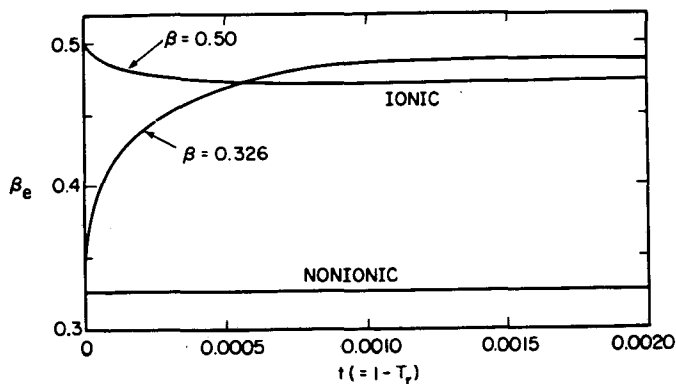


Figure 1-1. Plot of β_e from the two fits for the ionic system. β_e for a typical nonionic liquid-liquid system is also shown. (XBL 917-1667)

2. Monte Carlo Simulation of Phase Equilibria for the Two-Dimensional Lennard-Jones Fluid in the Gibbs Ensemble (Publication 7)

R.R. Singh, K.S. Pitzer, J.J. de Pablo, and J.M. Prausnitz

The coexistence curve of the two-dimensional Lennard-Jones fluid has been obtained by Monte Carlo simulation in the Gibbs ensemble. The calculated vapor-liquid equilibria show that the apparent critical exponent, β_e , has a value near that of an infinitely large system, rather than the classical value, even though the correlation length is constrained by the box size. These results are similar to those for the three-dimensional case.

3. Second Virial Coefficients for Mixed Gases of Low Polarity (Publication 8)

K.S. Pitzer

A simple method of calculation is presented for the cross second virial coefficient B_{12} for mixed gases. It is based on an equation in the acentric-factor system and is appropriate for cases where the pure components are normal fluids. While reasonable estimates can be made on the basis of the properties of the components alone, the more important type of application arises when there is one accurate experimental value of B_{12} . Then the equation predicts the entire temperature dependency with comparable precision (see Figure 3-1).

*This work was supported by the Director, Office of Energy Research, Office of Basic Energy Sciences, Chemical Sciences Division, of the U.S. Department of Energy under Contract No. DE-AC03-76SF00098.

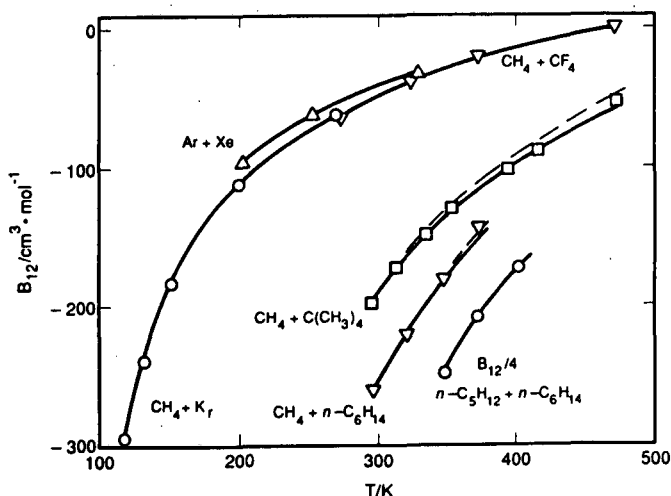


Figure 3-1. Calculated curves of the cross second virial coefficient B_{12} compared with experimental values. Solid curves were calculated with $V_{c,12} = (V_{c,1}^{1/3} - V_{c,2}^{1/3})^3/8$, while dashed curves were calculated for $V_{c,12} = (V_{c,1} + V_{c,2})/2$. For $n\text{-C}_5\text{H}_{12} + n\text{-C}_6\text{H}_{14}$, the quantity $B_{12}/4$ is shown. (XBL 917-1668)

experimental properties up to about 2000 K and Monte Carlo calculations for the ionic hard-sphere model that have very recently been extended to the critical region. Also in progress in collaboration with the LLNL is a project extending to a wide composition range an equation for the thermodynamic properties of the industrially and geologically important ternary system $\text{Na}_2\text{SO}_4\text{-H}_2\text{SO}_4\text{-H}_2\text{O}$.

1990 PUBLICATIONS AND REPORTS

Refereed Journals

1. D.R. Schreiber and K.S. Pitzer, "Equation of State in the Acentric Factor System," *Fluid Phase Equilib.* **46**, 113 (1989); LBL-25927.
2. J.C. Tanger IV and K.S. Pitzer, "Calculation of the Ionization Constant of H_2O to 2,273 K and 500 MPa," *AIChE J.* **35**, 1631 (1989); LBL-26855.
3. L.M. Connaughton, F.J. Millero, and K.S. Pitzer, "Volume Changes for Mixing the Major Sea Salts: Equations Valid to Ionic Strength 3.0 and Temperature to 95°C," *J. Sol. Chem.* **18**, 1007 (1989); LBL-27304.†
4. J.K. Hovey, K.S. Pitzer, J.C. Tanger IV, J.L. Bischoff, and R.J. Rosenbauer, "Vapor-Liquid Phase Equilibria of Potassium Chloride-Water Mixtures: Equation-of-State Representation for $\text{KCl-H}_2\text{O}$ and $\text{NaCl-H}_2\text{O}$," *J. Phys. Chem.* **94**, 1175 (1990); LBL-27558.†
5. R.R. Singh and K.S. Pitzer, "Rectilinear Diameters and Extended Corresponding States Theory," *J. Chem. Phys.* **92**, 3096 (1990); LBL-27824.
6. R.R. Singh and K.S. Pitzer, "Near-Critical Coexistence Curve and Critical Exponent of an Ionic Fluid," *J. Chem. Phys.* **92**, 6775 (1990); LBL-27560.
7. R.R. Singh, K.S. Pitzer, J.J. de Pablo, and J.M. Prausnitz, "Monte Carlo Simulation of Phase Equilibria for the Two-Dimensional Lennard-Jones Fluid in the Gibbs Ensemble," *J. Chem. Phys.* **92**, 5463 (1990); LBL-28069.
8. K.S. Pitzer, "Second Virial Coefficients for Mixed Gases of Low Polarity," *Fluid Phase Equilib.* **59**, 109 (1990); LBL-27989.

Other Publications

9. R.T. Pabalan and K.S. Pitzer, "Models for Aqueous Electrolyte Mixtures for Systems Extending from Dilute Solutions to Fused Salts," in *Chemical Modeling of Aqueous Systems II* (ACS Symposium Series 416), D.C. Melchior and R.L. Bassett, eds., American Chemical Society, Washington, D.C., 1990; LBL-26468.†

4. Critical Phenomena in Ionic Fluids (Publication 10)

K.S. Pitzer

The properties in the critical region, including those of the coexisting phases, have been widely investigated for neutral-molecule fluids. For ionic fluids, the investigation of these properties has been very difficult because, in most cases, the critical points occur at very high temperatures. This review summarizes several recent studies of ionic fluids, both experimental and theoretical, including the discovery of a model ionic fluid with a critical point at 44°C and the measurement of its properties.

5. Work in Progress

A comprehensive equation of state is being developed for pure fluid NaCl extending from the supercooled liquid below 1000 K to the critical point near 4000 K. It is based on vapor properties derived by statistical methods from the molecular parameters of both NaCl and its dimer Na_2Cl_2 in combination with theoretical calculations of this project of the equilibrium among various clusters in the vapor of the ionic hard-sphere model. For the liquid, there are

LBL Reports

10. K.S. Pitzer, "Critical Phenomena in Ionic Fluids," submitted to Acc. of Chem. Res.; LBL-28711.

Invited Talks

11. K.S. Pitzer, "Phase Equilibria and Critical Exponents for Ionic Fluids, Including a New System with $T_c = 317$ K," 11th International Conference on Chemical

Thermodynamics, Como, Italy, August 26-31, 1990.

12. K.S. Pitzer, "Ionic Fluids over Wide Ranges of Temperature and Composition," International Chemical Congress of Pacific Basin Societies, Honolulu, HI, December 17-22, 1989.

[†]This work was supported by the Director, Office of Energy Research, Office of Basic Energy Sciences, Engineering and Geosciences Division, of the U.S. Department of Energy under Contract No. DE-AC03-76SF00098.

Chemical Physics at High Photon Energies*

David A. Shirley, Investigator

INTRODUCTION

This program addresses both experimental and theoretical aspects of electron spectroscopy for the investigation of electronic structure of matter in the gaseous and condensed phases. Research is conducted using both laboratory sources at LBL and synchrotron radiation in the 5–5000 eV energy range available at SSRL, NSLS, and BESSY, with emphasis on developing the high-resolution spectroscopy in the 20–1000 eV energy range by using both plane grating (SX700 at BESSY) and spherical grating (SGMs at SSRL and at NSLS) monochromators. Effects are emphasized that can be refined and extended with the advent of third-generation light sources: e.g., threshold and near-edge photoexcitation phenomena, very fast processes, and processes requiring very high intensity and energy resolution. Electron correlations in atoms and molecules are studied, especially in the adiabatic (low-energy) limit, where the electronic structure of the continuum is important. Time-of-flight measurements with synchrotron radiation are used to measure angular distributions of photoelectrons and resonant photoemission phenomena in the gas phase. Of special interest are ultrahigh-resolution absorption and threshold photoemission studies. Ultrahigh-resolution photoelectron spectroscopy based on molecular beams is yielding new information about small molecules and about the transition from single metal atoms to behavior characteristic of a three-dimensional solid. Employing angle-resolved, variable-energy photoemission, this program examines the electronic structure of solids. The program also studies the geometric and electronic structure of surface-adsorbate systems using photoelectron diffraction and angle-resolved photoemission extended fine structure (ARPEFS).

*This work was supported by the Director, Office of Energy Research, Office of Basic Energy Sciences, Chemical Sciences Division, of the U.S. Department of Energy under Contract No. DE-AC03-76SF00098. It was performed at the National Synchrotron Light Source and Stanford Synchrotron Radiation Laboratory, which are supported by the Department of Energy's Office of Basic Energy Sciences.

1. Carbon and Oxygen K-Edge Photoionization of the CO Molecule (Publication 11)

M. Domke,[†] C. Xue,[†] A. Puschmann,[†] T. Mandel,[†] E. Hudson, D.A. Shirley, and G. Kaindl[†]

High-resolution, high-intensity photoionization studies were performed near the carbon and oxygen K-edges of gas-phase CO. At least 37 absorption lines were resolved at the carbon K-edge, and new information was obtained about the Π^* , Rydberg, and double-excitation resonances, including Rydberg states up to $n = 7$ and vibrational transitions up to $v' = 3$. Vibrational structures in oxygen $1s-1\Pi^*$ and Rydberg states were resolved for the first time (see Figure 1-1). The derived molecular structure parameters are consistent with the $Z + 1$ approximation. High-resolution, high-intensity core-level photoabsorption promises new opportunities in vibrational state-to-state chemistry and surface science.

[†]Permanent address: Institut für Experimentalphysik, Freie Universität Berlin, D-1000 Berlin 33, Germany.

2. Extensive Double Excitation States in Atomic Helium (Publication 16)

M. Domke,[†] C. Xue,[†] A. Puschmann,[†] T. Mandel,[†] E. Hudson, D.A. Shirley, G. Kaindl,[†] C.H. Greene,[‡] H.R. Sadeghpour,[‡] and H. Petersen^{||}

High-resolution photoionization studies of He have revealed more than 50 states below the $N = 2$ to 7 thresholds of He^+ , including sixteen ($sp,2n+$) and five ($sp,2n-$) states in the $N = 2$ series (see Figure 2-1). With a resolving power of $E/\Delta E \sim 10,000$, states as narrow as 0.1 meV could be observed, and linewidths were determined with an accuracy up to ± 0.5 meV. Interchannel interferences, evident through effects on positions, shapes, and intensities of Rydberg lines, were interpreted within the framework of the multichannel quantum defect theory.

[†]Permanent address: Institut für Experimentalphysik, Freie Universität Berlin, D-1000 Berlin 33, Germany.

[‡]Permanent address: Joint Institute of Laboratory Astrophysics and Department of Physics, University of Colorado, Boulder, CO 80309-0440.

^{||}Permanent address: BESSY GmbH, D-1000 Berlin 33, Germany.

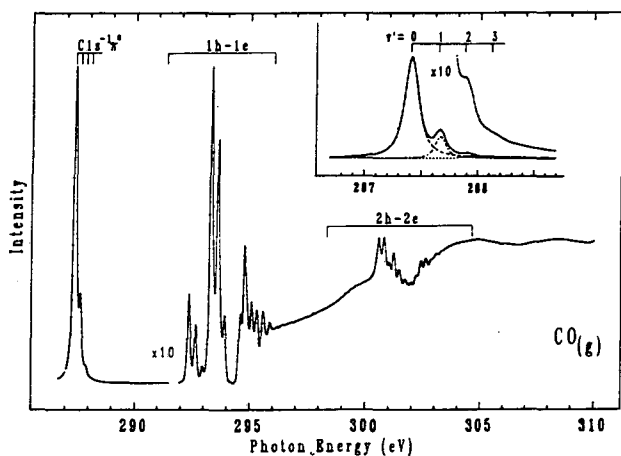


Figure 1-1. High-resolution photoionization spectrum at the C K-edge of gas-phase CO measured at the BESSY-SX700/II beamline. The inset shows the vibrational band of the C 1s-1 π^* resonance up to $v'=3$. Note that the baseline of the magnified region of the spectrum has been shifted. (XBL 917-1673)

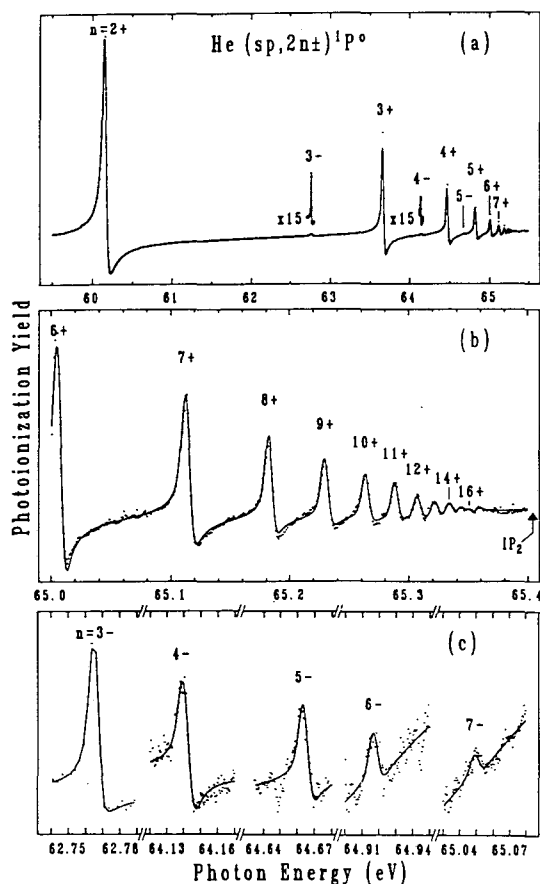


Figure 2-1. Autoionizing states of double-excited He below the $N = 2$ threshold (IP_2) of He: (a) overview, (b) magnification of the $n \geq 6$ region, (c) " $2n^-$ " states. (XBL 917-1674)

3. Vibrationally Resolved Threshold Photoemission of N_2 and CO at the N and C K-Edges (Publication 6)

L.J. Medhurst, P.A. Heimann, M.R.F. Siggel,[†] D.A. Shirley, C.T. Chen,[‡] Y. Ma,[‡] S. Modesti,[‡] and F. Sette[‡]

Zero-kinetic-energy photoelectron spectroscopy (ZKE-PES) was used to measure the Franck-Condon factors for the carbon and nitrogen K-shell ionized states in N_2 and CO. Corresponding features in the two spectra showed nearly identical energy spacings, both below and above the ionization threshold, as predicted by the equivalent core model (see Figure 3-1). The equilibrium bond length R_e for the CO C-1s-1 state was determined to be $1.077 \pm 0.005 \text{ \AA}$, and R_e for the N_2 N-1s-1 state was found to be $1.077 \pm 0.010 \text{ \AA}$, changes of 0.051 \AA for CO and -0.020 \AA for N_2 from their ground-state equilibrium bond lengths. The two-electron states corresponding to 1s-1 val-1 π^* were examined in the binding-energy region predicted by Green's function calculations. Two-electron states absent in the x-ray photoemission spectrum are present in both molecules and show evidence of vibrational structure.

[†]Permanent address: Daresbury Laboratory, Daresbury Warrington WA4 4AD, UK.

[‡]Permanent Address: AT&T, Bell Laboratories, Murray Hill, NJ 07974.

4. Threshold Behavior and Resonances in the Photoionization of Atoms and Molecules (Publication 2)

U. Becker[†] and D.A. Shirley

Threshold and near-threshold satellite intensities are examined with respect to threshold behavior, specifically for certain electron correlations contributing to the intensity of these satellites. It is assumed that the different dominant electron correlations give rise to at least four types of threshold behavior, making it possible to differentiate to a first approximation among them. These correlations are subdivided phenomenologically into two classes: "intrinsic" and "dynamic" correlations. Experimental evidence is presented for both inner- and outer-shell photoionization, substantiating this semiempirical concept. Our results are also compared with first *ab initio* calculations. The effect of resonances is emphasized as part of the threshold behavior but also with respect to their de-excitation into various decay channels. Multielectron processes such as resonant shake-off, as well as two-step autoionization and spectator Auger decay, are shown to play important roles in the decay of resonances and satellite states.

[†]Permanent address: Institut für Stahlungs und Kemphysik, Technische Universität Berlin, D-1000 Berlin 12, Germany.

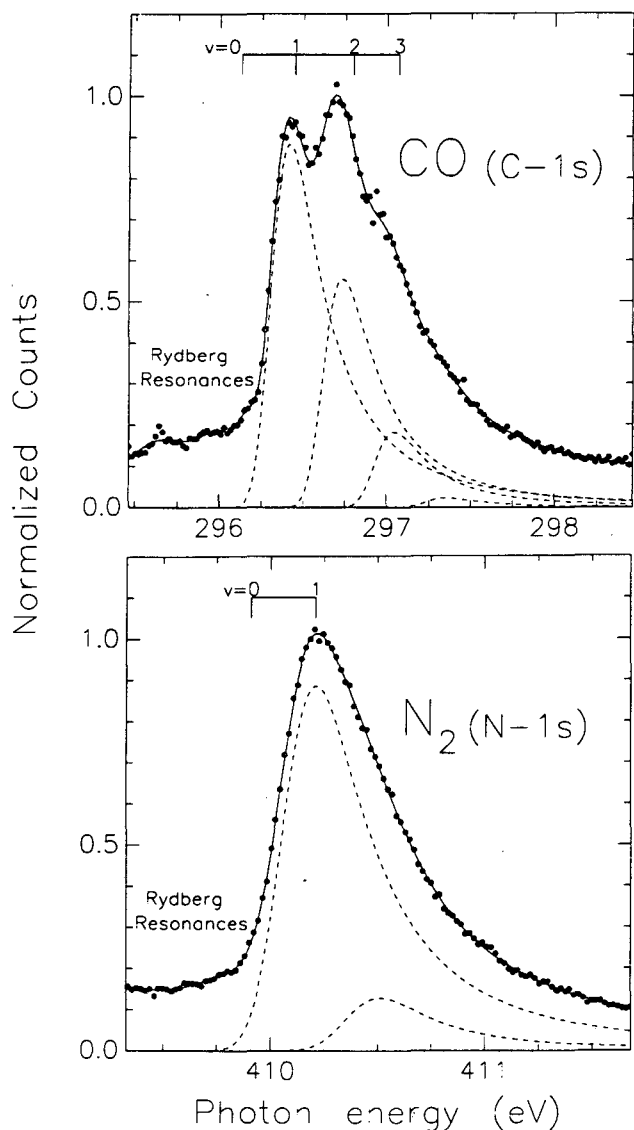


Figure 3-1. ZKE spectrum of CO at the C-1s ionization threshold and N₂ at the N-1s ionization threshold. The solid lines are fits to the data points. The individual peaks are shown with the dashed lines. The vertical lines at the top mark the thresholds for the different vibrational states. The maxima of the peaks are shifted from this by PCI. (XBL 911-131)

5. Photoelectron Spectroscopy and Electronic Structure of Clusters of the Group V Elements. I. Dimers (Publication 12)

L.S. Wang, Y.T. Lee, D.A. Shirley, K. Balasubramanian,[†] and P. Feng[†]

The HeI (584 Å) high-resolution photoelectron spectra of As₂⁺, Sb₂⁺, and Bi₂⁺ have been obtained with a high-

temperature molecular-beam source. A pure As₂ beam was produced by evaporating Cu₃As. Sb₂ was generated as a mixture with the atoms and tetramers by evaporating the pure element, while Bi₂ was generated as a mixture with only the atoms from the pure element. Vibrational structure was well resolved for the As₂⁺ spectrum (see Figure 5-1). Spectroscopic constants were derived and reported for the related ionic states. In addition, we have carried out relativistic complete-active-space self-consistent field followed by multireference single + double configuration-interaction calculations on these dimers, both for the neutral ground states and the related ionic states. The agreements between the calculated and experimentally derived spectroscopic constants were fairly good, although the calculations tended to consistently underestimate the strength of the bonding in these heavy homonuclear diatomics.

[†]Permanent address: Department of Chemistry, Purdue University, West Lafayette, IN 47907.

6. Photoelectron Spectroscopy and Electronic Structure of Clusters of the Group V Elements. II. Tetramers: Strong Jahn-Teller Coupling in the Tetrahedral ²E Ground States of P₄⁺, As₄⁺, and Sb₄⁺ (Publication 13)

L.S. Wang, B. Niu, Y.T. Lee, D.A. Shirley, E. Ghelichkhani,[†] and E.R. Grant[†]

High-resolution HeI (584 Å) photoelectron spectra have been obtained for the tetrameric clusters of the group V elements: P₄, As₄, and Sb₄. The spectra establish that

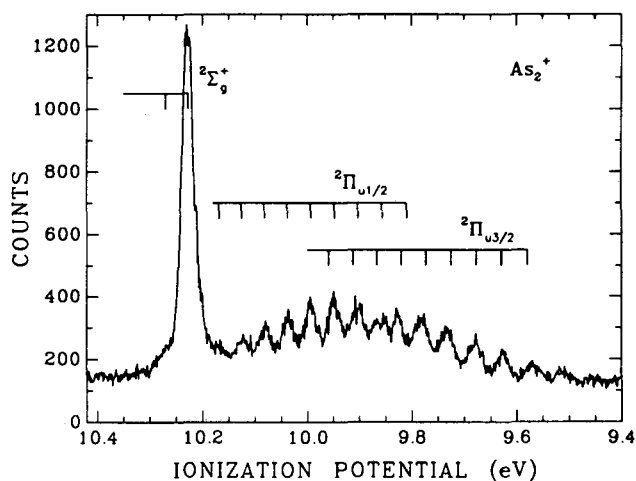


Figure 5-1. The HeI photoelectron spectrum of As₂⁺. (XBL 902-401)

the ground states of tetrahedral P_4^+ , As_4^+ , and Sb_4^+ are unstable with respect to the distortion in the $\nu_2(e)$ vibrational coordinate. The Exe Jahn-Teller Problem has been treated in detail, yielding simulated spectra to compare with experimental ones. Vibronic calculations, extended to second order (quadratic coupling) for P_4^+ , account for vibrational structure that is partially resolved in its photoelectron spectrum (see Figure 6-1). A Jahn-Teller stabilization energy of 0.65 eV is derived for P_4^+ , which can be characterized in its ground vibronic state as being highly distorted, and highly fluxional. Linear-only Jahn-Teller coupling calculations performed for As_4^+ and Sb_4^+ show good qualitative agreement with experimental spectra, yielding stabilization energies of 0.84 eV and 1.4 eV, respectively.

†Permanent address: Department of Chemistry, Purdue University, West Lafayette, IN 47907.

7. Photoelectron Spectroscopy and Electronic Structure of Clusters of the Group V Elements. III. Tetramers: The 2T_2 and 2A_1 Excited States of P_4^+ , As_4^+ , and Sb_4^+ (Publication 14)

L.S. Wang, B. Niu, Y.T. Lee, D.A. Shirley, E. Ghelichkhani,† and E.R. Grant†

Methods employing high-resolution HeI (584 Å) photoelectron spectroscopy have been applied to the tetrameric clusters of the group V elements, to resolve details of vibronic and spin-orbit structure in the first three electronic states of P_4^+ , As_4^+ , and Sb_4^+ (see Figure 7-1). Measured spacings of distinct vibrational progressions in the ν_1 mode for the 2A_1 states of P_4^+ and As_4^+ yield

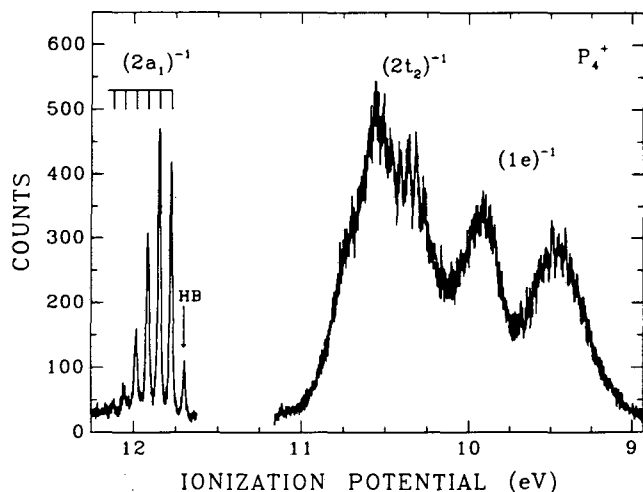


Figure 6-1. The HeI photoelectron spectrum of P_4^+ . (XBL 902-404)

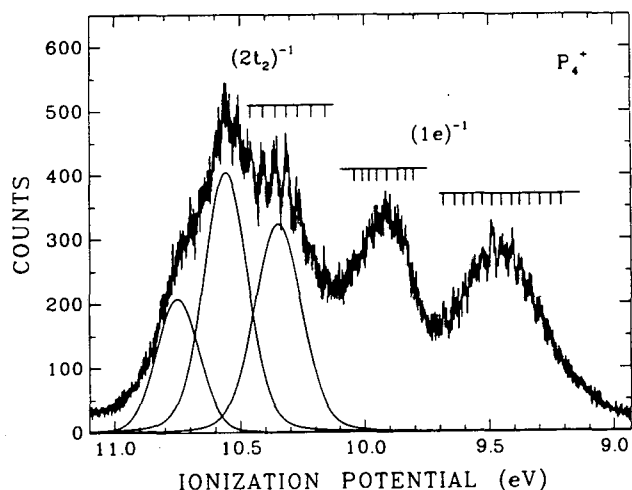


Figure 7-1. The $(1e)^{-1}$ and $(2t_2)^{-1}$ bands of the P_4^+ spectrum. Three Voigt functions are drawn to show the three components in the $(2t_2)^{-1}$ bands. (XBL 902-407)

vibrational frequencies of 577 (5) cm^{-1} for P_4^+ and 350 (6) cm^{-1} for As_4^+ . Franck-Condon factor calculations suggest bond-length changes for the ions in the 2A_1 states of 0.054 (3) Å for P_4^+ and 0.060 (3) Å for As_4^+ . Strong Jahn-Teller distortions in the $\nu_2(e)$ vibrational mode dominate the structure of the 2E ground states of the tetrameric ions. Both Jahn-Teller and spin-orbit effects appear in the spectra of the 2T_2 states of the tetrameric ions, with the spin-orbit effect being dominant in Sb_4^+ and the Jahn-Teller effect dominant in P_4^+ . Vibrational structure is resolved in the P_4^+ spectrum, and the $\nu_3(t_2)$ mode is found to be the one principally active in the Jahn-Teller coupling. A classical metal-droplet model is found to fit well with trends in the OPs of the clusters as a function of size.

†Permanent address: Department of Chemistry, Purdue University, West Lafayette, IN 47907.

8. A Detailed Study of $c(2 \times 2)Cl/Cu(001)$ Adsorbate Geometry and Substrate Surface Relaxation Using Temperature-Dependent Angle-Resolved Photoemission Extended Fine Structure (Publication 17)

L.-Q. Wang, A.E. Schach von Wittenau, Z.G. Ji,† L.S. Wang, Z.Q. Huang, and D.A. Shirley.

A detailed structural study of the $c(2 \times 2)Cl/Cu(001)$ adsorbate system was made, using the angle-resolved photoemission extended fine structure (ARPEFS) technique at low temperature, which yields both more accurate surface-structural information and near-surface-structural information for deeper substrate layers. Electrons were

detected along two emission directions, [001] and [011], and at two temperatures, 110 K and 300 K. The Fourier spectra for the [001] geometry at two temperatures are shown in Figure 8-1. The Cl atoms were found to adsorb in the four-fold hollow site, 1.604 (5) Å above the first copper layer, with a Cl-Cu bond length of 2.416 (3) Å; the errors in parentheses are statistical standard deviations only. These values are in excellent agreement with a previous LEED study by Jona *et al.* The $c(2 \times 2)$ Cl-covered first copper layer showed no relaxation with respect to the bulk position. However, a small corrugation of the second copper layer was found: the second-layer copper atoms below Cl atoms move 0.042 (12) Å away from the surface, while those in open positions remain in their bulk positions. The distances from the Cl atoms to the third and fourth copper layers were found to be 5.222 (25) Å and 7.023 (22) Å, respectively, yielding a bulk-like interlayer spacing. Thus the depth sensitivity of low-temperature ARPEFS facilitated definitive referencing of near-surface atomic positions to the underlying lattice.

†Permanent address: Department of Physics, Zhejiang University, Hangzhou, Zhejiang, People's Republic of China.

9. Energy Band Mapping of Silver (110) by Angle-Resolved Photoemission (Publication 7)

M.C. Mason,[†] J.G. Tobin,[‡] D.A. Shirley, Z. Hussain, and R.F. Davis^{||}

Angle-resolved photoemission spectra using synchrotron radiation are reported in the energy range $10 \geq h\nu \geq 34$ eV for Ag (110). Empirical dispersion relations are derived using a free-electron-like final state with parameters determined from previous energy coincidence measurements. The resulting initial state bands are in good agreement with theoretical band structure calculations, except for the lowest energy states, where the calculated energies appear to be low by as much as 0.4 eV. The validity of the free-electron model is examined in detail and found to be entirely consistent with all experimental results.

[†]Permanent address: Corporate Research Laboratories, Eastman Kodak Company, Rochester NY 14650.

[‡]Permanent address: Lawrence Livermore National Laboratory, Livermore, CA 94550.

^{||}Permanent address: Research Laboratories, Polaroid Corporation, Waltham, MA 02154.

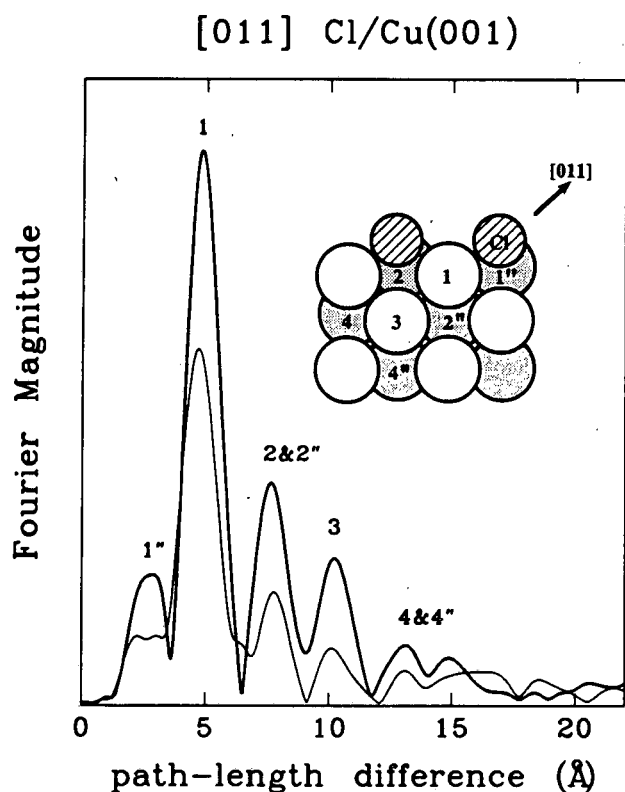


Figure 8-1. Fourier spectra for the [001] geometry at two temperatures, 110 K and 300 K. Each numbered peak is associated with a scattering path-length difference for a numbered atom in the inset. (XBL 9011-3833)

1990 PUBLICATIONS AND REPORTS

Refereed Journals

1. L.S. Wang, B. Niu, Y.T. Lee, and D.A. Shirley, "Photoelectron Spectroscopy and Electronic Structure of Heavy Group IV-VI Diatomics," *J. Chem. Phys.* **92**, 899 (1990); LBL-27699.
2. U. Becker and D.A. Shirley, "Threshold Behavior and Resonances in the Photoionization of Atoms and Molecules," *Physica Scripta* **T31**, 56 (1990).
3. P.A. Heimann, F. Senf, W. McKinney, M. Howells, R.D. Van Zee, L.J. Medhurst, T. Lauritzen, J. Chin, J. Meneghetti, W. Gath, H. Hogrefe, and D.A. Shirley, "High Resolution Results from the LBL 55-Meter SGM near the K-edge of Carbon and Nitrogen," *Physica Scripta* **T31**, 127 (1990); LBL-28744.
4. L.S. Wang, B. Niu, Y.T. Lee, and D.A. Shirley, "High Resolution Photoelectron Spectroscopy of Clusters of Group V Elements," *Physica Scripta* **41**, 867 (1990); LBL-27584.
5. L.S. Wang, J.E. Ruett-Robey, B. Niu, Y.T. Lee, and D.A. Shirley, "High Temperature and High Resolution UV Photoelectron Spectroscopy Using Supersonic Molecular Beams," *J. Electr. Spectrosc. Rel. Phenom.* **51**, 513 (1990); LBL-27583.
6. L.J. Medhurst, A. Schach von Wittenau, R.D. Van Zee, S. Zhang, S.H. Liu, D.A. Shirley, and D.W. Lindle, "Threshold Photoelectron Spectrum of the Argon 3s Satellites," *J. Electr. Spectrosc. Rel. Phenom.* **52**, 671 (1990); LBL-27468.

7. M.G. Mason, J.G. Tobin, D.A. Shirley, Z. Hussain, and R.F. Davis, "Energy Band Mapping of Silver (110) by Angle Resolved Photoemission," *Arabian J. Sci. Eng.* **15**, 309 (1990).
8. L.S. Wang, B. Niu, Y.T. Lee, and D.A. Shirley, "Electronic Structure and Chemical Bonding of the First Row Transition Metal Dichlorides, $MnCl_2$, $NiCl_2$, and $ZnCl_2$: A High Resolution Photoelectron Spectroscopic Study," *J. Chem. Phys.* **93**, 957 (1990); LBL-27925.
9. Z.Z. Yang, L.S. Wang, Y.T. Lee, D.A. Shirley, S.Y. Huang, and W.A. Lester, Jr., "Molecular Beam Photoelectron Spectroscopy of Allene," *Chem. Phys. Lett.* **171**, 9 (1990); LBL-27633.
10. L.J. Terminello, K.T. Leung, Z. Hussain, T. Hayashi, X.S. Zhang, and D.A. Shirley, "Surface Geometry of $(1 \times 1)PH_x/Ge(111)$ Determined with Angle-Resolved Photoemission Extended Fine Structure," *Phys. Rev. B* **41**, 12787 (1990); LBL-26151.
11. M. Domke, C. Xue, A. Puschmann, T. Mandel, E. Hudson, D.A. Shirley, and G. Kaindl, "Carbon and Oxygen K-Edge Photoionization of the CO Molecule," *Chem. Phys. Lett.* **173**, 122 (1990); Erratum **174**, 663 (1990).
12. L.S. Wang, Y.T. Lee, D.A. Shirley, K. Balasubramanian, and P. Feng, "Photoelectron Spectroscopy and Electronic Structure of Clusters of the Group V Elements. I. Dimers," *J. Chem. Phys.* **93**, 6310 (1990); LBL-28871.
13. L.S. Wang, B. Niu, Y.T. Lee, E. Ghelichkhani, E.R. Grant, and D.A. Shirley, "Photoelectron Spectroscopy and Electronic Structure of Clusters of the Group V Elements. II. Tetramers: Strong Jahn-Teller Coupling in the Tetrahedral 2E Ground States of P_4^+ , As_4^+ and Sb_4^+ ," *J. Chem. Phys.* **93**, 6318 (1990); LBL-28872.
14. L.S. Wang, B. Niu, Y.T. Lee, D.A. Shirley, E. Ghelichkhani, and E.R. Grant, "Photoelectron Spectroscopy and Electronic Structure of Clusters of the Group V Elements. III. Tetramers: The 2T_2 and 2A_1 Excited States of P_4^+ , As_4^+ and Sb_4^+ ," *J. Chem. Phys.* **93**, 6327 (1990); LBL-28873.
15. D.A. Shirley and G. Margaritondo, editors, "The 9th International Conference on Vacuum Ultraviolet Radiation Physics," Honolulu, Hawaii, July 17-21, (1989), *Physica Scripta T31* (1990).

Other Publications

16. M. Domke, C. Xue, A. Puschmann, T. Mandel, E. Hudson, D.A. Shirley, G. Kaindl, C.H. Greene, H.R. Sadeghpour, and H. Petersen, "Extensive Double Excitation States in Atomic Helium," *Phys. Rev. Lett.* (in press).

LBL Reports

17. L.-Q. Wang, A.E. Schach von Wittenau, Z.G. Ji, L.S. Wang, Z.Q. Huang, and D.A. Shirley, "A Detailed Study of $c(2 \times 2)Cl/Cu(001)$ Adsorbate Geometry and Substrate Surface Relaxation Using Temperature Dependent Angle-Resolved Photoemission Extended Fine Structure," LBL-28731.

Invited Talks

18. Z. Hussain, "Angle-Resolved Photoemission Study of Valence Bands of Solids: High Angular Resolution and Temperature Dependence," Surface Science and Catalysis Science Seminar, Center for Advanced Materials, Lawrence Berkeley Laboratory, January 11, 1990.
19. D.A. Shirley, "Surface Structures from Energy-Dependent Photoelectron Diffraction," Department of Theoretical Chemistry, Technical University, Brunswick, Germany, February 5, 1990.
20. D.A. Shirley, "Adsorbate Surface Structures and Properties from Energy Dependent Photoelectron Diffraction," Physik-Kolloquium Leipzig, Karl-Marx Universität, Leipzig, Germany, February 27, 1990.
21. D.A. Shirley, "Adsorbate Surface Structures and Properties From Energy Dependent Photoelectron Diffraction," Dresdener Seminar für Theoretische Physik, Technischen Universität Dresden, Germany, February 28, 1990.
22. D.A. Shirley, "Surface Structures from Energy-Dependent Photoelectron Diffraction," Physics Department, King Fahd University (UPM), Dharan, Saudi Arabia, March 13, 1990.
23. D.A. Shirley, "Surface Adsorbate Structures from Variable-Energy Photoelectron Diffraction," March Meeting, German Physical Society (DPG), Regensburg, Germany, March 26, 1990.
24. D.A. Shirley, "High Resolution Zero-Volt Spectroscopy in the Core Level Region," International Workshop on "Photoionization Today and Tomorrow," Ioffe Institute, USSR Academy of Sciences, Leningrad, USSR, April 26, 1990.
25. D.A. Shirley, "Photoelectron Diffraction in Surface Adsorbate Studies," Universität Bielefeld, Germany, May 5, 1990.
26. D.A. Shirley, "Surface Structures From Energy-Dependent Photoelectron Diffraction," Fritz-Haber-Institut, Berlin, Germany, May 8, 1990.
27. D.A. Shirley, "High-Resolution Zero-Volt Spectroscopy in the Core-Level Region," FB Physik, Technical University, Berlin, Germany, May 8, 1990.
28. D.A. Shirley, "Energy-Dependent Photoelectron Diffraction: New Insights," Physics Institute, University of Fribourg, Switzerland, May 14, 1990.
29. D.A. Shirley, "Energy-Dependent Photoelectron Diffraction: New Insights," Batiment des Sciences Physiques, Université de Lausanne, Switzerland, May 15, 1990.
30. D.A. Shirley, "Surface and Near-Surface Structures from Energy-Dependent Photoelectron Diffraction," Fakultät für Physik, Albert-Ludwigs Universität Freiburg, Germany, May 16, 1990.
31. D.A. Shirley, "Energy-Dependent Photoelectron Diffraction," ETH Zurich, Switzerland, May 17, 1990.
32. D.A. Shirley, "Energy-Dependent Photoelectron Diffraction," Institut für Grenzflächen—Forschung und Vacuum Physik, Jülich, Germany, May 31, 1990.
33. D.A. Shirley, "Energy-Dependent Photoelectron Diffraction: New Insights," Fakultät für Physik,

Technischen Universität Munchen, Germany, June 13, 1990.

34. D.A. Shirley, "Surface Structures from Energy Dependent Photoelectron Diffraction—New Results," DESY Colloquium, Deutscher Electronen Synchrotron, Hamburg, Germany, June 14, 1990.

35. D.A. Shirley, "How Will Photoemission Continuum-State Structure Affect Inverse Photoemission?" International

Seminar on Applications of Inverse Photoemission, Leningrad State University, Leningrad, USSR, June 27, 1990.

36. D.A. Shirley, "Energy-Dependent Photoelectron Diffraction," International Conference on Synchrotron Radiation (SR-90), Moscow State University, USSR, June 29, 1990.

ATOMIC PHYSICS

High-Energy Atomic Physics*

Harvey Gould, Investigator

INTRODUCTION

The goals of this program are (1) to search for an electron electric dipole moment (EDM), (2) to understand atomic collisions of relativistic ions, and (3) to test quantum electrodynamics in a strong static Coulomb field. Recent results include a new upper limit to the electron EDM of 1×10^{-26} e cm, a factor-of-7 improvement over all previous measurements and the smallest upper limit for any particle. Finding an electron EDM would be proof of new physics, not contained in the Standard Model, and would be as significant a discovery as the results expected from the Superconducting Super Collider. Present activities include (1) increasing the sensitivity of the EDM experiment, (2) developing a new, nonchanneling technique for measuring electron-impact ionization cross sections of highly stripped heavy ions, (3) an attempt to observe a new relativistic atomic collisions process—the capture of an electron by a (bare) ion when the electron is produced as part of an electron-positron pair by the motional Coulomb fields of a relativistic ion passing within atomic distances of a target nucleus, and (4) upgrades to meet applicable standards for environment, health, and safety.

1. A New Experimental Limit on the Electron Electric Dipole Moment (Publication 1)

K. Abdullah,[†] C. Carlberg,[‡] E. Commins, H. Gould, and S.B. Ross

The standard model of strong, weak, and electromagnetic interactions predicts an electron electric dipole moment (EDM) no greater than 10^{-37} e cm. But

many of the models beyond the standard model allow much larger electron EDMs, some as large as the current upper limit to the electron EDM. Higgs boson models of CP violation have found that an electron EDM of *greater* than 10^{-27} e cm is possible. The observation of an electron EDM would be proof of new physics not contained in the Standard Model and would be as important as any result expected from the Superconducting Super Collider. If the electron EDM is very small or absent, this sensitive experiment could impose useful constraints on many models and compliment high-energy particle-physics experiments.

The principle of the experiment is to search for the EDM by measuring its energy in an electric field. While this is impractical for a free electron, it is feasible using a valence electron in a $J = 1/2$ neutral atom of high atomic number. Here, due to relativistic effects, the ratio R of the atomic EDM to an electron EDM is much larger than unity. The experiment uses the ground state of thallium, where R is calculated to be -600 , and searches for the atomic EDM by looking for an energy splitting, which scales linearly in an applied electric field.

An atomic-beam magnetic-resonance apparatus with separated oscillatory fields is used to make the measurements. Beams of neutral thallium atoms at thermal velocities are produced by heating thallium in an oven. The thallium atoms are prepared into a single magnetic substate by optical pumping with 378-nm (UV) light linearly polarized along the direction of a weak applied magnetic field. Transitions between the levels being measured are induced by a pair of rf loops separated by about 1.2 m. In between the rf loops is a set of electrodes that produces an electric field of 105 V/cm. A difference in the transition frequency upon reversal of the electric field is the signature for the EDM.

While the shift in frequency due to electron EDM is no larger than 10^{-6} Hz/kV/cm, the shift due to the electron *magnetic* dipole moment is about 10^6 Hz/G. To prevent a magnetic dipole moment from mimicking an EDM, magnetic-field changes that are synchronous with the

*This work was supported by the Director, Office of Energy Research, Office of Basic Energy Sciences, Chemical Sciences Division, of the U.S. Department of Energy under Contract No. DE-AC03-76SF00098.

electric field are kept to below 10^{-10} G. One source of a synchronous magnetic field is the motional magnetic field of the atoms moving in the electric field if the electric field is not exactly parallel to the weak static magnetic field that defines the polarization axis. This effect is minimized by using two-counter propagating thallium beams so that the average velocity of the two beams is close to zero. Care is taken to achieve the same velocity distribution of atoms, a complete overlap of the beams, and uniform magnetic and electric fields.

[†]Present address: Salomon Brothers Inc., 1 New York Plaza, New York, NY 10004.

[‡]Present address: Manne Siegbahn Institute of Physics, Frescativ 24, 104 05, Stockholm, Sweden.

2. Work in Progress

Although electron-impact ionization cross sections of ions are usually measured by crossed beams of electrons and ions, this technique has not been applied to highly stripped heavy ions; high electron energies are needed to dislodge the tightly bound electrons, and very high electron densities are needed to measure the small cross sections. Channeling ions through a crystal lattice provides a much higher electron density, and this research group has channeled ions through Si single crystals to make the first measurement of the electron-impact ionization cross section of the L^- and K^- shells of a highly stripped heavy ion (uranium). Another group has since channeled ions to measure electron impact ionization cross sections of the L^- and M^- shells of xenon ($Z = 54$).

Measuring electron-impact ionization by channeling, however, requires that the electron density encountered by the ions is known, and that account is taken of the very large projectile ionization by the nuclei in the crystal from the fraction of ions that channel poorly or not at all. Also, because of the high density, one has to ensure that density-dependent effects, such as excitation with subsequent electron loss, do not affect the measurements. Channeling measurements of electron-impact ionization cross sections of the xenon M^- and L^- shells, done at GANIL, and the uranium K^- shell measurements, done at LBL, are not in agreement with calculations. An alternative experimental technique is needed to help resolve this discrepancy.

A new experiment is in progress that makes use of the fact that, for very high-energy highly stripped heavy-ion projectiles in hydrogen gas, the electron and proton in the hydrogen target will contribute about equally to the ionization of the projectile. Under these conditions, screening and molecular effects are negligible, and a measurement of the total ionization cross section of the projectile ion in hydrogen yields approximately twice the electron-impact ionization cross section.

1990 PUBLICATIONS AND REPORTS

Refereed Journals

1. K. Abdullah, C. Carlberg, E. Commins, H. Gould, and S.B. Ross, "A New Experimental Limit on the Electron Electric Dipole Moment," *Phys. Rev. Lett.* **65**, 2347 (1990); LBL-29516.

Other Publications

2. E.D. Commins, "Search for The Electric Dipole Moment of the Electron," *Bull. Am. Phys. Soc.* **35**, 1181 (1990); LBL-30210abs.
3. J. Schweppe, A. Belkacem, L. Blumenfeld, N. Claytor, B. Feinberg, H. Gould, V.E. Kostroun, L. Levy, S. Misawa, J.R. Mowat, and M.H. Prior, "Measurement of the Lamb Shift in Lithiumlike Uranium (U^{89+})," *Bull. Am. Phys. Soc.* **35**, 1178 (1990); LBL-30218abs.

LBL Reports

4. R. Mowat, B. Feinberg, H. Gould, M. Prior, and J. Schweppe, "Measurement of the Lamb Shift in Lithiumlike Uranium (U^{89+})," LBL-30214abs.
5. S.B. Ross, "Systematic Effects in the Berkeley Electron Electric Dipole Moment Experiment," LBL-29262abs.
6. J. Schweppe, A. Belkacem, L. Blumenfeld, N. Claytor, B. Feinberg, H. Gould, V.E. Kostroun, L. Levy, S. Misawa, J.R. Mowat, and M.H. Prior, "Measurement of the Lamb Shift in Lithiumlike Uranium (U^{89+})," LBL-30215abs.
7. K. Abdullah, C. Carlberg, E. Commins, H. Gould, and S.B. Ross, "The Electron Electric Dipole Moment Experiment," LBL-30216abs.
8. J. Schweppe, A. Belkacem, L. Blumenfeld, N. Claytor, B. Feinberg, H. Gould, V.E. Kostroun, L. Levy, S. Misawa, J.R. Mowat, and M.H. Prior, "Measurement of the Lamb Shift in Lithiumlike Uranium (U^{89+})," LBL-30217abs.

Invited Talks

9. A. Belkacem, "The Experimental Program at LBL," Brookhaven National Laboratory, Upton, NY, April 20-21, 1990.
10. E.D. Commins, "Search for The Electric Dipole Moment of the Electron," Physics Department, University of California at Berkeley, Berkeley, CA, Jan. 30, 1990; Department of Physics, Stanford University, Stanford, CA, Nov 20, 1990; Joint Institute for Laboratory Astrophysics/Department of Physics, University of Colorado, Boulder, CO, Dec. 12, 1990; Argonne National Laboratory, Argonne, IL, Jan 16, 1991; Department of Physics, Notre Dame University, Notre Dame, IN, Jan 17, 1991.
11. H. Gould, "A New Upper Limit to the Electron Electric Dipole Moment," CERN, July 30, 1990.
12. S.B. Ross, "An Experimental Limit to the Electric Dipole Moment of the Electron," Lawrence Livermore National Laboratory, Sept. 19, 1990.

Atomic Physics*

Michael H. Prior, Investigator

INTRODUCTION

This program performs challenging studies of the structure and interactions of atomic systems, to provide the most detailed description of their behavior, and to stimulate theoretical understanding of the observed phenomena. Emphasis is placed on research topics that are best addressed with unique research tools and expertise available at LBL. Often topics selected have relevance to plasma behavior and diagnostics in tokamak devices or advanced laser technology.

Currently the program exploits the ability of state-of-the-art electron cyclotron resonance (ECR) ion sources at LBL to produce intense, highly charged beams for ion-atom and ion-surface collision and Auger spectroscopic studies. The present studies emphasize detailed understanding of ion-atom collisions, with particular concentration on multiple-electron-transfer processes. A general goal of this work is to perform experiments that describe electron transfer between uniquely characterized initial and final states so that theoretical predictions can be tested at the finest scale possible. Of particular current interest are double-electron-transfer modes, where the two active electrons may exhibit a correlated behavior; that is, the transfer is not simply described as the incoherent sum of single-electron-transfer amplitudes. Also of interest are ion-surface studies, where the high potential energy carried by a multiply charged projectile can strongly influence secondary processes such as sputtering of neutrals and ions and Auger electron emission. In an applied sense, the combination of a highly ionized projectile and a neutral atom or surface in close proximity is a highly inverted, nonequilibrium system, and thus the detailed study of such collisions is relevant, for example, to the study of nonequilibrium plasmas important to advanced laser concepts and ion-wall interactions in plasma devices or space environments.

In addition to detailed collision studies, this program contains a component devoted to the description and understanding of energy-level structure and decay modes of highly excited atomic systems. Currently this work concentrates upon Auger electron spectroscopy, which provides energy-level data for multiply excited states. This

work complements photon spectroscopy in many cases, since levels that Auger decay prominently are usually weak photon emitters.

1. Light Emission from Na Atoms Sputtered by Multiply Charged Ar Ions (Publication 1)

R.E. Tribble,[†] M.H. Prior, and R.G. Stokstad[‡]

This study reports, for the first time, information on the projectile charge dependence of the production of excited neutral atoms by heavy ions impacting on a crystal surface. Production of excited singly charged surface ions was also observed. This was done by observing the optical spectrum emitted by atoms and ions sputtered from a NaCl crystal surface normal to a beam of Ar⁹⁺ ions produced by the LBL electron cyclotron resonance (ECR) ion source located at the 88-Inch Cyclotron. The yield of light following bombardment with heavy ions depends on the sputtering yield and on the probability that a sputtered atom or ion will be excited as it leaves the surface. For an insulating surface, both of these processes can depend in principle on the charge state, and hence on the electronic potential energy, of the incident ion. The sputtering yield could be increased by a direct electronic ejection of a surface atom—a Coulomb “explosion” accompanying the passage and neutralization of an incident ion. The probability that a sputtered atom or ion will become excited as it leaves the surface could be affected by the charge depletion on the surface induced by the incident ion, provided the time scales for relaxation of the surface charge and ejection of an atom are comparable. The excitation and subsequent emission of light by atoms remaining in the surface may also depend on the charge state of the bombarding ion. All of these phenomena are in principle sensitive to the neutralization process for the Ar ion as it approaches the target.

The experimental arrangement consisted of a NaCl crystal mounted on a target holder attached to a precision linear translator. The surface of the NaCl target was perpendicular to, and could be translated along, a line parallel to the ion-beam direction. A double collimator system was mounted in front of a Jarell-Ash (Model 82-410) 1/4 m grating spectrometer with the axis of the collimator system perpendicular to and intersecting the beam. This permitted a view of 600 μm along the beam path. The target position could be reproduced to within 10 μm relative to the spectrometer axis. The experimental

*This work was supported by the Director, Office of Energy Research, Office of Basic Energy Sciences, Chemical Sciences Division, of the U.S. Department of Energy under Contract No. DE-AC03-76SF00098.

arrangement, though optimized for measuring light emission by the sputtered target atoms, also permitted observation of light emitted at the surface of the target when it was positioned within 300 μm of the spectrometer axis.

Figure 1-1 is a survey spectrum showing all lines observed over the 280–600 nm region. The lines belong to the neutral and singly ionized sodium (Na I and Na II) spectra. There was no clear evidence of Cl lines, and this is not expected in this spectral range. The studies concentrated on the strong lines 3s-3p (the unresolved Na D lines) and 3s-4p, marked a and b in Figure 1-1. The intensities of these lines were measured, normalized to the ion beam flux, as a function of position in front of the NaCl surface. These curves show an intensity fall-off that depends on the velocity of the sputtered excited Na atoms, the lifetime of the excited states, and the variation of density of emitters within the viewing region of the spectrometer/collimator system. The curves show a rapid intensity fall-off in the region near the surface, followed by a slower, near-exponential drop where light is being emitted far from the surface by excited sputtered particles.

In Figure 1-2 we compare the light yield in the D lines as a function of the incident charge state for (a) light from the surface of the crystal (measured at the peak of the intensity curves) and (b) for light from the sputtered atoms (measured in the exponential region of the curve). The results shown in the figure indicate no significant change (i.e., not larger than 10% or two standard deviations) in the light yield from the sputtered atoms. However, there is a significant 25% increase in the yield of light from the surface as the charge state is increased from 4 to 12.

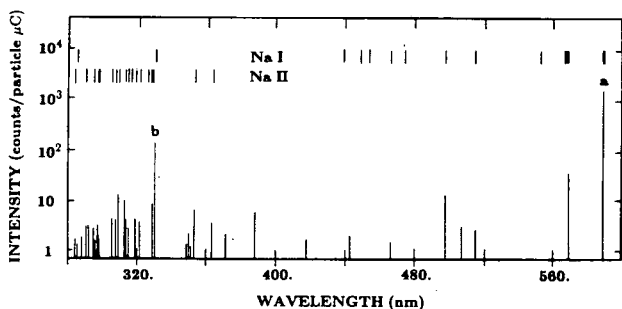


Figure 1-1. Survey of spectral lines observed from Ar^{8+} ions on the NaCl target. The intensity is in units of detected counts per particle μC . The two lines, a and b, are the atomic 3s-3p (unresolved D lines) and the 3s-4p transitions. Most of the other observed lines can be identified as transitions in Na atoms (Na I spectrum) or singly charged ions (Na II spectrum). The location of prominent lines in these spectra are indicated near the top of the figure. The spectrometer did not resolve lines spaced closer than about 1.0 nm. These data were taken with the target located 0.25 mm from the line normal to the spectrometer entrance slit. (XBL 895-1932)

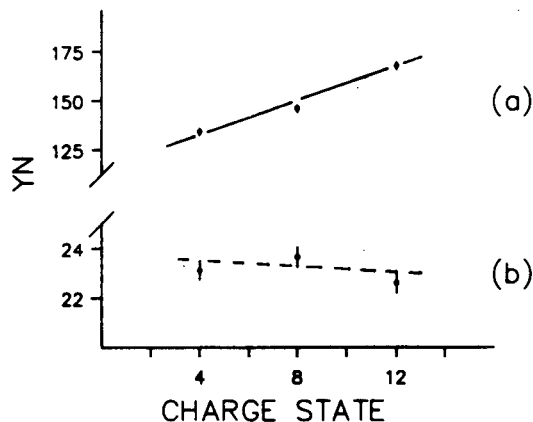


Figure 1-2. Normalized light yield (YN) for the Na D-lines, versus incident charge state at 48-keV bombardment energy for (a) the light from the surface region, and (b) the light from sputtered atoms well beyond the surface. (XBL 912-323)

The increase observed in the light emission at the surface with increasing charge state is probably a result of the additional energy required to neutralize the incoming ion. The potential energy between the ion and surface increases from 144 eV for Ar^{4+} to 2636 eV for Ar^{12+} . Thus, neutralizing the 12+ ions could cause a significant increase in surface excitation. This electronic excitation could be dissipated, at least in part, by excitation of the surface atoms, thus producing the increased light yield.

The production of a sputtered ion (as opposed to a neutral atom) is a process that is also determined by what happens at the end of the cascade as a struck atom is about to leave the surface. Studies of secondary-ion emission as a function of the charge of the incident ion have been reported for both semiconductors and insulators. The results are not totally consistent; but, in general, they do indicate an enhancement in the ion yield as the charge state of the projectile is increased. Our observation of no significant dependence of the sputtered-atom yield (curve b in Figure 1-2) appears to be inconsistent with the studies of secondary-ion emission. However, nature may be more subtle. An understanding of the mechanism(s) for the sputtering of excited atoms and of secondary ions requires a unified description of the processes before one can hope to explain the results from both types of measurement.

[†]Work performed while on leave at Lawrence Livermore National Laboratory from Texas A&M University.

[‡]LBL Nuclear Science Division.

2. Work in Progress

Using a large scattering chamber and a rotatable electron spectrometer, we measured the angular dependence of the Auger spectra following electron capture by C^{5+} from a He gas jet target. These are the first systematic studies of Auger angular distributions from states created in slow, highly charged ion-atom collisions. Nearly all published Auger spectra have been taken at a single fixed angle with respect to the projectile beam. Measurement of the electron emission angular dependence allows inference of the underlying alignment and hence the population of individual magnetic substates.

In any beam-gas inelastic collision, the final electronic magnetic substates of the products are not necessarily equally populated. This occurs because there is a preferred direction in the collision (the initial relative velocity vector), the system has cylindrical symmetry, and thus states with magnetic substate quantum numbers M_L and $-M_L$ will have equal population. Except for this restriction, the population of the different substates may differ. This variation of the magnetic substate population, termed alignment, can result in a significant variation of the Auger line intensities with emission angle measured from the beam direction.

Our observations show a striking variation of the magnetic substate populations for the Li-like $1s2p^2\ ^2D$ and $1s[2s2p\ ^1P]^2P$ states of the C^{3+} ion created by the double-electron capture. In particular, a substantial population of $M_L = 1$ states was observed, indicating the importance of rotational coupling (breakdown of the Born-Oppenheimer approximation) in this system. Strong variations of substate populations were observed over the narrow velocity range of 0.29 to 0.50 a.u. In the absence of relevant experimental data, theorists normally average their results over the magnetic substates; our results are the first to challenge theory at the finest quantum detail for a multiple-electron-transfer collision.

The study of the anisotropy of Auger electrons emitted from resolved multiply excited states formed in electron-capture collisions will be continued with systems similar to the $C^{5+} + He$ collision pair. Candidates are B^{4+} and $N^{6+} + He$. It is important to do this because the quasi-molecular level structure and the location of important real and

avoided crossings between initial and final states change markedly for the different three-electron systems. This will have strong effects on the anisotropy. Theory that can correctly reproduce the results for several related collision systems can be judged more reliable. From a practical point of view, it is essential to know the angular dependence of Auger spectra if one is to infer reliable production cross sections from measurements made at fixed angles. Our measurements show that enormous errors can be made if the angular distributions are ignored.

1990 PUBLICATIONS AND REPORTS

Refereed Journals

1. R.E. Tribble, M.H. Prior, and R.G. Stokstad, "Light Emission from Na Atoms Sputtered by Multiply-Charged Ar Ions," *Nucl. Instrum. Meth. Phys. Res. B* **44**, 412 (1990).
2. D. Schneider, M.H. Chen, S. Chantrenne, R. Hutton, and M.H. Prior, "Auger Electron Emission from Na-like Fe Ions Excited in Collisions of 170-keV Fe^{17+} on He and Ne," *Phys. Rev. A* **40**, 4313 (1989).

Other Publications

3. J. Schweppe, A. Belkacem, L. Blumenfeld, N. Claytor, B. Feinberg, H. Gould, V. Kostroun, L. Levy, S. Misawa, R. Mowat, and M. Prior, "Measurement of the Lamb Shift in Lithiumlike Uranium (U^{89+})," *Bull. Am. Phys. Soc.* **35**, 1178 (1990).
4. R. Hutton, M.H. Chen, M.W. Clark, D. DeWitt, J. McDonald, M.H. Prior, and D. Schneider, "Electron Spectroscopy of High Z Core-Excited Na-like Ions," *Bull. Am. Phys. Soc.* **35**, 1178 (1990).
5. R. Holt, D. Schneider, R. Hutton, and M.H. Prior, "Angular Dependence of Auger Spectra Following Double Electron Capture," *Bull. Am. Phys. Soc.* **35**, 1198 (1990).

LBL Reports

6. R.A. Holt, M.H. Prior, K.L. Randall, R. Hutton, J. McDonald, and D. Schneider, "Magnetic Substates Populated by Double Electron Capture," LBL-29292.

PROCESSES AND TECHNIQUES

CHEMICAL ENERGY

High-Energy Oxidizers and Delocalized-Electron Solids*

Neil Bartlett, Investigator

INTRODUCTION

The main aim of this program is the synthesis and characterization of new materials that may have utility in efficient storage or usage of energy. The novel materials include two-dimensional networks of light p-bonding atoms (boron, carbon, and nitrogen) with structures akin to graphite. Of these, the more metallic have possible applications as electrode materials for high-energy-density batteries, and those that are semiconducting could be useful in converting light to electrical energy. Good ionic conductors are also being sought, with emphasis on lithium-ion and fluoride-ion conductors, since batteries based on lithium and fluorine would be unsurpassed in their energy density. In addition, novel oxidation-state fluorides are being synthesized and structurally characterized to provide a comprehensive basis for better theoretical models, from which an improved capability to predict physical and chemical behavior ought to be forthcoming. Previously unknown or little-studied high-oxidation-state species constitute a large part of this effort. Such species are also investigated for their efficiency and specificity as chemical reagents.

1. Silver Trifluoride: Preparation, Crystal Structure, Some Properties, and Comparison with AuF₃ (Publication 7)

B. Zemva,[†] K. Lutart,[†] A. Jesih,[†] W.J. Casteel, Jr., A.P. Wilkinson,[‡] D.E. Cox,[§] R.B. Von Dreele,[¶] H. Borrmann, and N. Bartlett

It has been established that the bright red diamagnetic AgF₃ derived from AgF₄⁻ in AHF with BF₃ is thermodynamically unstable and, in contact with AHF, at

~20°C, loses F₂ in less than 19 hours according to the equation $3\text{AgF}_3 \rightarrow \text{Ag}_3\text{F}_8 + 1/2\text{F}_2$. To provide for meaningful comparisons, the structures of AuF₃ and AgF₃ have been determined using neutron-diffraction data. The structures of both AgF₃ and AuF₃ were successfully refined in space group P6₁22 - D₆₂ (No. 178) from time-of-flight neutron powder-diffraction data from 100-mg samples contained in 2-mm capillary tubes. The 7762 observations for AgF₃ yielded $a = 5.0782(2)$ Å, $c = 15.4524(8)$ Å, and $V = 345.10(2)$ Å³, the reliability parameters for the structure being $R_{\text{wp}} = 6.21$ and $R_p = 3.86\%$. From the 7646 observations for AuF₃, $a = 5.1508(1)$ Å, $c = 16.2637(7)$ Å, and $V = 373.68(2)$ Å³, with $R_{\text{wp}} = 11.21$ and $R_p = 7.58\%$. The silver or gold atom lies at the center of an elongated octahedron with two Ag-F(1) = 1.990(3) Å, two Au-F(1) = 1.998(2) Å, two Ag-F(2) = 1.863(4) Å, and two Au-F(2) = 1.868(3) Å, the approximately square, isodimensional AF₄ units being joined by symmetrical μ-fluorobridges [two F(1) in *cis* relationship in the AF₄ unit] to form the 6₁ (or 6₅) helical chains, the Ag-F(1)-Ag angle being 123.2(2)°, and the Au-F(1)-Au angle being 119.3(2)°. The ~5 Å³ smaller formula unit volume of AgF₃ compared with AuF₃ and the shorter z-axis interatomic distance [Ag-F = 2.540(4) Å, Au-F = 2.756(8) Å], is in accord with the tighter binding of the Ag(III) d-orbital electrons evident in the strong oxidizing properties of Ag(III).

Interaction of AgF⁺ with AgF₄⁻ (1:1) in AHF yields maroon Ag(II)Ag(III)F₅, which is probably the salt AgF⁺AgF₄⁻. The latter interacts with AgF₃ to yield Ag(II)Ag(III)₂F₈, a second mixed-oxidation-state fluoride that is identical to the product of the decomposition of AgF₃ at 20°C in AHF. The magnetic susceptibility of Ag(II)Ag(III)₂F₈ closely obeys the Curie-Weiss law (4 to 280 K) with $\theta = -4.2(5)^\circ$ and $\mu_{\text{eff}} = 1.924(3)$ B.M., this indicating that the material is magnetically dilute. This is consistent with Ag²⁺ separated by [AgF₄]⁻ ions as in the formulation Ag²⁺[AgF₄]⁻². Bougon *et al.*^{1,2} reported that their data for "AgF₃" obeyed the Curie-Weiss law over the temperature range 4 to 290 K. When the magnetic moment given by Bougon *et al.*^{1,2} for their "AgF₃" is adjusted to the formula Ag₃F₈, it becomes $\mu = 1.95 + 0.08$ B.M., which is not significantly different from the effective magnetic moment found here. The equivalence of the magnetic and

*This work was supported by the Director, Office of Energy Research, Office of Basic Energy Sciences, Chemical Sciences Division, of the U.S. Department of Energy under Contract No. DE-AC03-76SF00098.

x-ray powder data for Ag_3F_8 to that reported by Bougon *et al.*^{1,2} for the “ AgF_3 ” proves the identity of their latter with the former.

[†]Permanent address: Institut Jožef Stefan, Ljubljana, Yugoslavia.

[‡]Permanent address: University of Oxford, Oxford, England.

[§]Permanent address: Brookhaven National Laboratory, Upton, NY 11973.

[¶]Permanent address: Los Alamos National Laboratory, Los Alamos, NM 87545.

1. R. Bougon and M. Lance, *Comptes Rendus, Acad. Sci., Ser. 2* 297, 117 (1983).

2. R. Bougon, T. Bai Huy, M. Lance, and H. Abazli, *Inorg. Chem.* 23, 3667 (1984).

2. The Crystal Structure of $[\text{Ag}(\text{XeF}_2)_2]\text{AsF}_6$ Formed in the Oxidation of Xe by AgFAsF_6 (Publication 4)

R. Hagiwara, F. Hollander, C. Maines, and N. Bartlett

$[\text{Ag}(\text{XeF}_2)_2]\text{AsF}_6$ is formed by the oxidation of Xe with a solution of AgFAsF_6 in anhydrous hydrogen fluoride (AHF) at 20°C. It may also be made from AgAsF_6 and excess XeF_2 in AHF. It crystallizes in space group $I4c2$, with $a_0 = 8.4558(12)$ Å, $c_0 = 12.8645(19)$ Å, $V = 919.8(3)$ Å³, and $Z = 4$. The structure was solved by the Patterson method and refined to conventional R and wR values of 0.0189 and 0.0253, respectively. Sheets of the NaCl-type arrangement of AgAsF_6 occur in the structure. The XeF_2 molecules are located between those sheets, each being coordinated to two Ag^+ , one in the sheet above, the other below, as shown in Figure 2-1. Each Ag^+ is at the center of a roughly cubic arrangement of F ligands in two fourfold rectangular planar sets mutually at right angles (see Figure 2-2). The closely coordinated set involves F ligands of the XeF_2 with $\text{Ag}\cdots\text{F} = 2.466(3)$ Å. The four more distant F are ligands of the AsF_6^- with $\text{Ag}\cdots\text{F} = 2.732(3)$ Å. The XeF_2 and the AsF_6^- are approximately D_{oh} and O_h , respectively, with the bond lengths of $\text{Xe}-\text{F} = 1.979(3)$ Å, $\text{As}-\text{F}(\text{axial}) = 1.718(3)$ Å, and $\text{As}-\text{F}(\text{equatorial}) = 1.712(3)$ Å. This arrangement is simply a consequence of the interaction of the semi-ionic XeF_2 molecules $^{-1/2}\text{F}-\text{Xe}^+-\text{F}^{-1/2}$ with the $\text{Ag}(\text{I})$ cation. The compound slowly loses its XeF_2 in a vacuum at room temperature and falls to AgAsF_6 .

3. Synthesis and Characterization of Graphite-Like Boron-Carbon Materials (Publication 5)

B.C. Shen, O.K. Tse, J. Kouvetakos, K.M. Krishnan, K.-M. Yu, and N. Bartlett

The carbon-to-boron ratio of the graphite-like BC_X materials prepared from BCl_3 and benzene increases with

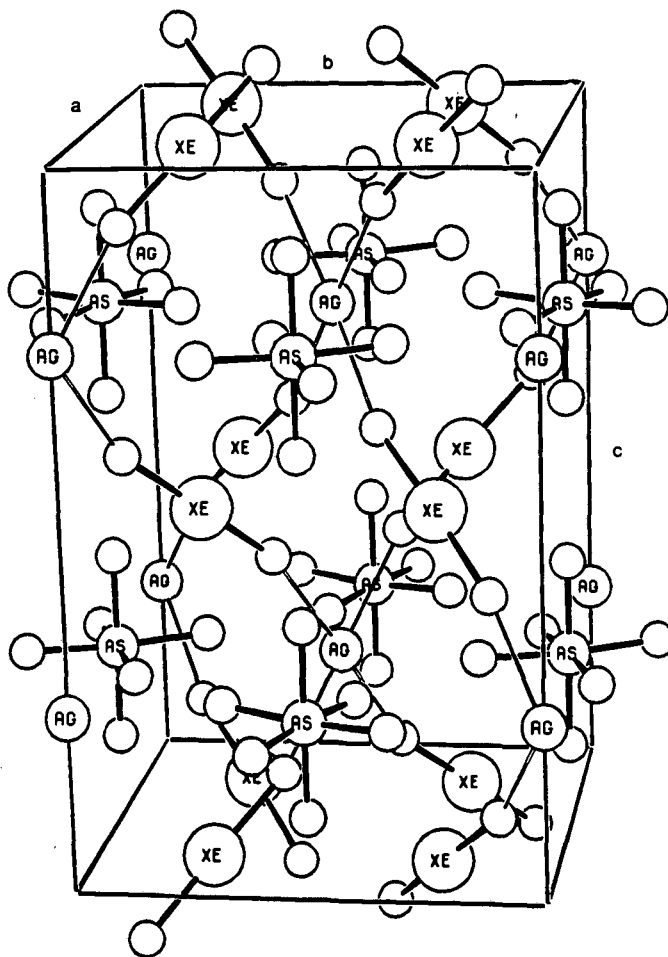


Figure 2-1. The unit cell of $[\text{Ag}(\text{XeF}_2)_2]\text{AsF}_6$. (XBL 917-1665)

increase in deposition temperature, from 3.1:1 at 800°C to 5.6:1 at 1000°C. Electron-energy-loss spectroscopy (EELS) shows graphite-like character with π^* features in the K-edge regions for both boron and carbon. The density (by flotation) is in the range 2.08–2.24 g cm⁻³, and the in-plane conductivity lies between 5×10^2 and 1×10^3 S cm⁻¹. X-ray photoelectron spectroscopy and Rutherford backscattering each reveal oxygen, chlorine, and silicon impurities in the BC_X deposits, these impurities being concentrated mainly in the surface layers exposed to the pyrolyzed gases. Chlorination of BC_X at ~300°C eliminates B (as BCl_3) completely, some volatile chlorinated carbons (including C_6Cl_6) also being formed. The resultant carbon does not reveal graphitic features in x-ray or electron diffraction or in the EELS spectra. Potassium metal intercalates BC_X to yield a black first-stage compound with an interlayer spacing of 5.3 to 5.4 Å. A deep blue first-stage compound formed with SO_3F radical has an interlayer spacing of 8.1 Å, akin to that in $(\text{BN})_3\text{SO}_3\text{F}$.

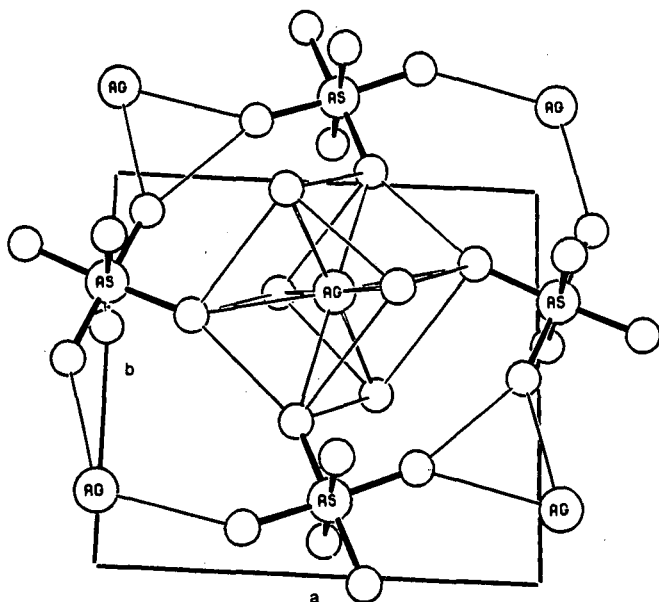


Figure 2-2. Ligand arrangement about the Ag(I) in $[Ag(XeF_2)_2]AsF_6$. (XBL 917-1666)

4. Work in Progress

X-ray synchrotron and time-of-flight neutron-diffraction data have established a novel structure type for the binary fluoride RuF_4 . In this structure the Ru atom is coordinated to six F ligands on an octahedral framework; four of the F are coplanar with the Ru, and each is symmetrically shared with another Ru, with $Ru-F-Ru = 133.0(6)^\circ$, to produce a puckered sheet structure. The unshared F ligands (trans to one another) have $Ru-F = 1.82(1) \text{ \AA}$, and the bridging interatomic distance is $2.00(3) \text{ \AA}$. These distances are very similar to those reported for the nonbridging and bridging distances in $(RuF_5)_4$ and for the bridging distance in RuF_3 . Higher precision is needed in the $(RuF_5)_4$ structure to prove this similarity. It is anticipated that distances of a given type will be similar throughout the binary fluoride set of RuF_6 , $(RuF_5)_4$, $(RuF_4)_n$, and $(RuF_3)_n$. Fragmentary evidence for the other transition elements, from group V through group VIII in the second and third transition series, indicates that this lack of dependence of the M-F distance upon the oxidation state is general.

Refereed Journals

1. B. Zemva, R. Hagiwara, W.J. Casteel, Jr., K. Lutar, A. Jesih, and N. Bartlett, "Spontaneous Oxidation of Xenon to Xe(II) by Cationic Ag(II) in Anhydrous Hydrogen Fluoride Solutions," *J. Am. Chem. Soc.* **112**, 4846 (1990); LBL-28299.
2. N. Bartlett, F. Okino, T.E. Mallouk, R. Hagiwara, M. Lerner, G.L. Rosenthal, and K. Kourtakis, "Oxidative Intercalation of Graphite by Fluoroanionic Species, Evidence for Thermodynamic Barrier," *Adv. Chem. Series* **226**, 391 (1990); LBL-28564.
3. J. Kouvetakis, T. Sasaki, C. Shen, R. Hagiwara, M. Lerner, K.M. Krishnan, and Neil Bartlett, "Novel Aspects of Graphite Intercalation by Fluorine and Fluorides and New B/C, C/N and B/C/N Materials Based on the Graphite Network," *Syn. Met.* **34**, 1 (1989); LBL-27565.

LBL Reports

4. R. Hagiwara, F. Hollander, C. Maines, and N. Bartlett, "The Crystal Structure of $[Ag(XeF_2)_2]AsF_6$ Formed in the Oxidation of Xe by $AgFAsF_6$," *European J. Solid State Inorg. Chem.* (in press); LBL-29869.
5. B.C. Shen, O.K. Tse, J. Kouvetakis, K.M. Krishnan, K.-M. Yu, and N. Bartlett, "Synthesis and Characterization of Graphite-Like Boron-Carbon Materials," LBL-30301.
6. B.C. Shen, C. Yom, and N. Bartlett, "A Simplified Synthesis of Lithium-Graphite Intercalation Compounds and Effect of Temperature on Staging," LBL-30302.
7. B. Zemva, K. Lutar, A. Jesih, W.J. Casteel, Jr., A.P. Wilkinson, D.E. Cox, R.B. Von Dreele, H. Borrmann, and N. Bartlett, "Silver Trifluoride: Preparation, Crystal Structure, Some Properties and Comparison with AuF_3 ," *J. Am. Chem. Soc.* (in press); LBL-28565.

Invited Talks

8. N. Bartlett, "Synthesis of Binary Transition Metal Fluorides," Conference on Synthetic Fluorine Chemistry, University of Southern California, Los Angeles, Feb. 15, 1990.
9. N. Bartlett, "Some Chemistry of Ag(III) and Cationic Ag(II)," University of Durham, England, May 31, 1990.
10. N. Bartlett, "Noble-Gas Chemistry," University of Nantes, France, June 5, 1990.

Catalytic Hydrogenation of CO*

Alexis T. Bell, Investigator

INTRODUCTION

The purpose of this project is to develop an understanding of the fundamental processes involved in the catalytic conversion of carbon monoxide and hydrogen to gaseous and liquid fuels. Attention is focused on defining the factors that limit catalyst activity, selectivity, and resistance to poisoning, and the relationship between catalyst composition/structure and performance. To meet these objectives, a variety of surface diagnostic techniques are used to characterize supported and unsupported catalysts before, during, and after reaction. The information is combined with detailed studies of reaction kinetics to elucidate reaction mechanisms and the influence of modifications in catalyst composition and/or structure on the elementary reactions involved in carbon monoxide hydrogenation.

1. An Isotopic Tracer Study of the Deactivation of Ru/TiO₂ Catalysts during Fischer-Tropsch Synthesis (Publication 9)

K.R. Krishna and A.T. Bell

An investigation of the causes of catalyst deactivation during Fischer-Tropsch synthesis over Ru/TiO₂ catalysts has been carried out. The effects of Ru dispersion, TiO₂ phase, and TiO₂ surface area on catalyst activity and selectivity were examined. CO chemisorption capacity and carbon species accumulation were determined as a function of reaction time using isotopic tracer techniques in conjunction with temperature-programmed surface reaction (TPSR). The results of this investigation show that all of the catalysts undergo deactivation with time, with no change in product selectivity. Initially, deactivation is very rapid followed by a slower activity loss. The long-term rate of deactivation is proportional to the initial CO turnover frequency, obtained by extrapolation of the long-term activity data. Deactivation is accompanied by a progressive loss in CO chemisorption capacity, as well as by an accumulation of various types of carbon species. The activity and the CO chemisorption capacity can be restored

to their initial values by reduction in H₂ or D₂. Differences in the initial activity (measured at 1 min after startup of reaction) of Ru supported on anatase and Degussa P-25 titania (70% anatase, 30% rutile) can be ascribed to differences in Ru dispersion; Ru supported on rutile exhibits a lower initial activity than the anatase-supported catalyst with the same dispersion. TiO₂-supported Ru has a higher activity than SiO₂- or Al₂O₃-supported Ru, and the formation of Ti³⁺ sites at the adlineation of Ru and titania is proposed to be the cause for this. Carbide carbon (C_α) and alkyl carbon chains (C_β) were observed to accumulate as reaction proceeds. C_β consists of two species: C_β[′], which is the precursor to C₂₊ hydrocarbons, and C_β[″], which consists of longer alkyl chains and does not participate in the production of gas-phase products. The inventory of the reactive C_α and C_β[′] passes through a maximum in the first 10 min of reaction, while the longer-chain C_β[″] grows monotonically. Both types of carbon result in a loss in CO chemisorption capacity. The rapid initial loss in activity in the first ten minutes correlates with the C_α + C_β[′] accumulation; the long-term loss in CO uptake and catalyst activity are probably due to C_β[″]. The alkyl chains comprising C_β[″] do not undergo hydrogenolysis under reaction conditions, probably due to inaccessibility to hydrogen.

2. A Review of Theoretical Models of Adsorption, Diffusion, Desorption, and Reaction Gases on Metal Surfaces (Publication 10)

S.J. Lombardo and A.T. Bell

A review is presented of the theoretical approaches available for describing the kinetics of gas adsorption, diffusion, desorption, and reaction on metal surfaces. The prediction of rate and diffusion coefficients based on molecular dynamics, transition-state theory, stochastic diffusion theory, and quantum mechanics is discussed, and the success of these theoretical approaches in representing experimental observation is examined. Consideration is also given to the effects of lateral interactions between adsorbates and to the ability of lattice-gas models to provide a representation of the dependences of rate and diffusion coefficients on adsorbate coverage. Finally, the utility of continuum and Monte Carlo models for describing the kinetics of complex surface processes in terms of elementary processes is addressed.

*This work was supported by the Director, Office of Energy Research, Office of Basic Energy Sciences, Chemical Sciences Division, of the U.S. Department of Energy under Contract No. DE-AC03-76SF00098.

3. Monte Carlo Simulations of The Effects of Pressure on Isothermal and Temperature-Programmed Desorption Kinetics (Publication 11)

S.J. Lombardo and A.T. Bell

A Monte Carlo simulation technique is presented for describing the adsorption, surface diffusion, and desorption kinetics of molecules from metal surfaces. Lateral interactions between adsorbed molecules are taken into account using the bond-order-conservation-Morse-potential (BOC-MP) method. The rate of desorption observed in the presence of a gas-phase species is higher than that observed in a vacuum. The increase in the apparent rate coefficient for desorption with increasing pressure can be ascribed to the effects of repulsive lateral interactions on the activation energy for desorption. The simulated kinetics are in good agreement with the experimentally observed kinetics for the isothermal desorption of CO from polycrystalline Pd and for the temperature-programmed desorption of CO from Ni(100).

4. An Analysis of Fischer-Tropsch Synthesis by the BOC-MP Approach (Publication 12)

E. Shustorovich and A.T. Bell

The BOC-MP approach has been used to calculate the heats of chemisorption of adspecies and activation barriers for elementary reaction steps envisioned to occur during Fischer-Tropsch (F-T) synthesis over the periodic series Fe/W(110), Ni(111), Pt(111), and Cu(111). Dissociative adsorption of CO to form carbidic carbon is projected to occur spontaneously on Fe/W(110) and with a small activation barrier on Ni(111). The calculated barrier heights for this reaction on Pt(111) and Cu(111) are high enough to preclude appreciable dissociation of CO. Hydrogen-assisted dissociation of CO_s is found to have an even smaller activation barrier on Fe/W and Ni, but not on Pt or Cu. On all the metal surfaces, the energetically preferred path for initiation of alkyl chain growth is via insertion of a CH₂ group into the carbon-metal bond of a CH₃ group. The activation barrier for CO insertion into the metal-carbon bond of a CH₃ group is greater than that for CH₂ insertion. As a consequence, the acetyl group formed by CO insertion serves mainly as a precursor to oxygenated products. On Fe/W, Ni, and Pt, the activation barrier for termination of alkyl chain growth by β-elimination of hydrogen is found to be lower than that for α-addition of hydrogen; and, as a consequence, olefins are projected to be formed more readily than paraffins. By using as examples

Fe(100) and Fe(100)-c(2×2)C,O, it is shown that carburization of an Fe(100) surface reduces the heats of adsorption of C, O, and CO, resulting in nondissociative chemisorption of CO, similar to that on Pt(111). The BOC-MP model projections are consistent with the available experimental data and contain claims that can be tested experimentally in the future.

5. An Analysis of Methanol Synthesis from CO and CO₂ by the BOC-MP Approach (Publication 13)

E. Shustorovich and A.T. Bell

The mechanisms of methanol synthesis from CO and CO₂ on Cu(111) and Pd(111) have been analyzed using the BOC-MP approach. The analysis was based on calculations of the heats of chemisorption *Q* for all adsorbed species and the activation barriers ΔE^* for all elementary reactions believed to be involved in the synthesis of methanol from CO and CO₂. The relevant experimental values of *Q* and ΔE^* , although scarce, agree well with the BOC-MP estimates. The formyl and formate routes to methanol were compared. On Cu(111), the activation barrier for hydrogenation of CO_s to HCO_s is found to be much larger than that for the desorption of CO_s, which makes formyl formation noncompetitive. By contrast, on Pd(111) the two barriers are calculated to be practically equal, making it very likely that formyl groups are formed. In the presence of OH_s groups, formate formation via the reaction CO_s + OH_s → HCOO_s is found to have a low activation barrier, particularly on Cu(111), where the formate route to methanol is preferred. The rate-determining step in this case is projected to be the hydrogenolysis of formate groups to form formaldehyde and atomic oxygen. On Cu(111) the formate route also appears to be efficient for the hydrogenation of CO₂ to methanol, since the activation barrier for H_s + CO_{2,s} → HCOO_s is calculated to be smaller than that for desorption of CO_{2,s}. The reverse is true for Pd(111), which makes the formate route to methanol energetically unfavorable in this case. The mechanism of the WGS reaction has also been considered. It appears that the reaction does not proceed via the formate intermediate, and the rate-determining step for this reaction is projected to be the dissociation of water. On Cu(111), the reverse WGS reaction is found to be competitive with methanol formation. The BOC-MP projections are generally consistent with the observed features of hydrogenation of CO and CO₂ on Cu and Pd catalysts. Some apparent inconsistencies are pointed out and discussed.

1990 PUBLICATIONS AND REPORTS

Refereed Journals

1. L.G. Tejuca and A.T. Bell, "TPD and IR Spectroscopic Studies of CO, CO₂, and H₂ Adsorption on LaCrO₃," *Appl. Surf. Sci.* **37**, 353 (1989).
2. A.T. Bell and E. Shustorovich, "A Comment on the Analysis of CO Hydrogenation Using the BOC-MP Approach," *J. Catal.* **121**, 1 (1990); LBL-26697.
3. E. Shustorovich and A.T. Bell, "An Analysis of Formic Acid Decomposition on Metal Surfaces by the Bond-Order-Conservation-Morse-Potential Approach," *Surf. Sci.* **222**, 371 (1989); LBL-26531.
4. J.L.G. Fierro, L.G. Tejuca, and A.T. Bell, "Preparation and Characterization of LaMn_{1-x}Cu_xO_{3+λ} Perovskite Oxides," *J. Catal.* **124**, 41 (1990).
5. J.A. Brown Bourzutschky, N. Homs, and A.T. Bell, "Conversion of Synthesis Gas over LaMn_{1-x}Cu_xO_{3+λ} Perovskites and Related Copper Catalysts," *J. Catal.* **124**, 52 (1990); LBL-27784.
6. J.A. Brown Bourzutschky, N. Homs, and A.T. Bell, "Hydrogenation of CO₂ and CO₂/CO Mixtures over Copper-Containing Catalysts," *J. Catal.* **124**, 73 (1990); LBL-27785.
7. A.T. Bell, "The Impact of Catalyst Science on Catalyst Design and Development," *Chem. Eng. Sci.* **45**, (8), 2013 (1990); LBL-30007.
8. A.T. Bell and E. Shustorovich, "Analysis of the Thermochemistry of C₂ Hydrocarbons on Transition Metal Surfaces Using a Refined BOC-MP Approach," *Surf. Sci.* **235**, 343 (1990); LBL-28073.

LBL Reports

9. K. Krishna and A.T. Bell, "An Isotopic Tracer Study of the Deactivation of Ru/TiO₂ Catalysts during Fischer-Tropsch Synthesis," *J. Catal.* (in press); LBL-29427.
10. S.J. Lombardo and A.T. Bell, "A Review of Theoretical Models of Adsorption, Diffusion, Desorption, and Reaction of Gases on Metal Surfaces," *Surf. Sci. Repts.* (in press); LBL-29470.
11. S.J. Lombardo and A.T. Bell, "Monte Carlo Simulations of the Effect of Pressure on Isothermal and Temperature-Programmed Desorption Kinetics," *Surf. Sci.* (in press); LBL-29460.
12. E. Shustorovich and A.T. Bell, "An Analysis of Fischer-Tropsch Synthesis by the Bond-Order-Conservation-Morse-Potential-Approach," *Surf. Sci.* (in press); LBL-29418.
13. E. Shustorovich and A.T. Bell, "Analysis of Methanol Synthesis from CO and CO₂ on Cu and Pd Surfaces by the Bond-Order-Conservation-Morse-Potential-Approach," submitted to *Surf. Sci.*; LBL-29624.

Invited Talks

14. A.T. Bell, "Catalysis at Metal-Metal Oxide Boundaries," *Frontiers in Chemical Research Series*, Department of Chemistry, Texas A&M University, College Station, TX, August 1989.
15. A.T. Bell, "Synthesis and Characterization of Dispersed Metal Oxide Catalysts and Supports," *Frontiers in Chemical Research Series*, Department of Chemistry, Texas A&M University, College Station, TX, August 1989.
16. A.T. Bell, "Theoretical and Experimental Studies of CO Hydrogenation," *Advances in Catalytic Chemistry IV*, Snowbird, UT, October 1989.
17. A.T. Bell, "Synthesis and Characterization of Dispersed Metal Oxide," *Mobil Research and Development Corp.*, Princeton, NJ, November 1989.
18. A.T. Bell, "New Approaches for Describing the Energetics and Kinetics of Surface Reactions," *Department of Chemical Engineering, University of Colorado*, Boulder, CO, November 1989.
19. A.T. Bell, "Illustration of the Application of Theory to the Prediction of Rate Parameters in Catalysis," *Department of Chemical Engineering, Purdue University*, West Lafayette, IN, December 1989.
20. A.T. Bell, "Catalysis by Design: Will It Ever Be Possible?," *College of Engineering 75th Anniversary Symposium*, The University of Akron, Akron, OH, February 1990.
21. A.T. Bell, "The Contributions of Catalyst Science to Catalyst Design of Development," *Engineering Foundation Meeting on Chemical Reaction Engineering III*, Santa Barbara, CA, February 1990.
22. A.T. Bell, "Studies of CO Hydrogenation over Ru Catalysts Using Transient Response Techniques," *AIChE Meeting*, Orlando, FL, March 1990.
23. A.T. Bell, "Simulation of Rate and Transport Processes in Catalytic Systems," *Department of Chemical Engineering and Materials Science, University of Minnesota*, Minneapolis, MN, April 1990.
24. A.T. Bell, "Characterization and Catalytic Reactivity of Dispersed Transition Metal Oxides," *Florida Catalysis Conference*, Palm Coast, FL, April 1990.
25. A.T. Bell, "The Impact of Catalyst Science on Catalyst Design and Development," *11th International Symposium on Chemical Reaction Engineering*, Toronto, Canada, July 1990.
26. A.T. Bell, "Mechanistic Studies of Hydrocarbon and Alcohol Synthesis from CO and H₂," *II International Workshop on Heterogeneous Catalysis*, Ensenada, Mexico, October 1990.
27. A.T. Bell, "The Relationship between Reaction Mechanisms and Kinetics in Heterogeneous Catalysis," *Symposium on The Mechanism of Heterogeneous Catalysis*, Lawrence Berkeley Laboratory, Berkeley, CA, November 1990.
28. A.T. Bell and K.R. Krishna, "Isotopic Tracer Studies of CO Hydrogenation over Ru/TiO₂," *4th Japan-China-USA*

- Symposium on Heterogeneous Catalysis, Sapporo, Japan, July 1989.
29. K.R. Krishna and A.T. Bell, "A Study of the Courses of Deactivation of Ru/TiO₂ during Hydrocarbon Synthesis," AIChE Meeting, San Francisco, CA, November 1989.
30. K.R. Krishna and A.T. Bell, "An Isotopic Tracer Study of Deactivation of Ru/TiO₂ Catalysts during Fischer-Tropsch Synthesis," California Catalysis Society Meeting, Berkeley, CA, March 1990.

Transition Metal-Catalyzed Conversion of CO, NO, H₂, and Organic Molecules to Fuels and Petrochemicals*

Robert G. Bergman, Investigator

INTRODUCTION

The goal of this program is the development of new chemical reactions in which transition metals interact with organic materials, and the understanding of how these reactions work. A recent discovery on this project was the finding that certain metal complexes undergo oxidative addition into the carbon-hydrogen bonds of completely saturated hydrocarbons ($M + R-H \rightarrow R-M-H$). This finding was the first example of a long-sought "alkane C-H activation" reaction; research is now being directed at examining the scope, selectivity, and mechanism of the process, extending it to other X-H bonds, and developing ways to convert the activated metal complexes X-M-H into functionalized organic molecules. During the current year, progress was made on the activation of molecules containing the heteroatoms oxygen and nitrogen, such as epoxides, alcohols, and amines. Most significant, however, was the finding that the liquified noble gases krypton and xenon could be used as inert solvents for C-H activation reactions. This technique now permits reaction of iridium and rhodium with C-H bonds in organic solids and very low boiling liquids (e.g., methane). It has also provided the first measurement of the fast rates and low activation energies of the direct C-H oxidative addition of rhodium to alkane C-H bonds.

1. Time-Resolved IR Spectroscopy in Liquid Rare Gases: Direct Rate Measurement of an Intermolecular Alkane C-H Oxidative Addition Reaction (Publication 1)

B.H. Weiller, E.P. Wasserman, R.G. Bergman, C.B. Moore, and G.C. Pimentel

The rate of oxidative addition of cyclohexane to form $Cp^*Rh(CO)(C_6H_{11})(H)$ [$Cp^* = (\eta^5-C_5Me_5)$] has been examined in liquified noble-gas solvents over a wide range

of temperatures and cyclohexane concentrations using a novel combination of low-temperature and IR laser flash-kinetic techniques. Photolysis of $Cp^*Rh(CO)_2$ in liquid xenon produces a monocarbonyl species that is much less reactive than the one generated in liquid krypton. We propose complexation with the noble-gas solvent $Cp^*Rh(CO)(Q)$ ($Q = Kr, Xe$) to account for this behavior. In the presence of C_6H_{12} , $Cp^*Rh(CO)(Kr)$ decays exponentially to form $Cp^*Rh(CO)(C_6H_{11})(H)$ with an observed rate constant that increases monotonically with increasing cyclohexane concentration and approaches an asymptotic value. When C_6D_{12} is used in place of C_6H_{12} , a significant isotope effect on the asymptotic rate constant is observed (see Figure 1-1). A mechanism that accounts for these data consists of a rapid exchange equilibrium between the krypton complex $Cp^*Rh(CO)(Kr)$ and an alkane complex $Cp^*Rh(CO)(C_6H_{12})$, characterized by an equilibrium constant K_1 , followed by unimolecular insertion with rate constant k_2 to form the alkyl hydride product. From the temperature dependence of the observed rate constants, activation parameters for the insertion reaction k_2 [$E_2 = 4.8 \pm 0.2$ kcal/mol, $\log(A_2) = 11.2 \pm 0.2$] are derived.

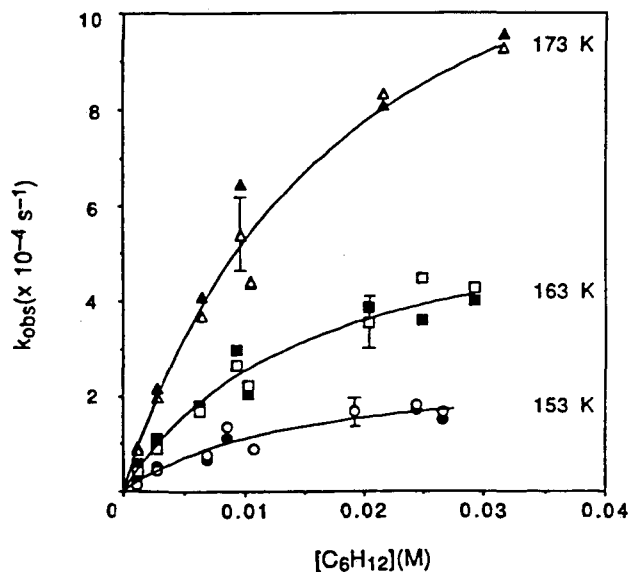


Figure 1-1. The observed rate constants (k_{obs}) for the decay of the transient at 1947 cm^{-1} (filled symbols) and for the formation of the product at 2003 cm^{-1} (open symbols) as a function of cyclohexane concentration and temperature. For clarity, only representative error bars are indicated explicitly. (XBL 917-1680)

*This work was supported by the Director, Office of Energy Research, Office of Basic Energy Sciences, Chemical Sciences Division, of the U.S. Department of Energy under Contract No. DE-AC03-76SF00098.

2. Mechanism of the C-C Cleavage of Acetone by the Ruthenium Benzyne Complex $(\text{PMe}_3)_4\text{Ru}(\eta^2\text{-C}_6\text{H}_4)$: Formation and Reactivity of an Oxametallacyclobutane Complex (Publication 2)

J.F. Hartwig, R.G. Bergman, and R.A. Andersen

The oxametallacyclobutane complex $(\text{PMe}_3)_4\text{Ru}[\eta^2\text{-CH}_2\text{C}(\text{Me})(\text{Ph})\text{O}]$ (complex 3 in Figure 2-1) was generated by an unusual β -migration of the Ru-bound phenyl group in the phenyl enolate complex $(\text{PMe}_3)_4\text{Ru}(\text{Ph})[\text{OC}(\text{CH}_2)\text{Me}]$. Mild thermolysis of 3 yielded methane and the orthometallated enolate complex 2 resulting from what appears to be a β -methyl migration reaction. These same products were previously observed in the reaction of acetone with the ruthenium benzyne complex $(\text{PMe}_3)_4\text{Ru}(\eta^2\text{-C}_6\text{H}_4)$, providing evidence that 3 is an intermediate in this C-C bond cleavage reaction. Reactivity studies on oxametallacyclobutane complex 3 led to the other unusual transformations shown in Figure 2-1, several of which cleave the C-O bond of the metallacycle to extrude α -methylstyrene.

3. Synthesis of $(\text{PMe}_3)_4\text{Ru}(\text{Me})[\text{OC}(\text{CH}_2)\text{Me}]$ as an Equilibrium Mixture of O- and C-Bound Transition-Metal Enolates and the Thermal Elimination of Methane to Form an η^4 -Oxatrimethylenemethane Complex (Publication 3)

J.F. Hartwig, R.A. Andersen, and R.G. Bergman

The ruthenium enolate $(\text{PMe}_3)_4\text{Ru}(\text{Me})[\text{OC}(\text{CH}_2)\text{Me}]$ (2) was synthesized by addition of the potassium enolate of acetone to $(\text{PMe}_3)_4\text{Ru}(\text{Me})(\text{Cl})$ (1). The complex was isolated as an equilibrium mixture of the O- and C-bound forms, as shown by measuring the ratio of isomers by ^1H NMR spectroscopy in the temperature range 5°C to 60°C . Thermolysis of the mixture of these two isomers at 65°C led to extrusion of methane and formation of metallacyclobutan-3-one $(\text{PMe}_3)_4\text{Ru}[(\text{CH}_2)_2\text{C}(\text{O})]$ (complex 3 in Figure 3-1). X-ray structural analysis of 3 shows that it has a buckled four-membered ring with a large dihedral angle $[45.6(5)^\circ]$. As shown by variable-temperature NMR spectroscopy (Figure 3-1), compound 3 undergoes reversible phosphine dissociation to form the

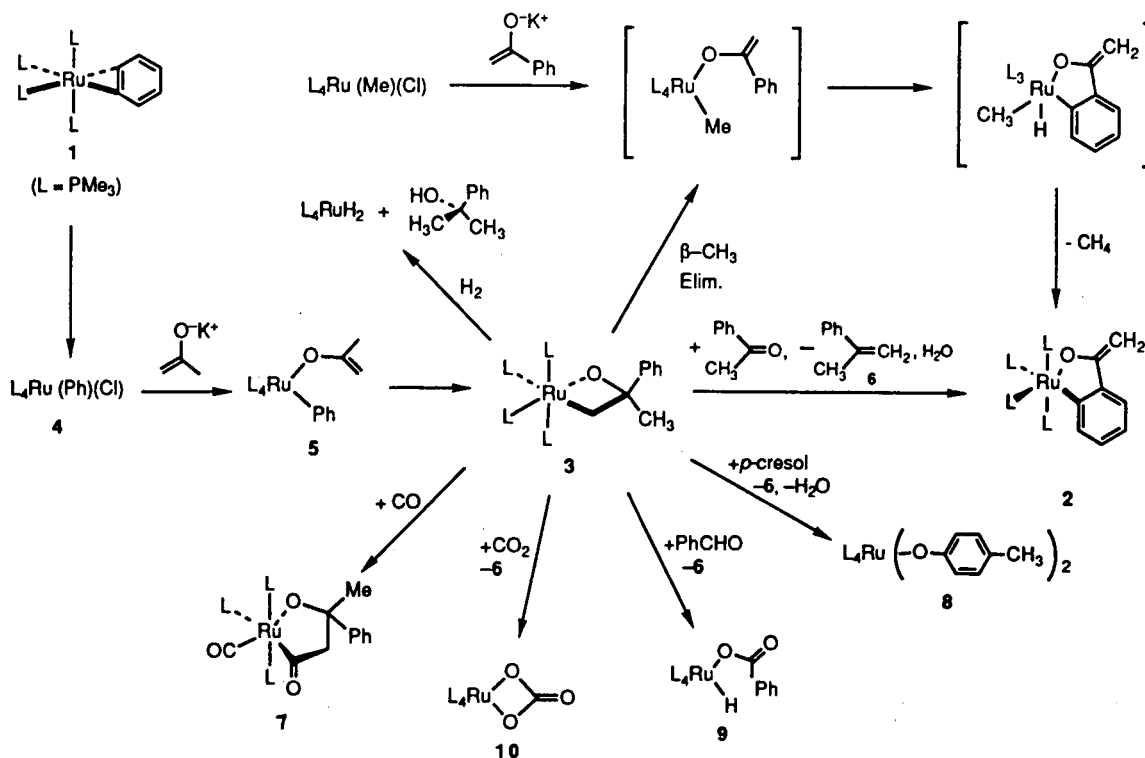


Figure 2-1. Synthesis and reactions of the tetrakis(trimethylphosphine)ruthenium oxametallacyclobutane complex 3. (XBL 917-1681)

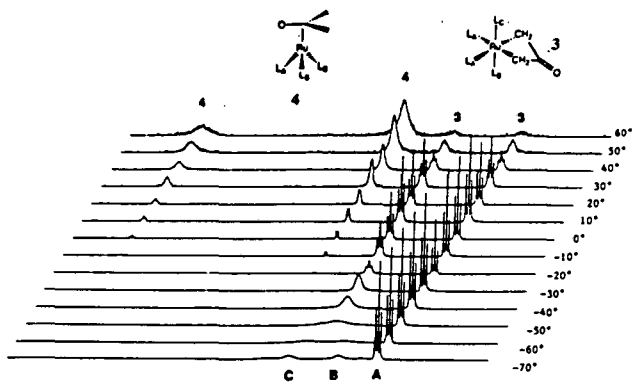


Figure 3-1. Variable-temperature $^{31}\text{P}\{^1\text{H}\}$ NMR spectra showing the interconversion of ruthenium metallacyclobutanone **3** and η^4 -oxatrimethylenemethane complex **4**. (XBL 917-1682)

oxatrimethyl-enemethane complex $(\text{PMe}_3)_3\text{Ru}[(\text{CH}_2)\text{C}(\text{O})]$ (**4**), which was isolated by removal of the labile phosphine under vacuum. X-ray structural analysis of **4** demonstrates that the oxatrimethylenemethane ligand is coordinated in a η^4 -fashion.

4. A Phosphorus-Carbon Bond-Cleavage Reaction of Coordinated Trimethylphosphine in $(\text{PMe}_3)_4\text{Ru}(\text{OC}_6\text{H}_4\text{Me})_2$ (Publication 4)

J.F. Hartwig, R.G. Bergman, and R.A. Andersen

A product resulting from cleavage of the P-C bond in a trimethylphosphine ligand forms upon thermolysis of $(\text{PMe}_3)_4\text{Ru}(\text{OC}_6\text{H}_4\text{Me})_2$ (**1**) or addition of p-cresol to the orthometallated complex $(\text{PMe}_3)_4\text{Ru}(\eta^2\text{-OC}_6\text{H}_3\text{Me})$ (**2**). The trimethylphosphine ligand has been transformed to a dimethylarylphosphinite ligand in the product $(\text{PMe}_3)_3(\eta^2\text{-PMe}_2\text{OC}_6\text{H}_3)\text{Ru}(\text{OC}_6\text{H}_4\text{Me})$ (**3**), the structure of which was determined by x-ray diffraction (Figure 4-1). Although complex **1** exists in equilibrium with complex **2** and free p-cresol at 65°C, kinetic evidence is presented indicating that complex **1** undergoes the P-C cleavage reaction.

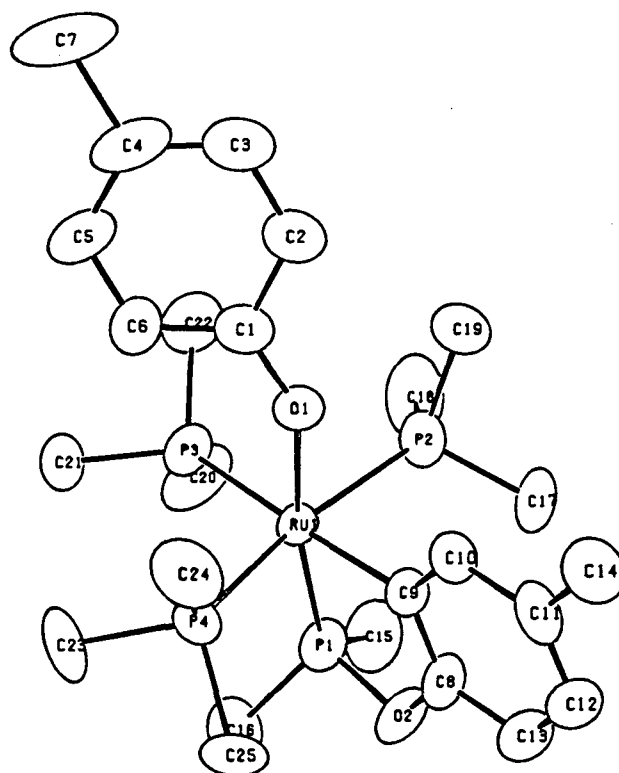


Figure 4-1. ORTEP diagram illustrating the x-ray crystallographically determined structure of phosphorus-carbon bond cleavage product **3**. (XBL 917-1683)

5. Work in Progress

Research is in progress in the following areas: (1) further exploration of the C-H, O-H, and N-H activation chemistry of tetrakis(trimethylphosphine)ruthenium complexes; (2) expansion of the use of liquified noble gases in preparative C-H activation chemistry; (2) infrared and uv-visible flash kinetic studies of the rapid steps involved in C-H oxidative addition reactions in liquified noble-gas solvents; (4) exploration of processes potentially leading to C-F activation reactions; and (5) development of reactions that can potentially convert the products of C-H oxidative addition reactions into functionalized organic molecules.

1990 PUBLICATIONS AND REPORTS

Refereed Journals

1. B.H. Weiller, E.P. Wasserman, R.G. Bergman, C.B. Moore, and G.C. Pimentel, "Time-resolved IR Spectroscopy in Liquid Rare Gases: Direct Rate Measurement of an Intermolecular Alkane C-H Oxidative Addition Reaction," *J. Am. Chem. Soc.* **111**, 8288 (1989); LBL-28049.
2. J.F. Hartwig, R.G. Bergman, and R.A. Andersen, "Mechanism of the C-C Cleavage of Acetone by the Ruthenium Benzyne Complex $(\text{PMe}_3)_4\text{Ru}(\eta^2\text{-C}_6\text{H}_4)$: Formation and Reactivity of an Oxametallacyclobutane Complex," *J. Am. Chem. Soc.* **112**, 3234 (1990); LBL-28287.
3. J.F. Hartwig, R.A. Andersen, and R.G. Bergman, "Synthesis of $(\text{PMe}_3)_4\text{Ru}(\text{Me})(\text{OC}(\text{CH}_2)\text{Me})$ as an Equilibrium Mixture of O- and C-Bound Transition Metal Enolates and the Thermal Elimination of Methane to Form an η^4 -Oxatrimethylene-methane Complex," *J. Am. Chem. Soc.* **112**, 5670 (1990); LBL-29325.
4. J.F. Hartwig, R.G. Bergman, and R.A. Andersen, "A Phosphorus-Carbon Bond Cleavage Reaction of Coordinated Trimethylphosphine in $(\text{PMe}_3)_4\text{Ru}(\text{OC}_6\text{H}_4\text{Me})_2$," *J. Organomet. Chem.* **394**, 417 (1990); LBL-29634.
5. R.G. Bergman, "A Physical Organic Road to Organometallic C-H Oxidative Addition Reactions," *J. Organomet. Chem.* **400**, 273 (1990); LBL-29326.

LBL Reports

6. J.F. Hartwig, R.A. Andersen, and R.G. Bergman, "Inter- and Intramolecular C-H Bond Forming Cleavage Reactivity of Two Different Types of Poly(trimethylphosphine) ruthenium Intermediates," submitted to *J. Am. Chem. Soc.*; LBL-29635.
7. J.F. Hartwig, R.G. Bergman, and R.A. Andersen, "The Structure, Synthesis and Chemistry of $(\text{PMe}_3)_4\text{Ru}(\eta^2\text{-Benzyne})$. Reactions with Arenes, Alkenes, and Heteroatom-containing Organic Compounds. Synthesis and Structure of a Monomeric Hydroxide Complex," submitted to *J. Am. Chem. Soc.*; LBL-29636.
8. J.F. Hartwig, R.A. Andersen, and R.G. Bergman, "Alkyl, Aryl, Hydrido, and Acetate Complexes of $(\text{DMPM})_2\text{Ru}$ [$\text{DMPM}=\text{bis}(\text{dimethylphosphino})\text{methane}$]: Reductive Elimination and Oxidative Addition of C-H Bonds," submitted to *Organometallics*; LBL-29637.
9. J.F. Hartwig, R.G. Bergman, and R.A. Andersen, "Insertion Reactions of CO and CO₂ with Ruthenium Benzyne, Arylamido, and Aryloxy Complexes: A Comparison of the Reactivity of Ruthenium-Carbon, Ruthenium-Nitrogen, and Ruthenium-Oxygen Bonds," submitted to *J. Am. Chem. Soc.*; LBL-30320.
10. J.F. Hartwig, R.G. Bergman, and R.A. Andersen,

"Oxygen- and Carbon-bound Ruthenium Enolates: Migratory Insertion, Reductive Elimination, β -Hydrogen Elimination, and Cyclometallation Reactions," submitted to *J. Am. Chem. Soc.*; LBL-30321

Invited Talks

11. R.G. Bergman, "Activation of C-H Bonds in Alkanes and Other Molecules Using Organotransition Metal Complexes," New Science in Homogeneous Transition Metal Catalyzed Reactions Symposium, American Chemical Society Meeting, Boston, MA, April 25, 1990.
12. R.G. Bergman, "Exploratory and Mechanistic Investigations of Metal-Mediated Transformations of Organic Compounds," International Chemical Congress of Pacific Basin Societies, Honolulu, HI, December 17-22, 1989.
13. R.G. Bergman, "Irreproducibility in the Scientific Literature: When do Scientists Tell the Whole Truth and Nothing but the Truth?" Department of Chemistry and Biochemistry, California State University, Los Angeles, November 14, 1989.
14. R.G. Bergman, "Models for Metal Mediated Oxidation Reactions: The Chemistry of Complexes with Metal-Heteroatom Bonds," Department of Chemistry, University of Washington, November 7-8, 1989; Department of Chemistry and Biochemistry, California State University, Los Angeles, November 14, 1989; Department of Chemistry, University of San Diego, December 4, 1989; Technische Universität Berlin, Berlin, Germany, July 6, 1990.
15. R.G. Bergman, "The Role of Alkane Complexes in C-H Activation Reactions," Department of Chemistry, Columbia University, New York, NY, March 30, 1990; Technische Universität Berlin, Berlin, Germany, July 2, 1990.
16. R.G. Bergman, "Transformation of Organic Compounds Using Organotransition Metal Complexes," Charles A. Stiefvater Memorial Lecture, University of Nebraska, October 26, 1989; Edgar Fahs Smith Memorial Symposium, Philadelphia Section, American Chemical Society, March 29, 1990; Graduate Colloquium Seminar, Northern Illinois University, DeKalb, April 17, 1990; Krug Lecture, University of Illinois, April 19, 1990; Remsen Lecture, Maryland Section, American Chemical Society, Baltimore, May 16, 1990; The Royal Society of Chemistry, Dalton Division, Fourth International Conference of the Platinum Group Metals, Cambridge, England, July 9-13, 1990; John K. Stille Memorial Symposium, Washington, D.C., August 29, 1990.
17. R.G. Bergman, "Using Kryptochemistry to Deal with Xenophobia: C-H Activation in Liquefied Noble Gas Solvents," Lind Lecture, East Tennessee Section, American Chemical Society, October 24-25, 1989; Union Carbide, South Charleston, WV, March 28, 1990.
18. R.G. Bergman, "C-H Activation," Stanford University, Stanford, CA, May 8, 1990.

Formation of Oxyacids of Sulfur from SO₂*

Robert E. Connick, Investigator

INTRODUCTION

The stimulus for this research is the existence of acid rain. Coal-burning power plants produce sulfur dioxide, which is oxidized in air to form sulfuric acid, the principal component of acid rain. In most commercial flue-gas desulfurization processes, the sulfur dioxide is absorbed in an aqueous solution of low acidity, where it may be oxidized by O₂. Control of the rate of this latter reaction is of major importance to these processes. While recent research of the project has been concentrated on this reaction, investigation of the fundamental chemistry of species formed from sulfur dioxide and reactions of these species remains the primary goal. The oxidation-reduction chemistry of sulfur should be studied, particularly reactions between two oxidation states of the element, e.g., reactions involving HSO₃⁻, H₂S, S₈, and the polythionates. A secondary and not closely related goal is to determine the factors controlling the rate of substitution reactions in the first coordination sphere of metal ions in solution. Computer modeling has been extended to three dimensions, and configurations of activated complexes have been determined. The usual concept of a transition state with reflection coefficient near unity is quite inadequate.

1. Work in Progress

Rate Law and Mechanism of the Oxidation of Bisulfite Ion by Oxygen

The rate law for the reaction of HSO₃⁻ with HSO₅⁻ has been determined to be of the form $k_1 [\text{HSO}_3^-][\text{HSO}_5^-][\text{H}^+] + k_2 [\text{HSO}_3^-][\text{HSO}_5^-][\text{H}^+]^{-1}$ in the pH range 3.5 to 7.8. Since S₂O₇²⁻ is formed in the reaction, just as in the HSO₃⁻-O₂ reaction, the species HSO₅⁻ is presumed to be an intermediate in the latter reaction. The yield of S₂O₇²⁻ as a function of pH was measured for comparison with the yield in the O₂ reaction. They are not the same, but related. The HSO₃⁻-HSO₅⁻ reaction gives ~90% S₂O₇²⁻ from pH 3.5 to ~6, after which the yield falls off according to an [H⁺]⁻¹ dependence at higher pH. The yield in the HSO₃⁻-O₂ reaction is ~50% from pH 3.5 to ~5.2, at which region the yield breaks over rather abruptly to an [H⁺]⁻¹ dependence. The break occurs just where the second term of the HSO₃⁻-HSO₅⁻ rate law becomes appreciable, and the abruptness of the change is in agreement with a second power change in the dependence on hydrogen-ion concentration between the two paths in the HSO₃⁻-HSO₅⁻ rate law. Yet the S₂O₇²⁻ yield of the HSO₃⁻-HSO₅⁻ reaction does not break over to an [H⁺]⁻¹ dependence until a higher pH is reached, and the breakover is not nearly as abrupt. To understand these discrepancies, experiments are under way to determine the effect of catalysts and inhibitors on the yield of S₂O₇²⁻ on the HSO₃⁻-O₂ reaction. While peroxymonosulfuric acid [HSO₅⁻] is clearly implicated as an intermediate in the HSO₃⁻-O₂ reaction, not all of the material appears to pass through this species, and the resulting yield of S₂O₇²⁻ is complex.

*This work was supported by the Director, Office of Energy Research, Office of Basic Energy Sciences, Chemical Sciences Division, of the U.S. Department of Energy under Contract No. DE-AC03-76SF00098.

Potentially Catalytic and Conducting Polyorganometallics*

K. Peter C. Vollhardt, Investigator

INTRODUCTION

The task being carried out under this program is the synthesis and evaluation of new molecules designed to exhibit novel chemical behavior, particularly (1) the catalysis of organic transformations of synthetic and industrial importance and (2) potential conductivity. It centers on the development and execution of synthetic methodology aimed at allowing access to sequences of extended strong π -ligands to multiple transition metals. This work has as its target a variety of novel organic systems. A major effort has focused on the exploitation of a new, iterative strategy that allows the continued elaboration of linked cyclopentadienyl chains and their complexation with control of the resulting oligometallic sequence. In this way, a number of hitherto unknown transition-metal arrays have become available in which the metallic centers adopt "unnatural" linear and angular configurations. These structures give rise to unprecedented reactivity when exposed to small molecules, pointing toward applications in catalysis. They also provide ideal models with which to probe the elementary steps of multimetallic ligand and electron transfer. The discovery of exciting novel chemistry of these systems, including thermally and photochemically induced intramolecular transfer of organic fragments, has justified the original premise of this research. Recent efforts have concentrated on exploring the reactivity patterns of the structures under investigation and expanding the range of available ligand chains, in particular those based on highly unsaturated carbon agglomerates, including oligomers of carbon.

1. Tercyclopentadienyl Trimetals (Publication 1)

R. Boese,[†] R.L. Myrabo, D.A. Newman, and K.P.C. Vollhardt

Preliminary results of this work were outlined in previous reports. The present account constitutes a summary of the current state of the art of one of the cornerstones of this program.

While the synthesis and chemistry of homo- and heterobimetallic organometallic compounds, often bridged by ligands intended to anchor the metals in close proximity, is well-explored, much less is known about the acyclic higher metal homologues. Linked pairs of η^5 -cyclopentadienyl (Cp) moieties, as in fulvalene, have played a significant role in these developments because of their exceptional binding ability. We report a rational (and potentially generalizable) synthesis of the first "cyclopentadienologs" of fulvalene, namely the two isomers of tercyclopentadienyl, their sequence-specific metal complexation (see Figure 1-1), the structure determination of two of these trimetallic products (see Figures 1-2 and 1-3), and some preliminary ligand transfer chemistry. The intramolecular nature of the latter bodes well for catalytic applications of systems of this type.

A prerequisite for potentially synergistic chemical behavior toward organic substrates of these systems is intramolecular metal-to-metal ligand transfer. Attempts to uncover such rearrangements has led to some remarkable observations. Thus, treatment of the cyclopentadiene intermediates **4a** and **4b** in Figure 1-1 with basic D_2O [CD_3COCD_3 , Et_3N , $23^\circ C$, 2 h] resulted in regiospecific deuterium incorporation (95%) into the uncomplexed ring, a process uncomplicated by potential metal transfer along the chain. Surprisingly, complete label scrambling between the two terminal rings occurred on conversion of $[D_5]4b$ into $[D_4]7b$, whereas $[D_4]7a$ was formed from $[D_5]4a$ bearing deuterium only on the $\eta^5-(C_5D_4)W(CO)_3CH_3$ substituent to the fulvalene unit! A possible rationale for this divergent behavior is that the metal-anion precursor before methylation is responsible for the scrambling in $[D_4]7b$ by reversible nucleophilic displacement of the metal-bound tungsten at the other terminus.

In contrast, in the analogous intermediate on route to $[D_4]7a$, steric constraints prevent coplanarity (or a favorable angle) of attack of the cyclopentadienyl ring of the attached non-metal-bound anionic tungsten. In support of this mechanism, following the course of the reaction of $[D_5]4b$ with $[W(NCMe)_3(CO)_3]$ ($23^\circ C$, 2 h, 40% conversion) by 1H NMR spectroscopy revealed the generation of $\{\eta^5-(C_5D_4)W(D)(CO)_3[\eta^5:\eta^5-(C_5H_3-C_5H_4)]W_2(CO)_6\}$, $[D_5]-17b$, "exchange" of label taking place only with time ($23^\circ C$, 19 h), presumably by dedeuteration at tungsten, since scrambling was suppressed in the presence of added CH_3COOD . Conversely, metalation of $[D_4]4b^{\theta}$ at $23^\circ C$ led to instant label redistribution in the resulting anion between two outer Cp units. This process was sufficiently slow at $-78^\circ C$ to allow

*This work was supported by the Director, Office of Energy Research, Office of Basic Energy Sciences, Chemical Sciences Division, of the U.S. Department of Energy under Contract No. DE-AC03-76SF00098.

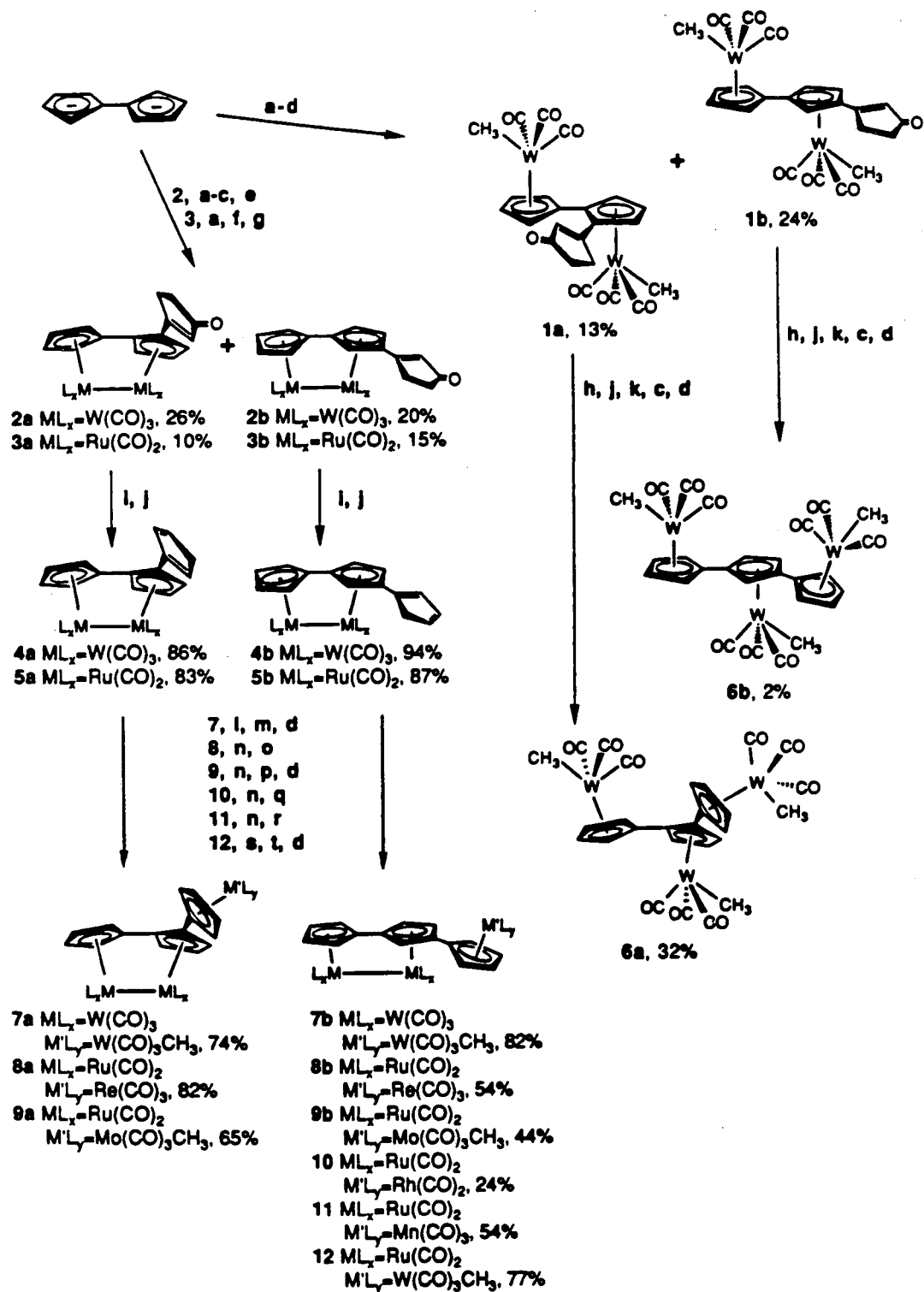


Figure 1-1. Synthesis of tercyclopentadienyl complexes. (a) 3-Chloro-2-cyclopentenone, THF, -78°C or -20°C , 5 min; (b) $\text{CH}_3\text{CH}_2\text{CH}_2\text{CH}_2\text{Li}$, -78°C to 23°C ; (c) $\text{W}(\text{NCCH}_3)_3(\text{CO})_3$ (xs) in DME, 23°C , 3 h; (d) CH_3I , 23°C , 30 min; (e) AgBF_4 (2.2 equiv), THF, -78°C to 23°C , 12 h; (f) $\text{CH}_3\text{CO}_2\text{H}$, -78°C ; (g) $\text{Ru}_3(\text{CO})_{12}$, DME, Δ , 18 h; (h) LiAlH_4 , Et_2O , 0°C to 23°C , 1 h; (i) $[(\text{CH}_3)_2\text{CHCH}_2]_2\text{AlH}$, CH_2Cl_2 , 0°C , 2 h; (j) cat. $4\text{-CH}_3\text{C}_6\text{H}_4\text{SO}_3\text{H}$, C_6H_6 , 60°C , 2 min; (k) $\text{KOC}(\text{CH}_3)_3$, CME, 23°C , 10 min; (l) $\text{W}(\text{NCCH}_3)_3(\text{CO})_3$, THF, 23°C , 12 h; (m) $\text{Li}[\text{Si}(\text{CH}_3)_3]_2$, THF, -78°C , 5 min; (n) NaNH_2 , THF, 23°C , 5 min; (o) $[\text{Re}(\text{CO})_3\text{Br}(\text{THF})]_2$, THF, 23°C , 1 h; (p) $\text{Mo}(\text{NCCH}_3)_3(\text{CO})_3$, THF, 23°C , 30 min; (q) $[\text{Rh}(\text{CO})_2\text{Cl}]_2$, THF, 23°C , 1 h; (r) $[\text{Mn}(\text{CO})_4\text{Br}]_2$, THF, 23°C , 30 min; (s) $\text{KOC}(\text{CH}_3)_3$, THF, 23°C , 5 min; (t) $\text{W}(\text{NCCH}_3)_3(\text{CO})_3$, THF, 23°C , 30 min. (XBL 917-1675)

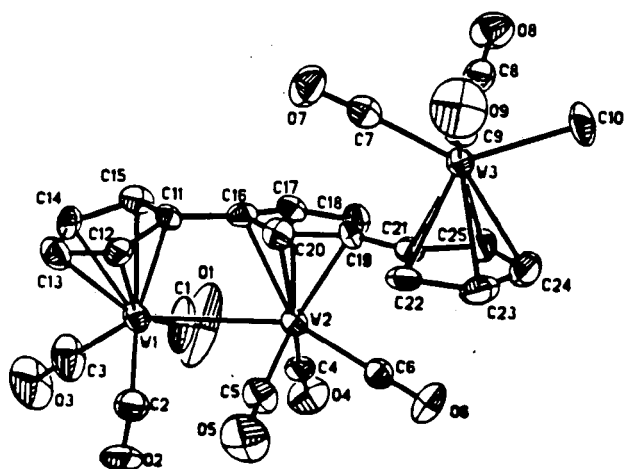


Figure 1-2. Molecular structure of 1,1':3',1''-tercyclopentadienyl compound **7b** (SHELXTL). Selected distances (Å) and angles (°): W1–W2, 3.266(1); W–CO (avg.) 1.96; W3–C10, 2.324(11); W1–Cp1 (ring centroid), 1.975; W2–Cp2, 1.994; W3–Cp3, 2.017; C23–C24, 1.375(18); C22–C23, 1.459(16); C11–C16, 1.453(13); C19–C21, 1.468(14); C21–C22–C23, 106.2(9); C22–C23–C24, 109.2(10); C12–C11–C16, 124.1(9); Cp2–Cp3, 9.6; C15–C11–C16–C20, 179.9(1.1); C12–C11–C16–C17, 153.7(1.0). (XBL 917-1676)

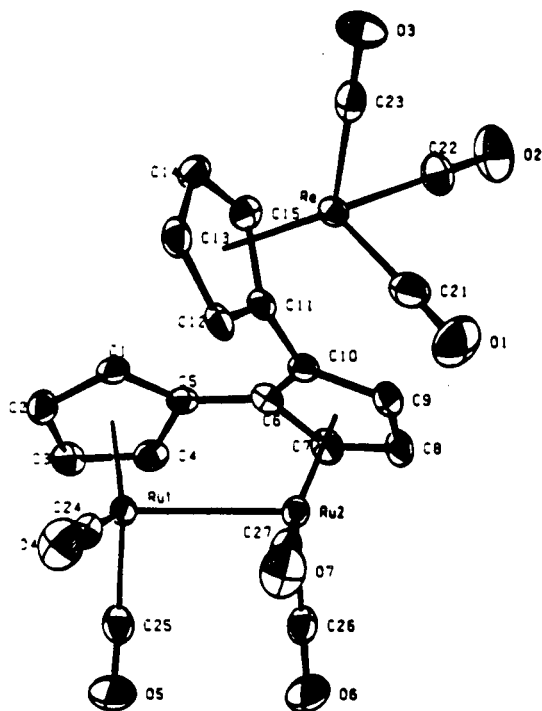


Figure 1-3. Molecular structure of the 1,1':2',1''-isomer **8a** (ORTEP). Selected distances (Å) and angles (°): Ru1–Ru2, 2.8190(4); Ru–CO (avg.), 1.86; Re–CO (avg.), 1.91; Ru1–Cp1, 1.8981(3); Ru2–Cp2, 1.8993(3); Re–Cp3, 1.9531(2); C14–C15, 1.397(6); C6–C10, 1.457(6); C5–C6, 1.436(6); C10–C11, 1.491(5); C1–C5–C4, 106.1(4); C8–C9–C10, 109.3(4); C4–C5–C6, 123.8(4); Cp2–Cp3, 104.7(2); C1–C5–C6–C7, 162.6(6); C4–C5–C6–C10, 154.1(6). (XBL 917-1677)

access to regiochemically deuterated $[D_4]7b$ by methylation, the stability of the latter ruling out methyl transfer as another pathway for exchange. This species is also stable in this regard on irradiation, significant, considering that chlorination of $[D_5]17a$ and $[D_5]17b$ (CCl_4 , THF, $23^\circ C$, 10 min) to tetradeuteriated $[\eta^5-(C_5H_4)W(CO)_3(Cl)][\eta^5:\eta^5-(C_5H_3-C_5H_4)]W_2(CO)_6$ provided results that completely paralleled those obtained in the generation of $[D_4]7a$ and $[D_4]7b$ with respect to the integrity of the position of the label.

Methyl migration could, however, be induced by reduction of the W–W bond in **7b** (1% Na–Hg, THF, $23^\circ C$, 1 h) to furnish $[\eta^5:\eta^5:\eta^5-(C_{15}H_{11})W_3(CO)_9CH_3]$ ²⁰ in the form of two isomers bearing the methyl group at both the terminal and internal positions in a ratio of 1:2.7, respectively, changing to 1:6 on prolonged standing. Treatment with CD_3I furnished $[D_6]6b$, the unlabeled methyl remaining mainly (2.2:0.9) bound to the central tungsten. Isomer **7a** behaved similarly, being converted into the corresponding dianions (1.5:1) and, ultimately, $[D_6]6a$ (1.2:1.8). The uniquely intramolecular nature of these processes could be established by cross-over experiments involving **7a** and **7b**, respectively, admixed with their $[(\eta^5-C_5D_4)W(CO)_3(CD_3)]$ -substituted counterparts. It appears that in reduced **7a** the terminal Cp-metal fragments are sufficiently mobile to allow for methyl transfer, although other details of this transformation have yet to be established.

†Permanent address: Institute of Inorganic Chemistry, University-GH Essen, D-4300 Essen 1, Germany.

2. Activated Molybdenum-Molybdenum Quadruple Bonds. Synthesis, Structure, and Properties of $[Mo_2(O_2CMe)_2(en)_4][[(O_2CMe)_2] \bullet en]$: A Solid-State Model for a Solvent-Shared Ion Pair (Publication 2)

B.W. Eichhorn,[†] M.C. Kerby,[‡] R.C. Haushalter,^{||} and K.P.C. Vollhardt

$Mo_2(O_2CMe)_4$ reacts with neat en at room temperature to form the $[Mo_2(O_2CMe)_2(en)_4][[(O_2CMe)_2] \bullet en]$ complex in high yield. Under mild thermal conditions ($\sim 120^\circ C$), this compound reverts back to $Mo_2(O_2CMe)_4$ in the solid state. The complex has an unusual solid-state structure incorporating two acetate counterions that are hydrogen bonded to the spanning en ligands (see Figure 2-1).

The extent of acetate displacement in solution is not clear; however, NMR studies suggest that solvent-for-acetate substitution is more extensive in D_2O than in en. This observation is consistent with the findings of Taube and Bowen nearly two decades ago. Their studies showed that stable, red solutions of aquated Mo_2^{4+} could be

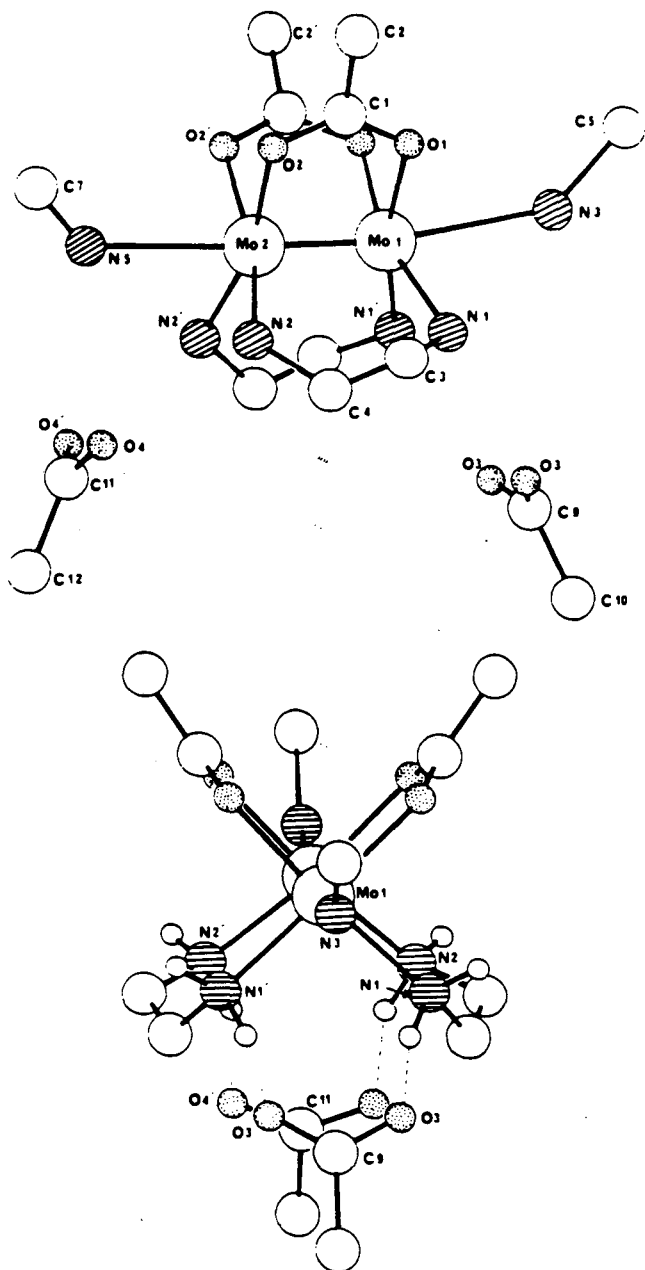


Figure 2-1. Two Chem-X views of the $[\text{Mo}_2(\text{O}_2\text{CMe})_2(\text{en})_4][\text{O}_2\text{CMe})_2]$ complex. For clarity, only the first nitrogen and carbon atoms of the axial en ligands are shown. Top: perspective perpendicular to the M-M vector showing the coordination environment. Bottom: a view down the M-M vector illustrating the N-H...O hydrogen bonds and the eclipsed M_2L_8 core. (XBL 917-1678)

produced from $\text{K}_4\text{Mo}_2\text{Cl}_8 \cdot 2\text{H}_2\text{O}$ in 0.1 M aqueous trifluoromethanesulfonic acid. Furthermore, they prepared a compound of composition $\text{Mo}_2(\text{en})_4\text{Cl}_4$ that forms stable, yellow-orange aqueous solutions that presumably contain $\text{Mo}_2(\text{en})_4^{4+}$ ions. Except for a few ligand exchange

reactions, the chemistry of these compounds remains unexplored.

It appears that the ability of the polar en solvent to displace the acetate ligands from the coordination sphere of the Mo_2 center in the title compound tends to activate the complex toward reactions with external small organic molecules such as terminal alkynes. The potential of these solvated Mo_2^{4+} ions for use as 8-e reductants in polar solvents is intriguing, and our preliminary studies show that the chemistry of these compounds is quite rich.

[†]Permanent address: Department of Chemistry and Biochemistry, University of Maryland, College Park, MD 20742.

[‡]Permanent address: Exxon Research and Development Laboratories, Baton Rouge, LA 70821.

[§]Permanent address: Exxon Research and Engineering Company, Clinton Township, Annandale, NJ 08801.

3. Oligomerization of Alkynes by the RhCl_3 -Aliquat 336 Catalyst System (Publications 3 and 4)

I. Amer,[†] T. Bernstein,[†] M. Eisen,[†] J. Blum,[†] and K.P.C. Vollhardt

The cyclo-oligomerization of several terminal and internal alkynes under phase-transfer conditions by the RhCl_3 -Aliquat 336 catalyst is described. The kinetics of 1-heptyne cyclotrimerization at 90°C in 1,1,2,2-tetrachloroethane/water were found to follow the second-order rate law $d[\text{arene}]/dt = -k[\text{alkyne}][\text{RhCl}_3]$ when the molar ratio of substrate:rhodium chloride:quat was approximately 25:1:1. The activation energy of $E_a = 12.5 \text{ kcal mol}^{-1}$ suggests that the catalysis is both chemically and diffusion controlled. Product analysis is compatible with a mechanism that involves rhodacyclopentadiene rather than metal cyclobutadiene intermediates.

The RhCl_3 -Aliquat 336 ion pair in 1,1,2,2-tetrachloroethane was shown to catalyze both cyclodimerization and trimerization of internal phenylalkynes in a highly regioselective manner. Thus, 1-phenyl-1-propyne, 1-phenyl-1-butyne, and 4-phenyl-3-butyne-2-one result in the corresponding 2,3-disubstituted 1-phenylnaphthalenes, in addition to the respective 3,5,6-trisubstituted 1,2,4-triphenylbenzenes as the only cyclotrimerization products. Diphenylacetylene yields 1,2,3-triphenylnaphthalene and hexaphenylbenzene. Formation of small amounts of 1-chloro-2,3-dimethyl-4-phenylnaphthalene and 1-(2-chlorophenyl)-2,3-dimethylnaphthalene, in the cyclo-oligomerization of 1-phenyl-1-propyne, supports a mechanism in which initial oxidative coupling of the alkyne functions produces a 2,5-diphenylrhodacyclopentadiene capable of subsequent

ortho-metallation of the phenyl substituents, followed by metal hydride transfer and reductive elimination of the resultant benzometallacycloheptatriene intermediate.

†Permanent address: Department of Chemistry, The Hebrew University, Jerusalem 91904, Israel.

4. Facile Hydrogenation of the Central Cyclohexatriene of Tris(benzocyclobutadieno)benzene: Synthesis, Structure, and Thermal and Photochemical Isomerization of all-*cis*-Tris(benzocyclobuta)cyclohexane (Publication 5)

D.L. Mohler, K.P.C. Vollhardt, and S. Wolff

We describe the first chemical reaction of hydrocarbon **1** (see Figure 4-1), namely its facile and stereoselective hydrogenation to **2**, whose x-ray structural analysis reveals the presence of an unusually bond-fixed, planar cyclohexane ring. The latter undergoes stereospecific thermal retrocyclization exclusively to the hexaene **3**, a feature that, in conjunction with the associated kinetic data, suggests the occurrence of an unprecedented all-disrotatory process. In contrast, irradiation of **2** effects the rearrangement of the new hydrocarbon **4** and, ultimately, phenanthrene and naphthalene, whereas **3** photoisomerizes

to **5** (See Figure 4-1). The reported chemistry expands significantly the range of the transformations recorded for the benzocyclobutene nucleus and the tribenzo-(CH)₁₂-manifold.

1990 PUBLICATIONS AND REPORTS

Refereed Journals

1. R. Boese, R.L. Myrabo, D.A. Newman, and K.P.C. Vollhardt, "On the Way to Ligating Oligocyclopentadienyls: Synthesis and Preliminary Reactions of the Two Isomeric Tercyclopentadienyls and their Transition Metal Complexes," *Angew. Chem.* **102**, 589 (1990); *Angew. Chem., Int. Ed. Engl.* **29**, 549 (1990); LBL-26646.
2. B.W. Eichhorn, M.C. Kerby, R.C. Haushalter, and K.P.C. Vollhardt, "Activated Molybdenum-Molybdenum Quadruple Bonds. Synthesis, Structure, and Properties of [Mo₂(O₂CMe)₂(en)₄][(O₂CMe)₂][•]en: A Solid-State Model for a Solvent-Shared Ion Pair," *Inorg. Chem.* **29**, 1319 (1990); LBL-26774.
3. I. Amer, T. Bernstein, M. Eisen, J. Blum, and K.P.C. Vollhardt, "Oligomerization of Alkynes by the RhCl₃-Aliquat 336 Catalyst System. Part 1. Formation of Benzene Derivatives," *J. Mol. Cat.* **60**, 313 (1990); LBL-28420.
4. I. Amer, J. Blum, and K.P.C. Vollhardt, "Oligomerization of Alkynes by the RhCl₃-Aliquat 336 Catalyst System. Part 2. Formation of 2,3-Disubstituted 1-Phenylnaphthalenes by Cyclodimerization of Phenylalkynes," *J. Mol. Cat.* **60**, 323 (1990); LBL-28424.
5. D.L. Mohler, K.P.C. Vollhardt, and S. Wolff, "Facile Hydrogenation of the Central Cyclohexatriene of Tris(benzocyclobutadieno)benzene: Synthesis, Structure, and Thermal and Photochemical Isomerization of all-*cis*-Tris(benzocyclobuta)cyclohexane," *Angew. Chem.* **102**, 1200 (1990); *Angew. Chem., Int. Ed. Engl.* **29**, 1151 (1990); LBL-30251.
6. A.P. Kahn, D.A. Newman, and K.P.C. Vollhardt, "Site-Specific Synthesis of Heterodinuclear Fulvalene Complexes," *Synlett*, 141 (1990); LBL-28425.
7. P.A. McGovern and K.P.C. Vollhardt, "The Synthesis and Novel Reactivity of Homo- and Heterodinuclear Fulvalene Metal Carbonyls," *Synlett*, 493 (1990); LBL-30252.
8. M.C. Kerby, B.W. Eichhorn, J.A. Creighton, and K.P.C. Vollhardt, "Models for Organometallic Polymers. Zigzag Chains of Mo₂(O₂CCH₃)₄ Units Linked by DMPE and TMED Ligands," *Inorg. Chem.* **29**, 1319 (1990); LBL-26775.
9. H. Schwager, S. Spyroudis, and K.P.C. Vollhardt, "Tandem Palladium-, Cobalt- and Nickel-catalyzed Syntheses of Polycyclic π -Systems Containing Cyclobutadiene, Benzene and Cyclooctatetraene Rings," *J. Organomet. Chem.* **382**, 191 (1990); LBL-28423.

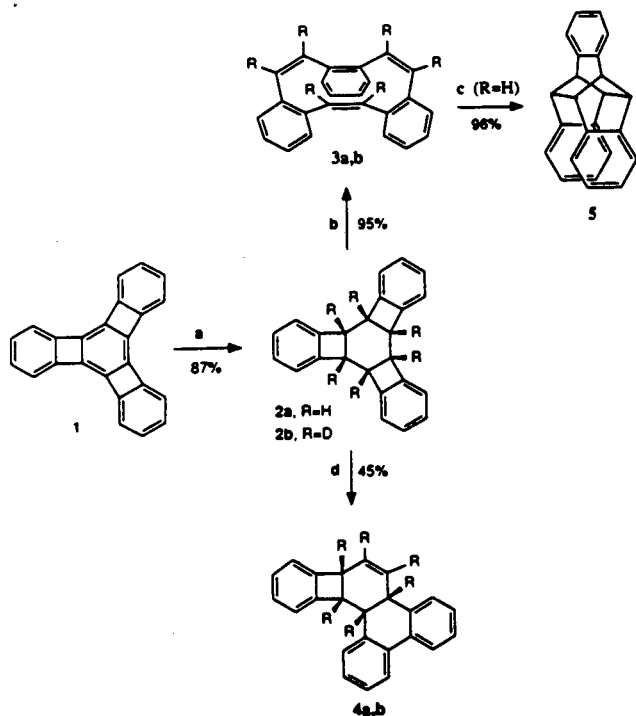


Figure 4-1. (a) H₂ or D₂ (1 atm), Pd-C, THF, 18 h; (b) C₆D₆, sealed tube, 125°C–160°C; (c) Et₂O, h ν 254 nm, –22°C, 4.5 h; (d) Et₂O, h ν 254 nm, –2°C, 3.5 h. (XBL 917-1679)

LBL Reports:

10. A.P. Kahn (Ph.D. Thesis), "I. Metal-specific Synthesis of Heterodinuclear Fulvalene Complexes. Reactions of (Fulvalene)[Tungsten(tricarbonyl)-(methyl)][Rhodium(Di-carbonyl)]. II. Alkyne Coupling and C-H Activation using (Cyclopentadienyl)Rhodium [Bis(Cyclooctene)]," LBL-30253.

Invited Talks

11. K.P.C. Vollhardt, "Oligocyclopentadienylmetals: Remarkable Organometallic Materials," Boston University, Boston, MA, Oct. 16, 1989.
12. K.P.C. Vollhardt, "Transition-metal Mediated Total Synthesis of Natural and Unnatural Products," Parke-Davis, Ann Arbor, MI, Oct. 12, 1989; Catalytica Associates, Menlo Park, CA, Oct. 25, 1989; University of Notre-Dame de la Paix (Namur), Belgium, Jan. 18, 1990; Catholic University of Louvain, Belgium, Jan. 19, 1990; University of Texas at Austin, Mar. 2, 1990; Ethyl Corporation, Baton Rouge, LA, Mar. 30, 1990; 73rd Canadian Chemical Conference, Symposium on Transition Metals in Organic Synthesis, Halifax, Nova Scotia, July 15-20, 1990; XXVIII International Conference on Coordination Chemistry, Gera, Germany, Aug. 13-18, 1990; 4th Symposium on the Latest Trends in Organic Synthesis, Blacksburg, VA, Oct. 14-17, 1990; University of California at Los Angeles, Nov. 1, 1990; Sandoz Pharma AG, Basel, Switzerland, Nov. 22, 1990; Bayer AG, Bayerwerk, Germany, Nov. 23, 1990.
13. K.P.C. Vollhardt, "Organic Transformations Involving Organocobalt: Mechanisms and Synthesis," Plenary Lecturer, Symposium on Organic Transformations Involving Organometallics: Mechanism and Synthesis, 1989 International Chemical Congress of Pacific Basin Societies, Honolulu, HI, Dec. 17-22, 1989.
14. K.P.C. Vollhardt, Discussion Leader, 1st J. Ficini Symposium, Namur, Belgium, Jan. 15-17, 1990.
15. K.P.C. Vollhardt, Plenary Lecturer, Organic Symposium of the Royal Netherlands Chemical Society, Wageningen, The Netherlands, April 5-6, 1990.
16. K.P.C. Vollhardt, Plenary Lecturer, Organometallics in Organic Synthesis, Ohio State University, Columbus, OH, April 7, 1990.
17. K.P.C. Vollhardt, 18th Lemieux Lectureship, University of Ottawa, Ontario, May 2-4, 1990.
18. K.P.C. Vollhardt, Lecturer, Organometallic Minicourse, Stockholm, Sweden, June 6-7, 1990.

HEAVY-ELEMENT CHEMISTRY

Actinide Chemistry*

Norman M. Edelstein, Richard A. Andersen, Kenneth N. Raymond, and Andrew Streitwieser, Jr., Investigators

INTRODUCTION

Development of new technological processes for the use, safe handling, storage, and disposal of actinide materials relies on the further understanding of basic actinide chemistry and the availability of a cadre of trained personnel. This research program is a comprehensive, multifaceted approach to the exploration of actinide chemistry and to the training of students. Research efforts include synthetic organic and inorganic chemistry for the development of new chemical agents and materials; chemical and physical characterization through such techniques as x-ray diffraction, optical and vibrational spectroscopy, magnetic resonance, and susceptibility; and thermodynamic and kinetic studies for the evaluation of complex formation. One aspect is the development and understanding of complexing agents that specifically and effectively sequester actinide ions. Such agents are intended for the decorporation of actinides in humans, in the environment, and in systems related to the nuclear fuel cycle. Extensive studies are under way to prepare organometallic and coordination compounds of the f-block elements that show the differences and similarities among the f-elements, and between the f- and d-transition series elements. Optical and magnetic studies on actinides as isolated ions in ionic solids, and in molecules, provide information about electronic properties as a function of atomic number.

SPECIFIC SEQUESTERING AGENTS FOR THE ACTINIDES

The coordination chemistry of the actinides and lanthanides is being studied in order to create agents that

selectively and strongly bind f-transition elements in their +4 or +3 oxidation states. Characterization of these compounds includes the use of NMR spectroscopy, x-ray crystallography, potentiometric and spectrophotometric titrations, and electrochemistry. Possible applications for these ligands include magnetic resonance imaging (MRI), plutonium decorporation, uranium extraction from sea water, and waste-actinide extraction and long-term storage.

1. Specific Complexation of Metal Oxo Cations (Publication 9)

T.S. Franczyk and K.N. Raymond

Certain tripodal tertiary amine carboxylates form monomers with the uranyl ion, employing the protonated amine as a hydrogen-bond donor to the uranyl oxygen. The hydrogen bond, along with the carbonyl groups, provides three-dimensional recognition (stereognosis) and a more stable complex. A formation constant with the uranyl ion in aqueous solution and the extraction ability of a hydrophobic complexing agent have been determined. These ligands could be used to extract uranium from sea water. Other such carboxylates form polymers with the uranyl ion but could still be used in industrial processes (see Figure 1-1).

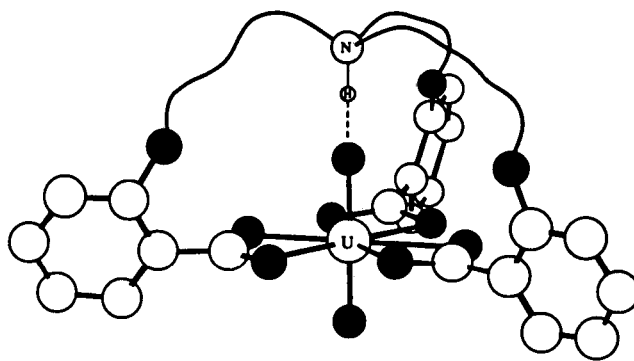


Figure 1-1. A schematic view of ligands designed for the stereognostic coordination of UO_2^{2+} . Selective recognition of the cation involves coordination to uranium and H-bonding to the oxo group. (XBL 911-155)

*This work was supported by the Director, Office of Energy Research, Office of Basic Energy Sciences, Chemical Sciences Division, of the U.S. Department of Energy under Contract No. DE-AC03-76SF00098.

2. Pu(IV) Coordination (Publication 10)

X. Jide and K.N. Raymond

Previous workers have determined that the tetracatecholates are not optimal ligands for decorporation of Pu(IV) due to their high pK_a 's.¹ However, the terephthalamides have lower pK_a 's and improved water solubility.² New chelators have been synthesized: DTPA analogs that contain only one or two catechol groups, tetracatechoylamides and tetraterphthalamides containing a polyaminomacrocyclic ring or H-shaped structure as a backbone, and macrotricyclic terephthalamides. Initial *in vivo* testing indicates that these tetracatecholates are not efficacious in removing Pu(IV) from mice (see Figure 2-1).

1. M.J. Kappel, H. Nitsche, and K.N. Raymond, *Inorg. Chem.* **24**, 606 (1985).

2. T.M. Garrett, P.W. Miller, and K.N. Raymond, *Inorg. Chem.* **28**, 128 (1989).

SYNTHETIC AND STRUCTURAL STUDIES OF ACTINIDES AND OTHER COMPOUNDS

3. Structural Studies on Cyclopentadienyl Compounds of Trivalent Cerium: Tetrameric $(MeC_5H_4)_3Ce$, Monomeric $(Me_3SiC_5H_4)_3Ce$, and $[(Me_3Si)_2C_5H_3]_3Ce$ and Their Coordination Chemistry (Publication 1)

S.D. Stults, R.A. Andersen, and A. Zalkin

The coordinated tetrahydrofuran in $(MeC_5H_4)_3Ce(thf)$ can be removed by Me_3Al in a Lewis acid-base reaction or

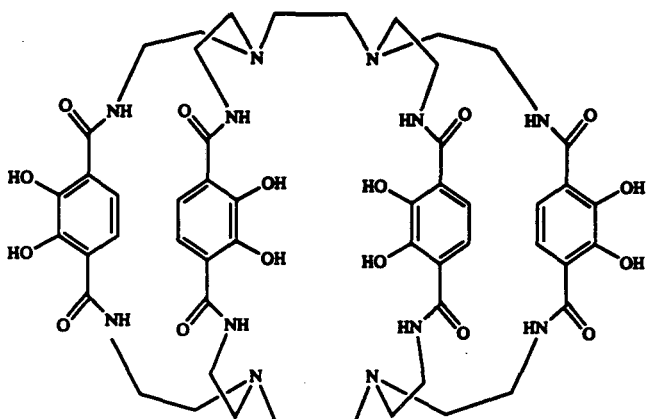


Figure 2-1. Structural formula of a new class of macrocyclic Pu(IV) chelating agents that are now under investigation as decontamination/decorporation agents. (XBL 911-154)

by the "toluene-reflux method" to give base-free $(MeC_5H_4)_3Ce$, which is a monomer in the gas phase though a tetramer in solid state; the crystals are monoclinic, $P2_1/a$, with $a = 12.497(5)$ Å, $b = 26.002(8)$ Å, $c = 9.664(3)$ Å, $\beta = 97.33(3)^\circ$, $R = 0.041$ for 2117 data, and $F^2 > 2\sigma(F^2)$. The structure, shown in Figure 3-1, is made up of a cyclic tetramer in which two MeC_5H_4 rings are η^5 -bonded to each cerium atom and one MeC_5H_4 ring bridges two cerium atoms such that the MeC_5H_4 ring is η^5 -bonded to one cerium and η^1 -bonded to the other. With larger cyclopentadienyl groups, the binary metallocenes (η^5 - $Me_3SiC_5H_4$)₃Ce, (η^5 - $Me_3CC_5H_4$)₃Ce, and $[\eta^5$ - $(Me_3Si)_2C_5H_3$]₃Ce are monomeric in gas phase and solid state. The structure of the latter, shown in Figure 3-2, is based upon a trigonal planar geometry; the crystals are monoclinic, $I2/c$, with $a = 22.752(5)$ Å, $b = 11.386(3)$ Å, $c = 17.431(4)$ Å, $\beta = 105.70(3)^\circ$, $R = 0.046$ for 2519 data, and $F^2 > 3\sigma(F^2)$. All of the binary metallocenes form 1:1 complexes with isocyanides and organocyanides, and the

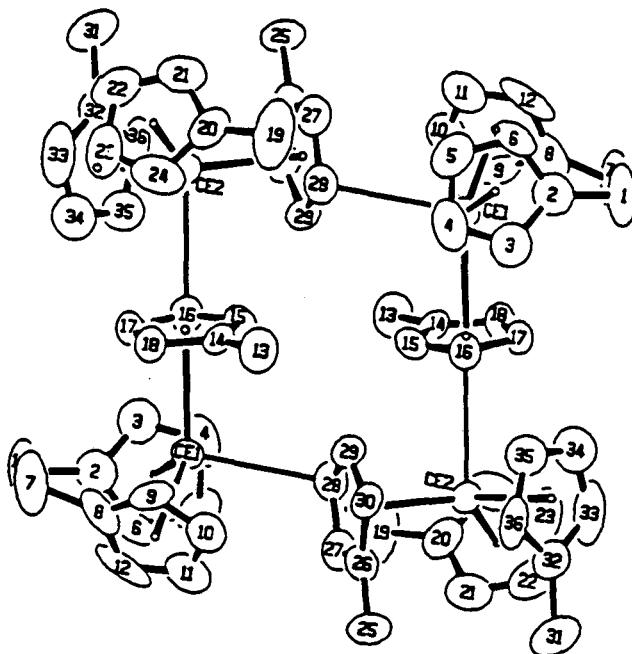


Figure 3-1. ORTEP diagram of $(\eta^5\text{-}MeC_5H_4)_8(\mu\text{-}\eta^5,\eta^1\text{-}MeC_5H_4)_4Ce_4$, 50% probability ellipsoids, Cp 1 = ring centroid of C(2-6), Cp 2 = ring centroid of C(8-12), Cp 3 = ring centroid of C(14-18), Cp 4 = ring centroid of C(20-24), Cp 5 = ring centroid of C(26-30), Cp 6 = ring centroid of C(32-36); Ce(1)C(2-6, 8-12) and Ce(2)C(20-24, 32-36) = 2.80(3) Å (avg.); Ce-Cp(1,2,4,6) = 2.54 Å; Ce(1)-C(14-18) and Ce(2)-C(26-30) = 2.88(4) Å (avg.); Ce-Cp(3,5) = 2.62 Å; Cp(1)-Ce(1)-Cp(2) and Cp(4)-Ce(2)-Cp(6) = 117°; Cp(1)-Ce(1)-Cp(2), Cp(2)-Ce(1)-Cp(3), Cp(4)-Ce(2)-Cp(5), and Cp(6)-Ce(2)-Cp(5) = 116° (avg.); Ce(1)-C(28) = 3.09(1) Å; Ce(2)-C(16) = 2.97(1) Å; Cp(1)-Ce-C(28), Cp(2)-Ce-C(28), Cp(4)-Ce-C(16), Cp(6)-Ce-C(16) = 100° (avg.). (XBL 912-174)

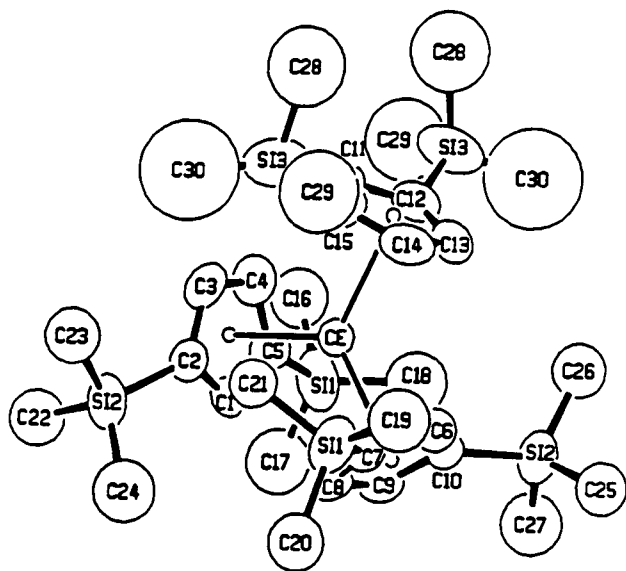


Figure 3-2. ORTEP drawing of $[\eta^5-(\text{Me}_3\text{Si})_2\text{C}_5\text{H}_3]_3\text{Ce}$, 50% probability ellipsoids; Ce-C = 2.83(4) Å (avg.), Ce-ring centroid = 2.57 Å (avg.), and ring centroid-Ce-ring centroid = 120° (avg.). (XBL 912-175)

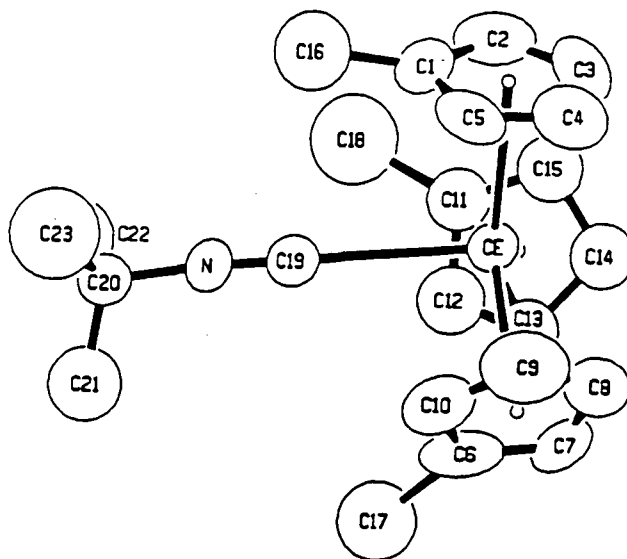


Figure 3-3. ORTEP drawing of $(\eta^5\text{-MeC}_5\text{H}_4)_3\text{Ce}(\text{CNCMe}_3)$, 50% probability ellipsoids; Ce-C(Cp) = 2.79(3) Å, Ce-ring centroid = 2.55 Å (avg.), ring centroid-Ce-ring centroid = 119° (avg.), Ce-C(19) = 2.71(2) Å, ring centroid-Ce-C(19) = 97° (avg.). (XBL 912-176)

crystal structure of two of them have been determined: (1) $(\text{MeC}_5\text{H}_4)_3\text{Ce}(\text{CNCMe}_3)$ is monoclinic, $P2_1/c$, with $a = 14.259(3)$ Å, $b = 9.382(2)$ Å, $c = 17.652(3)$ Å, $\beta = 106.16(3)^\circ$, $R = 0.050$ for 1501 data, and $F^2 > 3\sigma(F^2)$; (2) $[(\text{Me}_3\text{Si})_2\text{C}_5\text{H}_3]_3\text{Ce}(\text{CNCMe}_3)$ is also monoclinic, $P2_1/c$, with $a = 11.462(3)$ Å, $b = 17.146(4)$ Å, $c = 26.826(6)$ Å, $\beta = 112.93(3)^\circ$, $R = 0.047$ for 2437 data, and $F^2 > 3\sigma(F^2)$, as shown in Figures 3-3 and 3-4, respectively.

4. Chemistry of Trivalent Cerium and Uranium Metallocenes: Reactions with Alcohols and Thiols (Publication 2)

S.D. Stults, R.A. Andersen, and A. Zalkin

The trivalent cerium metallocene $(\text{Me}_3\text{CC}_5\text{H}_4)_3\text{Ce}$ reacts with alcohols, HOR ($R = \text{CHMe}_2$ or Ph), or thiols, HSR ($R = \text{CHMe}_2$ or Ph), to give the dimers $(\text{Me}_3\text{CC}_5\text{H}_4)_4\text{Ce}_2$ ($\mu\text{-ER}$)₂, as shown by x-ray crystallography for the isopropoxide and isopropylthiolate derivatives. Crystals of $(\text{Me}_3\text{CC}_5\text{H}_4)_4\text{Ce}_2$ ($\mu\text{-OCHMe}_2$)₂ (Figure 4-1) are monoclinic, $P2_1/c$, with $a = 11.962(4)$ Å, $b = 14.489(5)$ Å, $c = 12.384(5)$ Å, $\beta = 103.31(3)^\circ$, and $V = 2089$ Å³; the structure was refined by full-matrix least squares to a conventional R-factor of 0.028 for 2874 data, with $F^2 > 2\sigma(F^2)$. The Ce_2O_2 unit is planar; the geometry about the cerium atom is pseudotetrahedral, and the geometry is planar about the oxygen atom. Crystals of $(\text{Me}_3\text{CC}_5\text{H}_4)_4\text{Ce}_2$ ($\mu\text{-SCHMe}_2$)₂ (Figure 4-2) are also

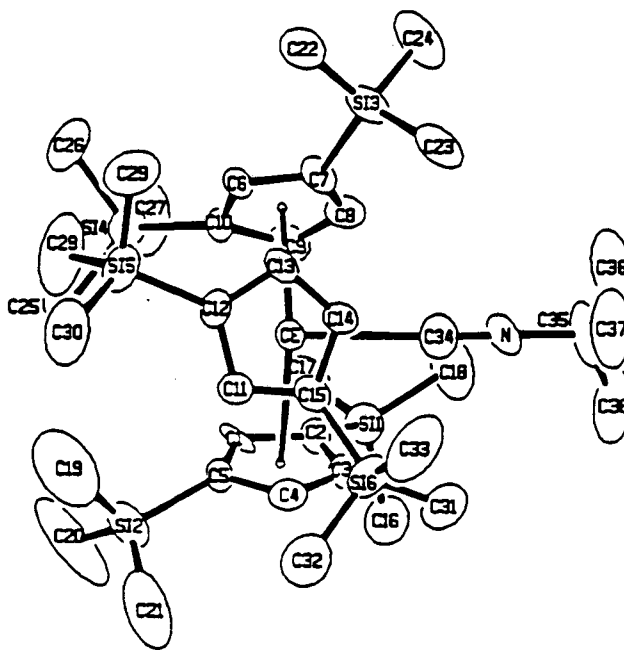


Figure 3-4. ORTEP drawing of $[\eta^5-(\text{Me}_3\text{Si})_2\text{C}_5\text{H}_3]_3\text{Ce}(\text{CNCMe}_3)$, 50% probability ellipsoids; Ce-C(Cp) = 2.87(3) Å (avg.), Ce-ring centroid = 2.60 Å (avg.), ring centroid-Ce-ring centroid = 119.5° (avg.), Ce-C(34) = 2.70(1) Å, ring centroid-Ce-C(34) = 94° (avg.). (XBL 912-177)

monoclinic, $P2_1/n$, with $a = 14.255(9)$ Å, $b = 13.585(9)$ Å, $c = 11.265(7)$ Å, $\beta = 96.02(5)^\circ$, and $V = 2170$ Å³; the structure was refined by full-matrix least squares to a

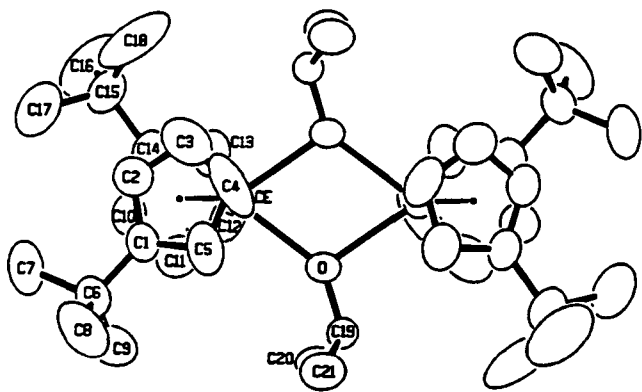


Figure 4-1. ORTEP diagram of $(\text{Me}_3\text{CC}_5\text{H}_4)_4\text{Ce}_2(\mu\text{-OCHMe}_2)$, 50% probability ellipsoids; C(19) is disordered and refined as two isotropic half-atoms, only one conformation of which is shown. Ce-C (avg.) = 2.83 ± 0.04 Å; Ce-Cp (cent.) = 2.58 Å; Ce-O = $2.373(3)$ Å, $2.369(3)$ Å; Ce...Ce = $3.844(2)$ Å; Ce-O-Ce = $108.3(1)^\circ$; O-Ce-O = $71.7(1)^\circ$; Ce-O-C(19) = $143.3(5)^\circ$, $108.2(5)^\circ$; Cp (cent.)-Ce-Cp (cent.) = 128.5° . (XBL 912-172)

conventional R-factor of 0.028 for 2899 data, with $F^2 > 2\sigma(F^2)$. The Ce_2S_2 unit is planar, and the geometry about cerium is pseudotetrahedral, though the geometry is pyramidal at sulfur so that the isopropyl groups are anti relative to the Ce_2S_2 ring. Methanol or water give an insoluble solid, presumably $\text{Ce}(\text{OMe})_3$ or $\text{Ce}(\text{OH})_3$,

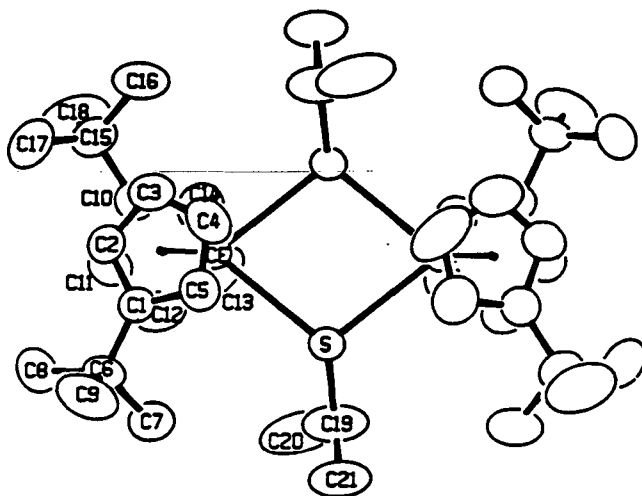


Figure 4-2. ORTEP diagram of $(\text{Me}_3\text{CC}_5\text{H}_4)_4\text{Ce}_2(\mu\text{-SCHMe}_2)_2$, 50% probability ellipsoids; Ce-C (avg.) = 2.78 ± 0.02 Å; Ce-Cp (cent.) = 2.52 Å; Ce-S = $2.870(2)$, $2.894(2)$ Å; Ce...Ce = $4.449(2)$ Å; Ce-S-Ce = $101.06(6)^\circ$; S-Ce-S = $78.94(6)^\circ$; Ce-S-C(19) = $128.5(3)^\circ$, $118.2(4)^\circ$; Cp (cent.)-Ce-Cp (cent.) = 131° . (XBL 912-173)

whereas HECMe_3 (E = O or S) does not react with $(\text{Me}_3\text{CC}_5\text{H}_4)_3\text{Ce}$; but the thiol does react with the sterically less bulky metallocene $(\text{MeC}_5\text{H}_4)_3\text{Ce}(\text{thf})$ to give $(\text{MeC}_5\text{H}_4)_4\text{Ce}_2(\mu\text{-SCMe}_3)_2$. The pKa's (H_2O) of the organic acids generally predict the thermodynamic outcome of the proton exchange reactions, though the latter set of experiments show that kinetic (i.e., steric) factors play a role. The uranium metallocene $(\text{Me}_3\text{CC}_5\text{H}_4)_3\text{U}$ reacts with HSPh at low temperature to give isolable $(\text{Me}_3\text{CC}_5\text{H}_4)_4\text{U}_2(\mu\text{-SPh})_2$, which rearranges in solution to the monomeric, tetravalent species $(\text{Me}_3\text{CC}_5\text{H}_4)_3\text{USPh}$ and unidentified material. The dimeric intermediate cannot be detected with the sterically smaller metallocene $(\text{MeC}_5\text{H}_4)_3\text{U}(\text{thf})$, as only $(\text{MeC}_5\text{H}_4)_3\text{UER}$ (ER = OMe, OCHMe₂, OPh, and SCHMe₂) is isolated.

5. $[(\text{MeC}_5\text{H}_4)_3\text{U}]_2[\mu\text{-1,4-N}_2\text{C}_6\text{H}_4]$: A Bimetallic Molecule with Antiferromagnetic Coupling Between the Uranium Centers (Publication 3)

R.K. Rosen, R.A. Andersen, and N.M. Edelstein

The two bimetallic, pentavalent uranium metallocene compounds $[(\text{MeC}_5\text{H}_4)_3\text{U}]_2(\mu\text{-1,4-N}_2\text{C}_6\text{H}_4)$, **1** in Figure 5-1, and $[(\text{MeC}_5\text{H}_4)_3\text{U}]_2(\mu\text{-1,3-N}_2\text{C}_6\text{H}_4)$, **2** in Figure 5-1, have been prepared from $(\text{MeC}_5\text{H}_4)_3\text{U}(\text{thf})$ and 1,4-diazido- and 1,3-diazido-benzene at room temperature, respectively. Magnetic-susceptibility studies on these solids from 5 to 280 K show that the spins on **1** antiferromagnetically couple at ~ 20 K while those on **2** do not couple to 5 K (see Figure 5-2). The susceptibility curve for **1** can be fit to a one-dimensional exchange between the two metal centers with a J of ~ 19 cm⁻¹ (see Figure 5-3). A super-exchange model is postulated to account for these results, since the imido-nitrogens of the bridging ligand in **1** are in the 1,4-positions of the benzene ring and they can conjugate, while the bridging ligand in **2** has the imido-nitrogen on the 1,3-positions of the benzene ring and they cannot conjugate.

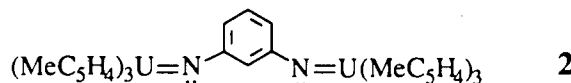
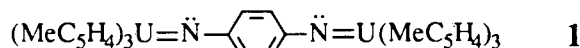


Figure 5-1. Two bimetallic, pentavalent uranium metallocene compounds. (XBL 918-1685)

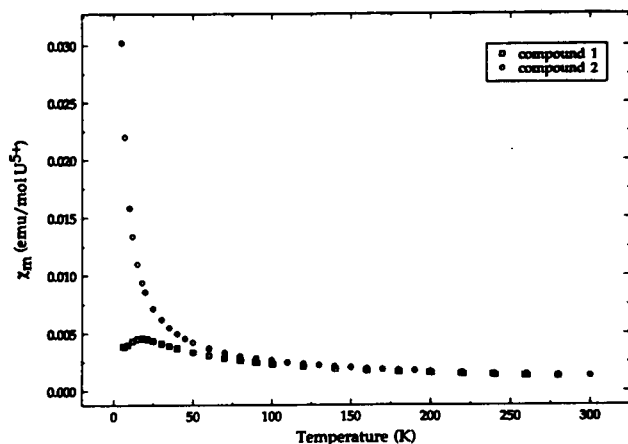


Figure 5-2. Experimental magnetic susceptibility data of 1 and 2 as a function of temperature. (XBL 901-210)

6. The Uranocene Half-Sandwich: Mono[8]annuleneuranium(IV) Dichloride and Some Derivatives (Publication 5)

T.R. Boussie, R.M. Moore, Jr., A. Streitwieser, A. Zalkin, J. Brennen, and K.A. Smith

A facile synthesis of [8]annulene uranium(IV) dichloride (1) has been developed via the reduction of cyclooctatetraene (COT) by UCl_3 , or through reaction of UCl_4 , COT, and NaH. Crystals of 1 solvated by tetrahydrofuran (THF) were not sufficiently stable for x-ray crystal analysis, but a crystal structure of the bis-pyridine adduct, [8]annuleneuranium(IV) dichloride bis(pyridine),

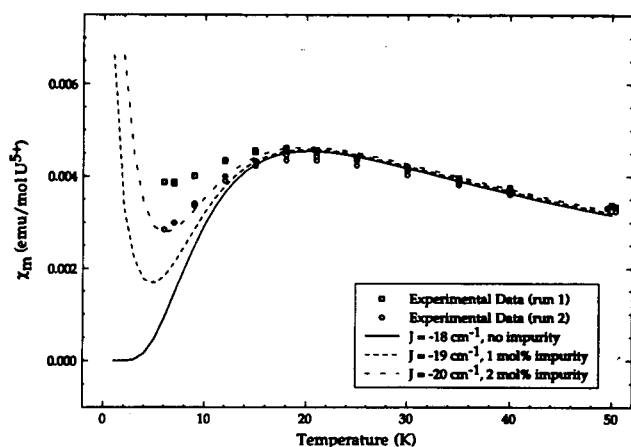


Figure 5-3. Comparison of experimental magnetic susceptibility data with calculated values for 1. The calculations are with $g_{||} = 2.6$. The impurity is assumed to be $(\text{MeC}_5\text{H}_4)_3\text{U}(\text{thf})$, and three calculated curves are shown for $J = -18 \text{ cm}^{-1}$ (no impurity), $J = -19 \text{ cm}^{-1}$ (1 mole% impurity), and $J = -20 \text{ cm}^{-1}$ (2 mole% impurity). (XBL 901-211)

$(\text{C}_8\text{H}_8)\text{UCl}_2(\text{NC}_5\text{H}_5)_2$ (2), was determined (see Figure 6-1). Crystals of 2 are monoclinic, $P2_1/c$, with $a = 15.431(3) \text{ \AA}$, $b = 7.744(2) \text{ \AA}$, $c = 15.665(3) \text{ \AA}$, $Z = 4$, and $R_f = 2.8\%$. Reaction of 1 with sodium acetylacetonate gave the corresponding half-sandwich derivative [8]annulene uranium(IV) bis(acetylacetonate), $(\text{C}_8\text{H}_8)\text{U}(\text{CH}_3\text{COCHCOCH}_3)_2$ (3). The crystal structure of 3 is shown in Figure 6-2. Crystals of 3 are monoclinic, $P2_1/n$, with $a = 19.166(4) \text{ \AA}$, $b = 10.312(2) \text{ \AA}$, $c = 9.227(2) \text{ \AA}$, $Z = 4$, and $R_f = 2.7\%$.

The ^1H NMR spectrum of 1 in THF- d_8 at 30°C shows a single resonance at -31.8 ppm with a line width of 18 Hz corresponding to the [8]annulene protons. Replacement of the coordinating THF ligands with pyridine results in only a small change in the ring proton resonance.

Reaction of 1 with COT dianion gives uranocene. Reaction with a substituted COT dianion gives a statistical mixture of the possible uranocenes. Attempted alkylations of 1 with organolithium or Grignard reagents failed to produce isolable products in which the chlorides were replaced. Similarly, attempted reactions of 1 with metal alkoxides gave no isolable products. The reaction chemistry of these half-sandwich compounds is clearly limited.

The activation parameters for the coordination of trimethylphosphine (PMe_3) to 1 in THF solution have been measured by variable-temperature NMR: $\Delta H^\ddagger = 12.7 \text{ kcal mol}^{-1}$, $\Delta S^\ddagger = 2.2 \text{ e.u.}$, and $\Delta G^\ddagger = 12.1 \text{ kcal mol}^{-1}$.

7. Structures of Organo-f-Element Compounds Differing in the Oxidation State of the f-Element: Crystal Structures of Bis([8]annulene) Complexes of Cerium(IV), Ytterbium(III), and Uranium(III) (Publication 13)

T.R. Boussie, D.C. Eisenberg, J.T. Rigsbee, A. Streitwieser, and A. Zalkin

Crystal structures of the first organometallic compound of cerium(IV), 1,1'-dimethylcerocene, 3, and of a reduced

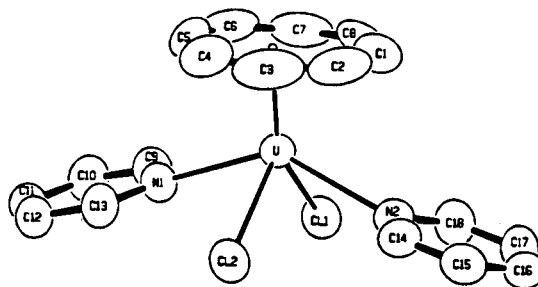


Figure 6-1. ORTEP drawing of 2. (XBL 892-550)

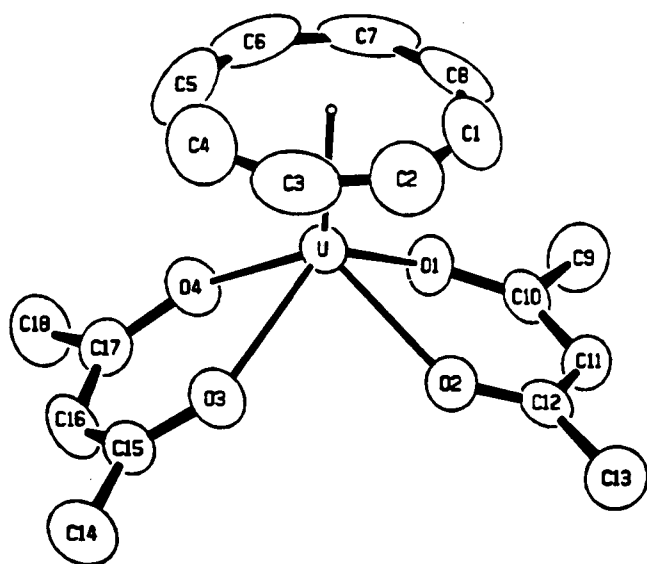


Figure 6-2. ORTEP drawing of 3. (XBL 892-551)

uranocene, (diethylene glycol dimethyl ether)potassium bis(methyl[8]annuleny)uranate(III), 7, have been obtained and are shown in Figures 7-1 and 7-2, respectively. They provide valuable comparisons with related organometallic structures derived from cyclooctatetraene (COT) dianion. The results show that the effective size of the [8]annulene ring (r_{COT}) varies over a wide range. A selection of the available data is summarized in Table 7-1.

For a given oxidation state, the metal ligand distance normally increases as the coordination number (C.N.) increases. Comparisons of 10-coordinated uranocene, 1, and thorocene, 2, with their 9-coordinate half-sandwich analogs 4, 5, and 6 show a reversal of this generalization. The generalization holds for the cerium(III) compounds 8 and 11. In the potassium sandwich salts 7, 8, and 9, the two rings have different effect sizes; the COT ring that is also coordinated to K^+ is farther from the central f-element. Especially dramatic is the comparison of these potassium salts with 12. The coordination environment around the potassium is the same in all four cases, yet the K-COT distance varies widely.

The results can be rationalized by the recognition that the ring-metal distance depends not just on some intrinsic function of coordination number on metal cation radius but also on the mutual repulsions of the ligands. In 4, 5, and 6, the repulsions between the one COT dianion ring and the other ligands is greater than between the two COT dianion rings of 1 and 2. In 7, 8, and 9, one COT ring is attracted

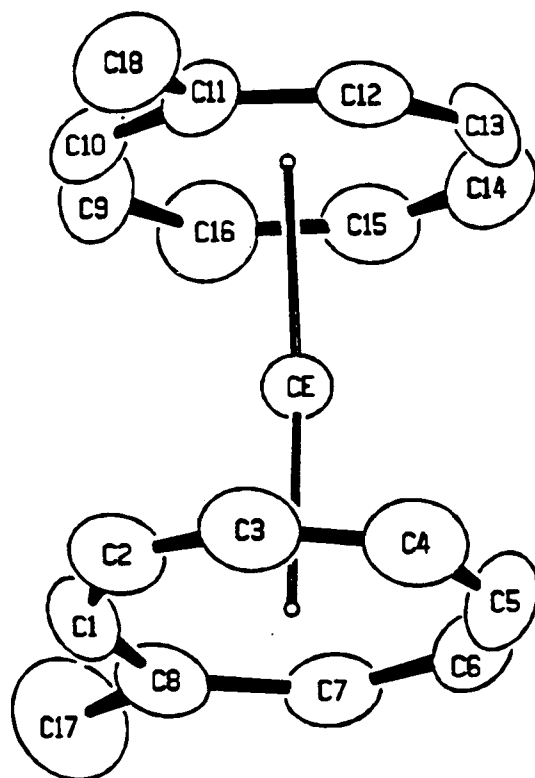


Figure 7-1. ORTEP drawing of 3. (XBL 904-1349)

only to a central trivalent cation while the other is attracted to a K^+ as well. In these compounds the K^+ is repelled by the central trivalent cation, whereas in 12 only the repulsion of two monovalent cations is involved.

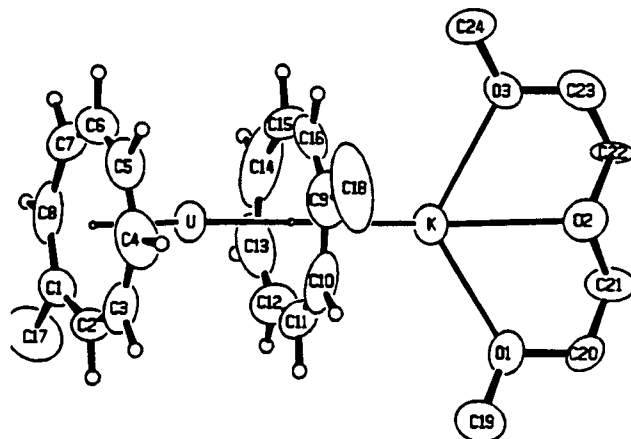


Figure 7-2. ORTEP drawing of 7. (XBL 904-1351)

Table 7-1. Comparison of M-C bond lengths and r_{COT} for several [8]annulene complexes.

Compound	M	M C.N.	M-C Dist., Å	r_{metal} , Å	r_{COT} , Å
1. $\text{U}(\text{C}_8\text{H}_8)_2$	U^{4+}	10	2.64	1.08	1.57
2. $\text{Th}(\text{C}_8\text{H}_8)_2$	Th^{4+}	10	2.70	1.13	1.57
3. $\text{Ce}(\text{MeC}_8\text{H}_7)_2$	Ce^{4+}	10	2.69	1.07	1.62
4. $(\text{C}_8\text{H}_8)\text{UCl}_2(\text{NC}_5\text{H}_5)_2$	U^{4+}	9	2.68	1.05	1.63
5. $(\text{C}_8\text{H}_8)\text{U}(\text{acac})_2$	U^{4+}	9	2.69	1.05	1.64
6. $(\text{C}_8\text{H}_8)\text{ThCl}_2(\text{thf})_2$	Th^{4+}	9	2.72	1.09	1.63
			2.71	1.09	1.62
			2.72	1.09	1.63
7. $[\text{K}(\text{diglyme})][\text{U}(\text{MeC}_8\text{H}_7)_2]^{\text{a}}$	U^{3+}	10	2.73	1.22	1.51
	U^{3+}	10	2.71	1.22	1.49
	K^+	8	3.26	1.51	1.75
8. $[\text{K}(\text{diglyme})][\text{Ce}(\text{C}_8\text{H}_8)_2]^{\text{a}}$	Ce^{3+}	10	2.73	1.25	1.48
	Ce^{3+}	10	2.75	1.25	1.50
	K^+	8	3.17	1.51	1.66
9. $[\text{K}(\text{diglyme})][\text{Yb}(\text{C}_8\text{H}_8)_2]^{\text{a}}$	Yb^{3+}	10	2.61	1.10	1.51
	Yb^{3+}	10	2.60	1.10	1.50
	K^+	8	3.19	1.51	1.68
10. $(\text{C}_8\text{H}_8)\text{Lu}(\text{C}_5\text{Me}_5)$	Lu^{3+}	8	2.43	0.977	1.46
11. $[(\text{C}_8\text{H}_8)\text{CeCl}(\text{thf})_2]_2$	Ce^{3+}	9	2.71	1.20	1.51
12. $[\text{K}(\text{diglyme})]_2(\text{Me}_4\text{C}_8\text{H}_4)$	K^+	8	3.00	1.51	1.49

^aThe [8]annulene rings are in different coordination environments.

PHYSICAL AND SPECTROSCOPIC PROPERTIES

8. The $6d \rightarrow 5f$ Fluorescence Spectra of PaCl_6^{2-} in a Cs_2ZrCl_6 Crystal (Publication 15)

D. Piehler, W.K. Kot, and N. Edelstein

Emission spectra from the parity-allowed electronic transitions between the lowest crystal-field level of the $6d^1$ configuration to all the electronic levels of the $5f^1$ configuration of Pa^{4+} (see Figure 8-1) diluted into single crystals of Cs_2ZrCl_6 at 4.2 K show highly structured

vibronic sidebands (see Figure 8-2). Vibronic progressions are seen along the 310 cm^{-1} totally symmetric stretch of the PaCl_6^{2-} complex. Most vibronic peaks correspond to even parity vibrations of the PaCl_6^{2-} complex or the host lattice. Additionally, electronic Raman scattering was observed between the two lowest crystal-field levels of the $5f^1$ configuration by exciting with an argon-ion laser in near resonance with the lowest level of the $5d^1$ configuration.

The spectra allow four levels of the $5f$ configuration, as well as the lowest Γ_{8g} level of the excited $6d$ configuration of $\text{Pa}^{4+}/\text{Cs}_2\text{ZrCl}_6$, to be measured accurately. An analysis of vibronic structure indicated that the Pa-Cl bond distance is $\sim 0.1 \text{ \AA}$ longer in the $6d$ excited state than in the ground

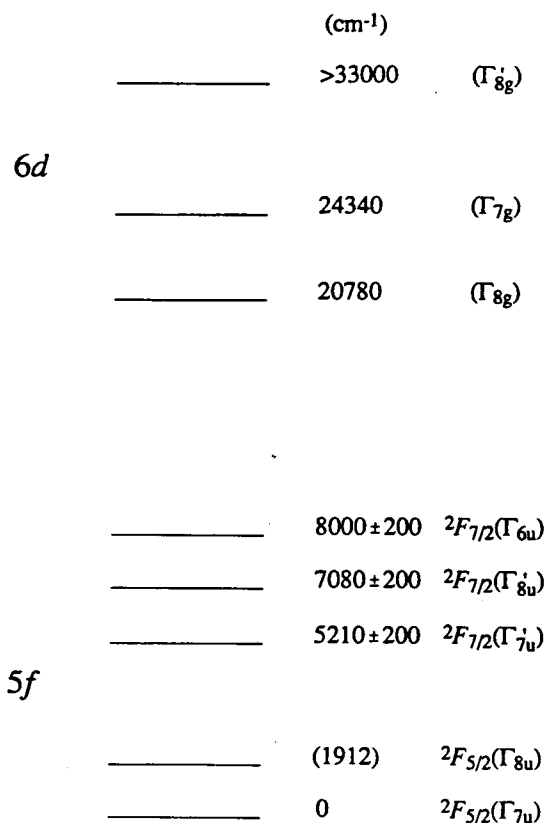


Figure 8-1. Schematic energy-level diagram for the 5f and 6d configurations of Pa⁴⁺/Cs₂ZrCl₆. (XBL 911-6)

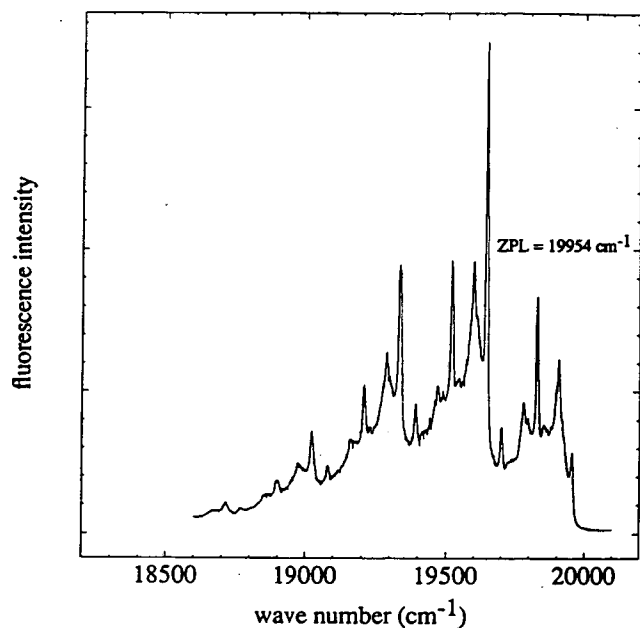


Figure 8-2. Fluorescence spectrum from the 6d(Γ_{8g}) level to the 5f(Γ_{7u}) level. (XBL 911-7)

5f configuration. The simple crystal-field model cannot accurately reproduce the energies of the 5f configuration and the g value of the ground state. The relative strengths of the fluorescent bands are reproduced quite well by a calculation of the relative electric-dipole intensities between the 6d(Γ_{8g}) state and the 5f levels.

9. Luminescence of Sm²⁺ Ions as a Probe of Pressure-Induced Phase Transitions in SrF₂ (Publication 19)

C.S. Yoo,[†] H.B. Radousky,[†] N.C. Holmes,[†] and N.M. Edelstein

The luminescence spectra of Sm²⁺ diluted in SrF₂ are characteristic of the local site symmetry and bulk crystal phase of SrF₂. In this paper the change in these spectra are used to monitor the β (cubic) to α (orthorhombic) phase transition of SrF₂ at 5 GPa and 300 K. Several spectra at various temperatures and pressures are shown in Figure 9-1. The Sm²⁺ spectra in the α phase show a series of

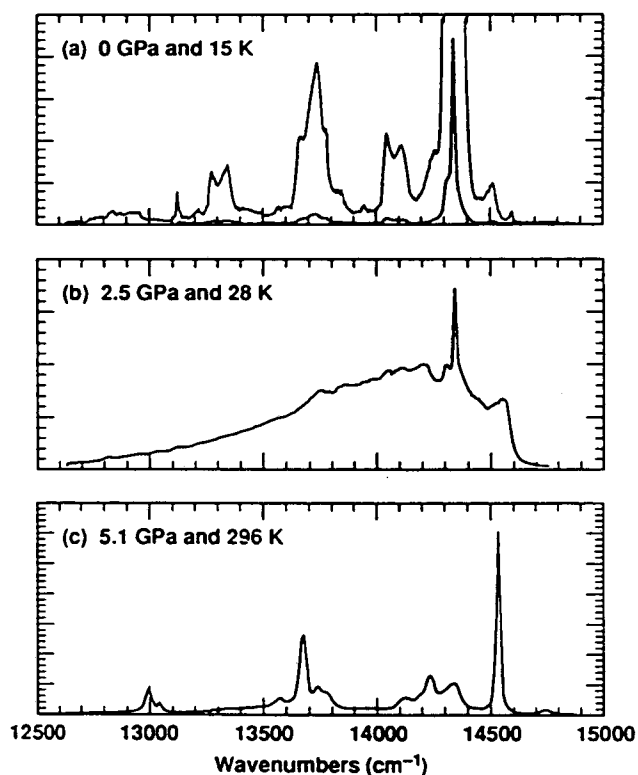


Figure 9-1. Luminescence spectra of Sm²⁺ ions doped in SrF₂ crystals; (a) 4f-4f transitions in β -SrF₂ at 0 GPa and 15 K, (b) 4f-4f and 5d-4f transitions in β -SrF₂ at 2.5 GPa and 28 K, and (c) 4f-4f transitions in α -SrF₂ at 5.1 GPa and 296 K. (XBL 911-4)

sharp 4f-4f transition bands originating from the 5D_0 level to 7F_J multiplets, including a strong transition for $\Delta J = 0$. The high-pressure α phase is metastable and can be recovered at 1 atmosphere and 30 K. At low temperatures, these transitions are not observed; instead, the $4f^55d^1$ band of the Sm^{2+} ion in the β phase shifts below the 5D_0 ($4f^6$) level at 4.5 GPa and 30 K. The relative energies of the low-energy $4f^55d^1$ band edge and the $^5D_0 \rightarrow ^7F_1$ fluorescent line as a function of pressure are shown in Figure 9-2. This band crossing occurs reversibly in the β phase. The nature of the Sm^{2+} luminescence spectra in the α - and β -phases of SrF_2 at several pressures and temperatures is discussed.

†Permanent address: Lawrence Livermore National Laboratory, Livermore, CA 94550.

10. The Electronic Structure of Metalloorganic Compounds of f-Elements XXVII. Interpretation of the Optical, Magnetic, EPR, and NMR Spectroscopic Properties of the Neutral Base Adducts of Tris(η^5 -cyclopentadienyl)Nd(III) (Publication 20)

H. Reddmann,† H. Schultze,† H.-D. Amberger,† G.V. Shalimoff, and N.M. Edelstein

The absorption spectrum of $(Cp-d_5)_3Nd \cdot THF-d_8$ was measured in hydrocarbon glasses and in KBr and teflon pellets at room and low temperatures. The bands were assigned based on calculations assuming the crystal-field

parameters of the Nd complex were the same as for the previously analyzed $Cp_3Pr \cdot MeTHF$. The parameters of the empirical Hamiltonian were fitted to the energies of 96 levels to give an r.m.s. deviation of 26 cm^{-1} . On the basis of the wave functions of the crystal-field ground state obtained from these calculations, the observed EPR spectrum of $Cp_3Nd_{0.06}La_{0.94} \cdot THF$ could be explained. The calculated wave functions and eigenvalues were used to simulate the experimentally determined temperature dependence of μ_{eff} of powdered $Cp_3Nd \cdot THF$ and of an oriented single crystal of $Cp_3Nd \cdot NCCCH_3$. With the assumption that the methyl protons of the γ -picoline ligand of $Cp_3Nd \cdot \gamma\text{-pic}$ and $(MeCp)_3Nd \cdot \gamma\text{-pic}$, respectively, experience an NMR shift due only to dipolar coupling, the paramagnetic anisotropy $\chi_{\parallel} - \chi_{\perp}$ was estimated.

†Permanent address: Institut für Anorganische und Angewandte Chemie der Universität Hamburg, Martin-Luther-King-Platz 6, D-2000 Hamburg 13, Germany.

11. Photoreduction of Ce(IV) in $Ce_2(O^iPr)_8(iPrOH)_2$. Characterization and Structure of $Ce_4O(O^iPr)_{13}(iPrOH)$ (Publication 21)

K. Yunlu,† P.S. Gradoff,† N. Edelstein, W. Kot, G. Shalimoff, W.E. Streib,‡ B.A. Vaaristra,‡ and K.G. Caulton‡

Visible irradiation of $Ce_2(O^iPr)_8(iPrOH)_2$ yields the mixed-valence compound $Ce_4O(O^iPr)_{13}(iPrOH)$, which has been characterized by 1H NMR, infrared spectra, elemental analysis, and x-ray diffraction. The structure is described by $Ce_4(\mu_4-O)(\mu_3-O^iPr)_2(\mu_2-O^iPr)_4(O^iPr)_7(iPrOH)$ (see Figure 11-1). The $Ce_4(\mu_4-O)$ core has a butterfly form, with a crystallographic C_2 axis that passes through the oxide ion and the center of a symmetric hydrogen bond between the coordinated alcohol and one terminal alkoxide. This photoredox reaction cannot be thermally induced and requires that hydrogen be present on the carbon α to the alkoxide oxygen. Magnetic susceptibility and EPR studies show the compound to be paramagnetic. Two temperature ranges of Curie-Weiss behavior are observed, with $\mu_{\text{eff}} = 2.7 \text{ BM}$ from 80–300 K. Crystal data (-130°C): $a = 21.405(6) \text{ \AA}$, $b = 14.077(3) \text{ \AA}$, $c = 20.622(6) \text{ \AA}$, $\beta = 103.97(1)^\circ$, with $Z = 4$ in space group $C2/c$.

†Permanent address: Rhone-Poulenc, Inc., New Brunswick, NJ 08901.

‡Permanent address: Department of Chemistry and Molecular Structure Center, Indiana University, Bloomington, IN 47405.

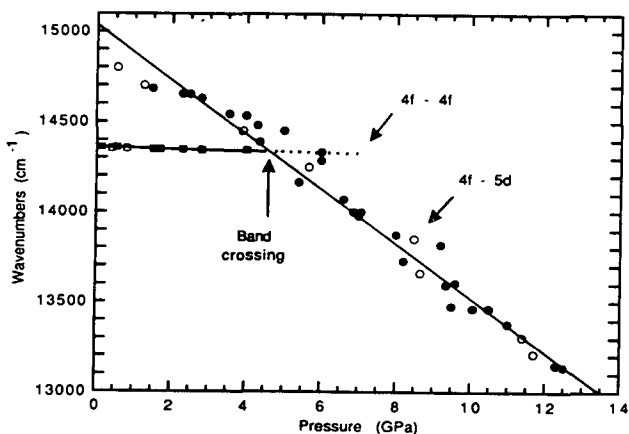


Figure 9-2. Peak position of the 4f-4f band and the red edge position of the 4f-5d band in the β phase as a function of pressure, showing the band crossing at 4.5 GPa and 30 K. Closed and open circles represent the up and down strokes in pressure, respectively. (XBL 911-5)

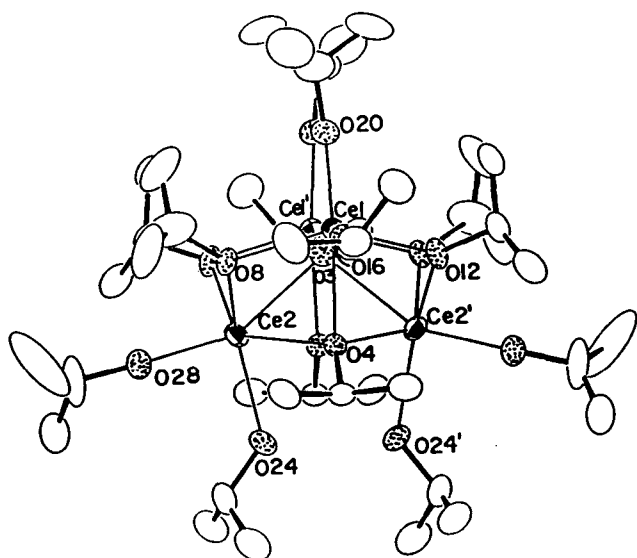


Figure 11-1. ORTEP drawing of the nonhydrogen atoms of $\text{Ce}_4\text{O}(\text{OPr})_{13}(\text{iPrOH})$, showing selected atom labeling. The crystallographic C_2 axis (which creates primed from unprimed atoms) lies vertically in both drawings. Oxygens are stippled. (XBL 911-15)

12. Electronic Coherent Anti-Stokes Raman Spectroscopy in CeF_3 (Publication 17)

D. Piehler

The coherent anti-Stokes Raman spectra (CARS) of the electronic states of the Ce^{3+} ion in a CeF_3 crystal at 3.8 K have been measured. CARS resonances involving the ground state of the $^2F_{5/2}$ manifold and the Stark components of the $^2F_{7/2}$ manifold at 2161 cm^{-1} and 2239 cm^{-1} have been detected. Measurements were made with both visible ($\lambda_1 \approx 476 \text{ nm}$, $\lambda_2 = 532 \text{ nm}$) and near-ultraviolet ($\lambda_1 = 355 \text{ nm}$, $\lambda_2 \approx 385 \text{ nm}$) lasers. The energy-level diagram and experimental frequencies for the singly resonant electronic CARS experiment are shown in Figure 12-1. The intensity of a normalized CARS signal is shown in Figure 12-2. The enhancement of the third-order susceptibility due to the electronic transitions, $|\chi^{(3)R}/\chi^{(3)NR}|_{\text{max}}$, is as great as 4.8. This represents an order-of-magnitude increase over singly resonant electronic CARS experiments in other rare-earth crystals. The CARS data also yielded accurate measurement of the Ce^{3+} electronic Raman cross sections. In the visible region, $\sigma_{zz}(2161 \text{ cm}^{-1}) = (5.0 \pm 1.1) \times 10^{-30} \text{ cm}^2$, and $\sigma_{zz}(2239 \text{ cm}^{-1}) = (1.9 \pm 0.7) \times 10^{-30} \text{ cm}^2$. Both the absolute magnitude and dispersion of $|\chi^{(3)R}|_{\text{max}}$ could be calculated by modeling the virtual intermediate states as a single degenerate 5d state at 45000 cm^{-1} .

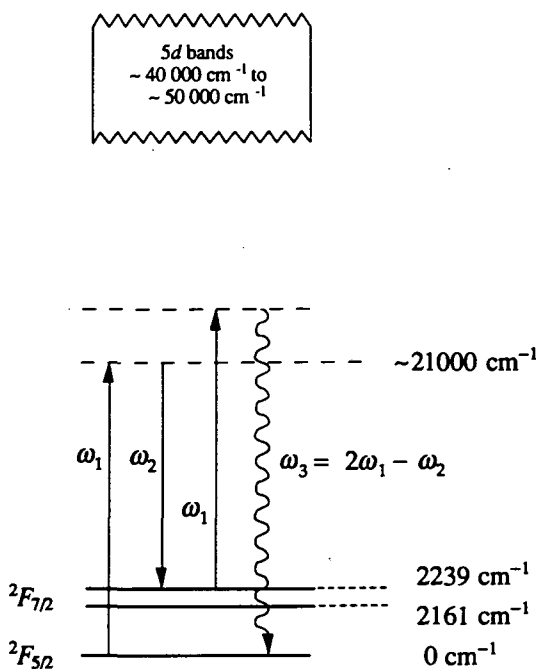


Figure 12-1. Schematic diagram of single resonant electronic CARS in CeF_3 using visible lasers. A frequency-doubled $\text{Nd}^{3+}:\text{YAG}$ laser provided a fixed $\omega_2/2\pi c = 18794 \text{ cm}^{-1}$. A tuneable dye laser provided $\omega_1/2\pi c = 21000 \text{ cm}^{-1}$. Energy levels are not drawn to scale. (XBL 911-16)

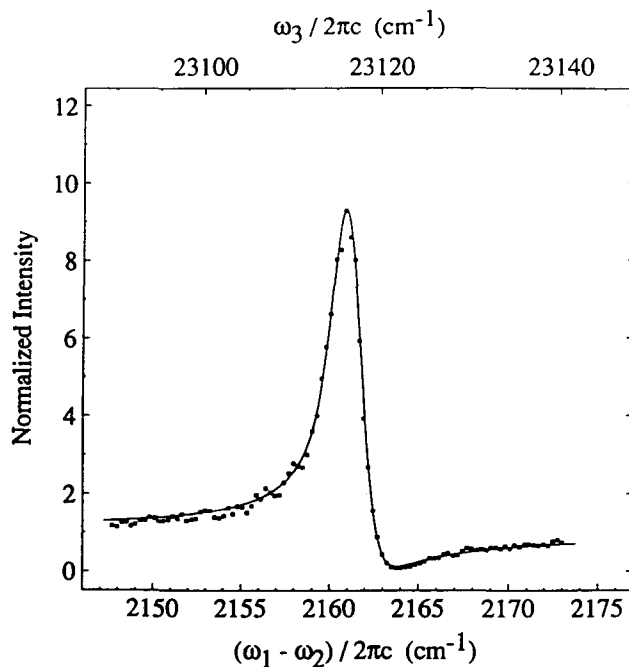


Figure 12-2. Intensity of a CARS signal, normalized to the off-resonance intensity, at frequency ω_3 as a function of $\omega_1 - \omega_2$ with the visible lasers polarized in the z direction. The solid line is from an empirical fit. (XBL 911-17)

1990 PUBLICATIONS AND REPORTS

Refereed Journals

1. S.D. Stults, R.A. Andersen, and A. Zalkin, "Structural Studies on Cyclopentadienyl Compounds of Trivalent Cerium: Tetrameric $(\text{MeC}_5\text{H}_4)_3\text{Ce}$, Monomeric $(\text{Me}_3\text{SiC}_5\text{H}_4)_3\text{Ce}$ and $[(\text{Me}_3\text{Si})_2\text{C}_5\text{H}_3]_3\text{Ce}$ and Their Coordination Chemistry," *Organometallics* **9**, 115 (1990); LBL-26279.
2. S.D. Stults, R.A. Andersen, and A. Zalkin, "Chemistry of Trivalent Cerium and Uranium Metallocenes: Reactions with Alcohols and Thiols," *Organometallics* **9**, 1625 (1990); LBL-27041.
3. R.K. Rosen, R.A. Andersen, and N.M. Edelstein, " $[(\text{MeC}_5\text{H}_4)_3\text{U}]_2[\mu\text{-}1,4\text{-N}_2\text{C}_6\text{H}_4]$: A Bimetallic Molecule with Antiferromagnetic Coupling between the Uranium Centers," *J. Am. Chem. Soc.* **112**, 4508 (1990); LBL-28093.
4. D.C. Eisenberg, A. Streitwieser, and W.K. Kot, "Electron Transfer in Some Organouranium and Transuranium Systems," *Inorg. Chem.* **29**, 10-14 (1990); LBL-25585.
5. T.R. Boussie, R.M. Moore, Jr., A. Streitwieser, A. Zalkin, J. Brennen, and K.A. Smith, "The Uranocene Half-Sandwich: Mono[8]annuleneuranium(IV) Dichloride and Some Derivatives," *Organometallics* **9**, 2010 (1990).
6. S. Xia, G.M. Williams, and N.M. Edelstein, "Contributions From the Energy Level Structure of the $4f^{11}5d^1$ Intermediate Configuration to the Electronic Raman Scattering Intensities of TmPO_4 ," *Chem. Phys.* **138**, 255 (1989); LBL-26122.
7. L.R. Morss, J.W. Richardson, Jr., C.W. Williams, G.H. Lander, A.C. Lawson, N.M. Edelstein, and G.V. Shalimoff, "Powder Neutron Diffraction and Magnetic Susceptibility of $^{248}\text{CmO}_2$," *J. Less Common Metals* **156**, 273 (1989); LBL-28438.
8. D. Piehler and N. Edelstein, "Doubly Resonant Coherent Anti-Stokes Raman Spectroscopy of Ce^{3+} in LuPO_4 ," *Phys. Rev. A* **41**, 6406 (1990); LBL-28203.
9. K.N. Raymond and T.S. Franczyk, "Specific Complexation of Metal Oxo Cations," Patent Application, DOE Case No. IB-803.
10. X. Jide and K.N. Raymond, "Pu(IV) Coordination," LBL-30331.
11. L. Gong and A. Streitwieser, "Organolanthanide Catalysis of a Mukaiyama Addition Reaction," *J. Org. Chem.* (in press); LBL-27759.
12. A. Streitwieser and L. Gong, "Kinetic Study of a Lanthanide Catalyzed Mukaiyama Addition Reaction," *Eur. J. Solid State and Inorg. Chem.* (in press); LBL-30185.
13. T.R. Boussie, D.C. Eisenberg, J.T. Rigsbee, A. Streitwieser, and A. Zalkin, "Structures of Organo-f-Element Compounds Differing in the Oxidation State of the f-Element: Crystal Structures of Bis([8]annulene) Complexes of Cerium(IV), Ytterbium(III) and Uranium(III)," *Organometallics* (in press); LBL-29655.
14. A. Streitwieser and T.R. Boussie, "Sandwiches, Half-Sandwiches and Related f-Element Organometallics," *Eur. J. Solid State and Inorg. Chem.* (in press); LBL-30186.
15. D. Piehler, W. Kot, and N. Edelstein, "The $6d \rightarrow 5f$ Fluorescence Spectra of PaCl_6^{2-} in a Cs_2ZrCl_6 Crystal," *J. Chem. Phys.* (in press); LBL-29451.
16. D. Piehler (Ph.D. Thesis), "Nonlinear Optical Spectroscopy of Ce^{3+} Ions in Insulating Crystals," LBL-29883.
17. D. Piehler, "Electronic Coherent Anti-Stokes Raman Spectroscopy in CeF_3 ," *J. Op. Soc. Am. B* (in press); LBL-29802.
18. N. Edelstein, "Magnetic and Optical Properties of Np and Pu Ions and Compounds," ACS symposium volume to commemorate the 50th Anniversary of the Discovery of the Transuranium Elements (in press); LBL-29305.
19. C.S. Yoo, H.B. Radousky, N.C. Holmes, and N.M. Edelstein, "Luminescence of Sm^{2+} Ions as a Probe of Pressure-Induced Phase Transitions in SrF_2 ," LBL-30130.
20. H. Reddmann, H. Schultze, H.-D. Amberger, G.V. Shalimoff, and N.M. Edelstein, "The Electronic Structure of Metalloorganic Compounds of f-Elements XXVII. Interpretation of the Optical, Magnetic, EPR, and NMR Spectroscopic Properties of the Neutral Base Adducts of $\text{Tris}(\eta^5\text{-cyclopentadienyl})\text{Nd(III)}$," LBL-30167.
21. K. Yunlu, P.S. Gradeff, N. Edelstein, W. Kot, G. Shalimoff, W.E. Streib, B.A. Vaartstra, and K.G. Caulton, "Photoreduction of Ce(IV) in $\text{Ce}_2(\text{O}^i\text{Pr})_8(\text{}^i\text{PrOH})_2$. Characterization and Structure of $\text{Ce}_4\text{O}(\text{O}^i\text{Pr})_{13}(\text{}^i\text{PrOH})$," LBL-30168.
22. N. Edelstein, "Studies of f^1 and d^1 Configurations in the Lanthanide and Actinide Series," in *Proc. First Int. Conf. on f-Elements*, Leuven, Belgium, Sept. 4-7, 1990, *Eur. J. Solid State and Inorg. Chem.* (in press); LBL-29652.

Invited Talks

23. K.N. Raymond, "Metal Ion Encapsulation: From Microbes to Macrocycles," Brigham Young University, Provo, UT, Feb. 22, 1990.
24. K.N. Raymond, "New Coordination Chemistry of the Siderophores," UCLA Colloquium, Taos, NM, Feb. 28, 1990.
25. K.N. Raymond, "Coordination Chemistry and Microbial Iron Transport," American Physical Society Meeting, Anaheim, CA, Mar. 14, 1990.
26. K.N. Raymond, "Siderophore-like Iron Macrocyclic Complexes," Annual Congress of the Royal Society of Chemistry, Belfast, Northern Ireland, Apr. 11, 1990.
27. K.N. Raymond, "Biomimetic Metal Encapsulators," Basolo 70 Symposium, Evanston, IL, Aug. 17-18, 1990.
28. K.N. Raymond, "The Electrochemistry, Thermodynamic Stability and Structure of Catechol Metal Complex Analogs of Iron Sequestering Agents and Vanadium Tunichromes," ACS Symposium, Washington D.C., Aug. 26-31, 1990.

LBL Reports

10. X. Jide and K.N. Raymond, "Pu(IV) Coordination," LBL-30331.
11. L. Gong and A. Streitwieser, "Organolanthanide Catalysis of a Mukaiyama Addition Reaction," *J. Org. Chem.* (in press); LBL-27759.
12. A. Streitwieser and L. Gong, "Kinetic Study of a Lanthanide Catalyzed Mukaiyama Addition Reaction," *Eur. J. Solid State and Inorg. Chem.* (in press); LBL-30185.
13. T.R. Boussie, D.C. Eisenberg, J.T. Rigsbee, A. Streitwieser, and A. Zalkin, "Structures of Organo-f-Element Compounds

29. K.N. Raymond, "Template Synthesis and Ligand Design for f-metal Ligands," International Conference on f-Elements, Leuven, Belgium, Sept. 4-7, 1990.
30. K.N. Raymond, "Biological Iron Transport," University of Geneva, Switzerland, Sept. 10, 1990.
31. K.N. Raymond, "From Microbes to Macrocycles: Metal-Ion Specific Sequestering Agents," University of Lausanne, Switzerland, Sept. 11-12, 1990.
32. K.N. Raymond, "Coordination Chemistry of Microbial Iron Transport" and "New Approaches to Metal-Ion Specific Sequestering Agents," University of Fribourg, Switzerland, Sept. 13-14, 1990.
33. K.N. Raymond, "Metal Ion-Specific and Stereognostic Coordination Chemistry," Los Alamos National Laboratory, Los Alamos, NM, Oct. 29, 1990.
34. K.N. Raymond, "Metal Ion-Specific and Stereognostic Coordination Chemistry," Harvard/MIT Inorganic Series Seminar, Cambridge, MA, Nov. 15, 1990.
35. A. Streitwieser, "f-Element Organometallic Chemistry," Department of Chemistry, Cornell University, Ithaca, NY, Oct. 9, 1989; Department of Chemistry, Northern Illinois University, DeKalb, IL, Oct. 16, 1989; Department of Chemistry, University of Illinois, Urbana, IL, Oct. 17, 1989; International Symposium on Modern Chemistry, University of Erlangen-Numberg, Germany, Apr. 26, 1990.
36. A. Streitwieser, "Discovery of Uranocene—Sandwiches, Half-sandwiches, and f-Element Organometallic Chemistry," Department of Chemistry, California Polytechnic University at Pomona, CA, Nov. 15, 1989.
37. A. Streitwieser, "Organolanthanide Catalysis of a Mukaiyama Reaction," First International Conference on f-Elements, Leuven, Belgium, Sept. 6, 1990.
38. N.M. Edelstein, "Recent Results in Thorium, Protactinium and Uranium Chemistry," Laboratoire de Reactivite et Mecanismes en Chimie Inorganique, CEA, Saclay, France, Sept. 22, 1989; University of Sussex, England, Oct. 18, 1989.
39. N.M. Edelstein, "Optical and Magnetic Properties of the Transuranium Elements," 1989 International Chemical Congress of Pacific Basin Societies, Honolulu, HI, Dec. 18, 1989.
40. N. Edelstein, "Magnetic Properties of Np and Pu Ions and Compounds," 200th National Meeting, American Chemical Society, Washington, D.C., Aug. 26-31, 1990.
41. N. Edelstein, "Florescence of Pa⁴⁺ Diluted in Cs₂ZrCl₆," First International Conference on f-Elements, Leuven, Belgium, Sept. 4-7, 1990; Laboratoire de Physico-Chimie des Materiaux Luminescents, Université Claude Bernard-Lyon, Villeurbanne, France, Sept. 6, 1990.

CHEMICAL ENGINEERING SCIENCES

Molecular Thermodynamics for Phase Equilibria in Mixtures*

John M. Prausnitz, Investigator

INTRODUCTION

Phase equilibria are required for design of efficient large-scale separation processes (e.g., distillation and extraction) in the chemical and related industries. In this context, "efficient" refers to optimum use of raw materials and to conservation of energy.

Since the variety of technologically important fluid mixtures is extremely large, it is not possible to obtain all equilibria from experiment. Therefore, the objective of this research is development of molecular thermodynamics for interpretation and correlation of reliable experimental data toward confident prediction of phase equilibria for engineering. The correlations are expressed through semi-theoretical, physicochemical models in a form suitable for computer-aided design. Particular attention is given to those materials that may be useful for innovative low-energy-consuming separation processes, such as polymers and gels and micellar systems, with possible applications in biotechnology. However, attention is also devoted to conventional materials for applications in fuel technology and for recovery of solutes from wastewater.

Development of molecular thermodynamics calls for a combination of theoretical, computational, and experimental work. Further, it requires simultaneous awareness of progress in molecular science and of realistic requirements for engineering design.

1. Thermodynamics of Liquid-Liquid Equilibria Including the Critical Region. Transformation to Non-Classical Coordinates Using Revised Scaling (Publication 1)

J.J. de Pablo and J.M. Prausnitz

Classical or mean-field models for equilibrium properties of fluids and fluid mixtures are inaccurate near a critical point. To improve the performance of such models near the critical point of a pure fluid, Fox proposed a method of transforming the coordinates of a classical equation of state to nonclassical coordinates. Recently, we have extended the method of Fox to binary liquid mixtures at constant pressure and to ternary liquid mixtures at constant pressure and temperature. However, our previous extension has used simple scaling, where transformation to nonclassical coordinates is symmetric with respect to the critical point. In this work, our extension is applied to binary and ternary liquid mixtures in a revised-scaling context that allows for the asymmetry found in real systems. Results are shown for binary and ternary liquid mixtures. For a few illustrative examples, good agreement is obtained between experimental and calculated coexistence curves.

2. Thermodynamics of Aqueous Systems Containing Hydrophilic Polymers or Gels (Publication 2)

M.M. Prange, H.H. Hooper, and J.M. Prausnitz

A quasicheical partition function is applied to represent the thermodynamic properties of aqueous solutions of nonelectrolytes, including linear polymers and crosslinked polymers (gels). The partition function extends conventional lattice theory; to take into account strong specific interactions (hydrogen bonds) as encountered in aqueous solutions, each molecule (polymer segment) may possess three energetically different types of contact sites. We distinguish between sites that interact through dispersion forces and sites that can participate in a hydrogen bond; hydrogen-bonding sites are divided into electron-pair donating sites and electron-pair accepting sites. The Helmholtz energy of the mixture is obtained using an oriented quasicheical approximation. The final

*This work was supported by the Director, Office of Energy Research, Office of Basic Energy Sciences, Chemical Sciences Division, of the U.S. Department of Energy under Contract No. DE-AC03-76SF00098.

equation contains three independent adjustable binary parameters; these are the exchange energies for different types of contact pairs. To represent quantitatively upper or lower critical solution phenomena, we include the semitheoretical fluctuation correction recently proposed by de Pablo. Comparison with experimental data indicates that the proposed molecular-thermodynamic model may be useful for representing phase equilibria for a variety of aqueous systems, including swelling equilibria for hydrophilic gels.

3. Molecular Thermodynamics of Fluid Mixtures at Low and High Densities (Publication 3)

D. Dimitrelis and J.M. Prausnitz

A molecular-thermodynamic framework is proposed to describe phase equilibria over a wide range of densities and compositions. The proposed framework is expressed through a model for the Helmholtz energy that incorporates arbitrary mixing rules at high densities, while at low densities the model reduces to the correct second-virial-coefficient limit. In effect, this framework provides density-dependent mixing rules. The proposed framework is illustrated with an equation of state of the Boublik-Mansoori-van der Waals form. Special attention is given to high-pressure vapor-liquid equilibria for systems containing water and hydrocarbons.

4. Swelling Equilibria for Positively Ionized Polyacrylamide Hydrogels (Publication 4)

H.H. Hooper, J.P. Baker, H.W. Blanch, and J.M. Prausnitz

Swelling equilibria are reported for polyacrylamide gels in water and for copolymer gels containing acrylamide and [(methacrylamido)propyl] trimethylammonium chloride (MAPTAC) in aqueous NaCl solutions. Gel swelling was investigated as a function of gel structure (cross-link density and monomer concentration), degree of gel ionization (relative amount of charged comonomer), and solution ionic strength. A gel-swelling model is presented that describes polymer/solvent mixing effects using a recently proposed lattice model developed for aqueous/polymer systems; this model accounts for hydrogen bonding in aqueous solutions by distinguishing between different types of contact sites on a solvent molecule or polymer segment. The elastic contribution to swelling is represented using a network theory that accounts for nonaffine displacement of network junctions under strain; polyelectrolyte effects on swelling are described using ideal Donnan theory. Swelling equilibria

for uncharged polyacrylamide networks in water are correlated using the gel-swelling model. The model describes reasonably well the effect of cross-link density on swelling but fails to reproduce accurately the dependence of swelling on monomer concentration at preparation. Exchange-energy parameters obtained from polyacrylamide gel-swelling measurements are used to predict swelling in salt solutions for acrylamide/MAPTAC copolymer gels. The model predicts well the effect of gel charge density and solution ionic strength on swelling; however, the effect of monomer concentration is not accurately predicted. Further work is needed to quantify the effect of monomer concentration on the swelling and elastic properties of polyacrylamide hydrogels.

5. Effect of a Dissolved Gas on the Solubility of an Electrolyte in Aqueous Solution (Publication 5)

H.R. Corti, M.E. Krenzer, J.J. de Pablo, and J.M. Prausnitz

The solubility of Na_2SO_4 in aqueous CO_2 solutions has been measured at 50°C and 75°C and at pressures to 200 bar. To calculate the effect of gas concentration on the solubility of the salt, we use thermodynamic-consistency equations that relate the solubility of the salt to the Setschenow constant and other thermodynamic properties. The effect of pressure on the salt solubility is estimated from volumetric data for the aqueous electrolyte solution and for the solid salt. Calculated and experimental results are in good agreement. By use of the thermodynamic-consistency analysis, predictions are made for the solubility of NaCl in aqueous solutions containing CO_2 or CH_4 , using available data for gas solubility in the respective binary electrolyte solutions. The predicted decrease of NaCl solubility with rising CO_2 concentration is confirmed experimentally at 50°C.

6. Biotechnology: A New Frontier for Molecular Thermodynamics (Publication 6)

J.M. Prausnitz

Thanks to growing scientific knowledge at the molecular level and to the awesome growing power of computers, it may now be possible to apply molecular thermodynamics toward the development and production of biochemicals. To illustrate that possibility, a few examples are presented; these include extraction for isolating solutes from dilute aqueous solution; extraction using organic solvents containing reverse micelles; phase separation in liquid solutions of large molecules using shear; entropy-driven adsorption of enzymes; and finally, molecular-

simulation calculations to determine the catalytic properties of a mutant enzyme.

While novel future applications will require much dedicated research, it is necessary to start now to build the necessary foundations. Emphasis must be directed toward establishing a representative data base and toward increasing familiarity with new experimental methods and new theoretical concepts. To apply molecular thermodynamics to biotechnology, it is particularly important for chemical-engineering thermodynamicists to give attention to the properties of aqueous systems containing salts and large, charged molecules.

7. Phase Equilibria for Fluid Mixtures from Monte Carlo Simulation (Publication 7)

J.J. de Pablo and J.M. Prausnitz

The Gibbs-ensemble Monte Carlo simulation method is extended for simulation of systems containing polyatomic molecules. This extension is used to predict phase equilibria in systems containing pure and mixed lower alkanes. To describe interactions between different groups, we use OPLS potential-energy functions. We also give results for the simulated vapor-liquid coexistence curve of water, using a TIP4P potential function.

8. Monte Carlo Simulation of Phase Equilibria for the Two-Dimensional Lennard-Jones Fluid in the Gibbs Ensemble (Publication 8)

R.R. Singh, K.S. Pitzer, J.J. de Pablo, and J.M. Prausnitz

The coexistence curve of the two-dimensional Lennard-Jones fluid has been obtained by Monte Carlo simulation in the Gibbs ensemble. The calculated vapor-liquid equilibria show that the apparent critical exponent β_c has a value near that of an infinitely large system, rather than the classical value, even though the correlation length is constrained by the box size. These results are similar to those for the three-dimensional case.

9. A Simple Perturbation Term for the Carnahan-Starling Equation of State (Publication 9)

R. Dohrn and J.M. Prausnitz

A simple perturbation term is presented for the Carnahan-Starling (CS) hard-sphere reference equation of state (EOS). This perturbed CS EOS is compared with seven other two-parameter equations of state; it represents

the critical isotherms of eight fluids with the lowest deviations in density and pressure. After a generalized temperature dependence is introduced for parameters a and b , the perturbed CS EOS is compared to the well-known Peng-Robinson equation. For nine nonpolar pure fluids, the perturbed CS EOS represents liquid densities significantly better, but it is not superior for vapor pressures. For mixtures, the CS reference term is given by the Boublik-Mansoori hard-sphere mixture EOS. Some calculations for binary mixtures are given, using conventional mixing rules for parameters a and b in the simple perturbation term.

10. Configurational Properties of Partially Ionized Polyelectrolytes from Monte Carlo Simulation (Publication 10)

H.H. Hooper, H.W. Blanch, and J.M. Prausnitz

Monte Carlo simulations have been performed for a lattice model of an isolated, partially ionized polyelectrolyte whose charged groups interact through screened Coulombic potentials. Configurational properties are reported as a function of chain ionization and Debye screening length for chains containing 20–140 segments. At high screening between fixed charges, the chains exhibit power-law scaling behavior for the dependence of the mean-square end-to-end distance $\langle r^2 \rangle$ on chain length. At lower screenings the chains undergo a transformation from flexible to stiff conformations as ionization rises. Long-chain scaling behavior was not observed at low screening due to the limits on the chain lengths studied here. Simulation results for poly-ion electrostatic energies and expansion factors are compared with predictions based on the theory of Katchalsky and Lifson and the uniform-expansion extension of this theory. Large discrepancies between theory and simulation are probably due to the assumed theoretical expressions used for describing distance probability distributions between charged groups.

11. Monte Carlo Simulations of Hydrophobic Polyelectrolytes. Evidence for a Structural Transition in Response to Increasing Chain Ionization (Publication 11)

H.H. Hooper, S. Beltran, A.P. Sassi, H.W. Blanch, and J.M. Prausnitz

Monte Carlo simulation has been used to study the configurational properties of a lattice-model isolated polyelectrolyte with attractive segment-segment interaction potentials. This model provides a simple representation of

a hydrophobic polyelectrolyte. Configurational properties were investigated as a function of chain ionization, Debye screening length, and segment-segment potential. For chains with highly attractive segment-segment potentials (i.e., hydrophobic chains), large global changes in polymer dimensions were observed with increasing ionization. The transformation from a collapsed chain at low ionization to an expanded chain at high ionization becomes increasingly sharp (i.e., occurs over a smaller range of ionization) with increasing chain hydrophobicity. The ionization-induced structural transitions for this model hydrophobic polyelectrolyte are analogous to pH-induced transitions seen in real polyelectrolytes and gels. These studies suggest a simple explanation for such transitions based on competing hydrophilic and hydrophobic interactions.

12. Swelling Equilibria for Ionized Temperature-Sensitive Gels in Water and in Aqueous Salt Solutions (Publication 12)

S. Beltran, H.H. Hooper, H.W. Blanch, and J.M. Prausnitz

Swelling equilibrium data in water and in aqueous NaCl solutions are presented for thermally sensitive N-isopropylacrylamide (NIPA) hydrogels containing 0–4 mol% quaternized amine (positively ionizable) comonomer. We report the effect of gel charge and solution ionic strength on the temperature-induced collapse of NIPA gels. Experimental swelling equilibria are compared with predictions based on a recently proposed oriented-quasichemical model. This model has been shown previously to describe lower critical solution behavior in uncharged aqueous polymer solutions and gels (i.e., aqueous NIPA gel). We apply the model here to ionized NIPA gel. Semiquantitative predictions are obtained for the effects of gel charge and solution ionic strength on temperature-dependent swelling behavior.

13. Phase Equilibria for Aqueous Systems Containing Salts and Carbon Dioxide. Application of Pitzer's Theory for Electrolyte Solutions (Publication 13)

H.R. Corti, J.J. de Pablo, and J.M. Prausnitz

The semiempirical specific-interaction model developed by Pitzer is applied to aqueous salt solutions that also contain a dissolved nonelectrolyte. Pitzer's model is used to describe phase equilibria for aqueous solutions containing either sodium chloride and carbon dioxide to 600 bar or sodium sulfate and carbon dioxide to 200 bar at

several temperatures. In contrast to predictions reported by previous authors, we find that over wide ranges of pressure and temperature, Pitzer's equations provide an excellent description of salt solubilities in these ternary systems.

14. Molecular Simulation of Water Along the Liquid-Vapor Coexistence Curve from 25°C to the Critical Point (Publication 14)

J.J. de Pablo, J.M. Prausnitz, H.J. Strauch, and P.T. Cummings

Previous work has shown that the simple point-charge (SPC) model can represent the experimental dielectric constant of water. In this work, we present results of Monte Carlo simulations of SPC water in the isothermal-isobaric (NPT) ensemble and in the Gibbs ensemble. Long-range intermolecular interactions are included in these simulations by use of the Ewald summation method. When Ewald sums are used, simulated, uniphase liquid potential energies are slightly lower (in absolute value) than those obtained for a simple spherical cutoff of the intermolecular potential. The coexistence curve of SPC water is obtained from 25°C to 300°C. The critical constants of SPC water are estimated by adjusting the coefficients of a Wegner expansion to fit the difference between simulated liquid and vapor orthobaric densities; the estimated critical temperature is 314°C, and the estimated critical density is 0.27 g/cm³.

15. Molecular Thermodynamics of Aqueous Polymers and Gels (Publication 15)

H.H. Hooper, H.W. Blanch, and J.M. Prausnitz

The phase behavior of aqueous polymer solutions and gels is often sensitive to prevailing conditions such as temperature, pH, ionic strength, or solvent composition. For crosslinked polymer gels, this solution sensitivity is indicated by large changes in gel volume in response to small changes in solution conditions. This chapter reviews recent work directed at developing a molecular-thermodynamic description of phase behavior in aqueous polymer systems. A theoretical description of phase equilibria correlates systematic experimental data obtained for model systems. Novel molecular-simulation studies of isolated polyelectrolytes provide detailed information on the relationship between expansion of polyelectrolytes in solution and pertinent parameters that characterize polymer and solution properties.

16. Work in Progress

Efforts are directed at experimental and molecular-thermodynamic studies of (a) phase equilibria for systems containing water, a water-soluble polymer, salt, an organic solvent (e.g., propanol) and carbon dioxide at high pressures, for separation of salts and polymers; (b) swelling equilibria and kinetics for hydrophilic gels in response to changes in temperature, pH, or ionic strength; (c) liquid-liquid equilibria in aqueous mixtures containing salt and an organic solvent that has an upper or lower consolute temperature in the region 10–120°C, for energy-efficient, solvent-induced crystallization; (d) molecular-simulation studies to determine the configurational properties of polymers in concentrated solution, and to determine chain configurations of a polyelectrolyte in dilute aqueous solution near a wall; (e) experimental measurement of liquid-liquid equilibria in polymer solvent systems over a large temperature range; (f) molecular simulations for natural-gas fluids and dilute fluid mixtures at high pressures in the retrograde region; (g) distribution of proteins and other water-soluble solutes between water and a well-defined gel; and (h) thermodynamic properties of hydrogels as a function of chemical composition, charge density, and extent of cross-linking.

1990 PUBLICATIONS AND REPORTS

Refereed Journals

1. J.J. de Pablo and J.M. Prausnitz, "Thermodynamics of Liquid-Liquid Equilibria Including the Critical Region: Transformation to Non-Classical Coordinates Using Revised Scaling," *Fluid Phase Equilibria* **59**, 1–14 (1990); LBL-26147.
2. M.M. Prange, H.H. Hooper, and J.M. Prausnitz, "Thermodynamics of Aqueous Systems Containing Hydrophilic Polymers or Gels," *AIChE J.* **35**, 803 (1989); LBL-26723.
3. D. Dimetrelis and J.M. Prausnitz, "Molecular Thermodynamics of Fluid Mixtures at Low and High Densities," *Chem. Eng. Sci.* **45**, 1503–1513 (1990); LBL-26794.
4. H.H. Hooper, J.P. Baker, H.W. Blanch, and J.M. Prausnitz, "Swelling Equilibria for Positively Ionized Polyacrylamide Hydrogels," *Macromolecules* **23**, 1096–1104 (1990); LBL-27284.
5. H.R. Corti, M.W. Krenzer, J.J. de Pablo, and J.M. Prausnitz, "Effect of a Dissolved Gas on the Solubility of an Electrolyte in Aqueous Solution," *I&EC Research* **29**, 1043–1055 (1990); LBL-27368.
6. J.M. Prausnitz, "Biotechnology: A New Frontier for Molecular Thermodynamics," *Fluid Phase Equilib.* **53**, 439 (1989); LBL-27685.

7. J.J. de Pablo and J.M. Prausnitz, "Phase Equilibria for Fluid Mixtures from Monte Carlo Simulation," *Fluid Phase Equilib.* **53**, 177–189 (1989); LBL-27721.
8. R.R. Singh, K.S. Pitzer, J.J. de Pablo, and J.M. Prausnitz, "Monte Carlo Simulation of Phase Equilibria for the Two-Dimensional Lennard-Jones Fluid in the Gibbs Ensemble," *J. Chem. Phys.* **92**, 5463 (1990); LBL-28069.
9. R. Dohrn and J.M. Prausnitz, "A Simple Perturbation Term for the Carnahan-Starling Equation of State," *Fluid Phase Equilib.* **61**, 53 (1990); LBL-28419.
10. H.H. Hooper, H.W. Blanch, and J.M. Prausnitz, "Configurational Properties of Partially Ionized Polyelectrolytes from Monte Carlo Simulation," *Macromolecules* **23**, 4820–4829 (1990); LBL-28665.
11. H.H. Hooper, S. Beltran, A.P. Sassi, H.W. Blanch, and J.M. Prausnitz, "Monte Carlo Simulations of Hydrophobic Polyelectrolytes. Evidence for a Structural Transition in Response to Increasing Chain Ionization," *J. Chem. Phys.* **93**, 2715–2723 (1990); LBL-28677.
12. S. Beltran, H.H. Hooper, H.W. Blanch, and J.M. Prausnitz, "Swelling Equilibria for Ionized Temperature-Sensitive Gels in Water and in Aqueous Salt Solutions," *J. Chem. Phys.* **92**, 2061 (1990); LBL-29053.
13. H.R. Corti, J.J. de Pablo, and J.M. Prausnitz, "Phase Equilibria for Aqueous Systems Containing Salts and Carbon Dioxide. Application of Pitzer's Theory for Electrolyte Solutions," *J. Phys. Chem.* **94**, 7876–7880 (1990); LBL-29147.
14. J.J. de Pablo, J.M. Prausnitz, H.J. Strauch, and P.T. Cummings, "Molecular Simulation of Water Along the Liquid-Vapor Coexistence Curve from 25°C to the Critical Point," *J. Chem. Phys.* **93**, 7355–7359 (1990); LBL-29213.

Other Publications

15. H.H. Hooper, H.W. Blanch, and J.M. Prausnitz, "Molecular Thermodynamics of Aqueous Polymers and Gels," in *Studies in Polymer Science*, Vol. 8, L. Brannon-Peppas and R. Harland, eds., Elsevier, 1990; LBL-28666.

LBL Reports

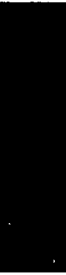
16. M.E. Krenzer, J.J. de Pablo, and J.M. Prausnitz, "Purification of Aqueous Hydroxyethylcellulose. Extraction of Sodium Acetate with Isopropanol and High-Pressure Carbon Dioxide," LBL-28102.
17. R. Dohrn, W. K nstler, and J.M. Prausnitz, "Correlation of High-Pressure Phase Equilibria in the Retrograde Region with Three Common Equations of State," submitted to *Can. J. Chem. Eng.*; LBL-28324.
18. T. Klein and J.M. Prausnitz, "Phase Behavior of Reverse Aqueous Micelles in Compressed Propane at 35°C and Pressures to 30 MPa Solubilization of Poly(ethylene glycol)," submitted to *J. Phys. Chem.*; LBL-28341.
19. A.P. B nz, R. Dohrn, and J.M. Prausnitz, "Three-Phase Flash Calculations for Multicomponent Systems," submitted to *Computers & Chem. Eng.*; LBL-28763.

20. S. Beltran, H.H. Hooper, H.W. Blanch, and J.M. Prausnitz, "A Monte Carlo Study of Polyelectrolyte Adsorption on a Planar Charged Surface," submitted to *Macromolecules*; LBL-29238.
21. K.A. Bartscherer, J.J. de Pablo, M.C. Bonnin, and J.M. Prausnitz, "Purification of Aqueous Cellulose Ethers. Extraction of Alkali Salts with Isopropanol and High-Pressure Carbon Dioxide," LBL-29452.
25. J.M. Prausnitz, "Recent Developments in Phase-Equilibrium Thermodynamics," Institute for Thermodynamics, Technical University of Berlin, September 1990.
26. J.M. Prausnitz, "Molecular Thermodynamics for Petroleum and Natural-Gas Production," Chemical Engineering Department and Institute for Petroleum Technology, University of Wyoming, Laramie, October 1989.
27. J.M. Prausnitz, "Synthetic Nature of Molecular Thermodynamics," Chemical Engineering Department, University of Pennsylvania, Philadelphia, November 1989.
28. J.M. Prausnitz, "Phase Equilibria for Natural-Gas Systems in the Retrograde Region," Annual Thermodynamics Conference, Gas Research Institute (Technical Meeting), Phoenix, AZ, February 1990.
29. H.H. Hooper, "Swelling of Thermally-Sensitive Hydrogels," AIChE Annual Meeting, San Francisco, CA, November 1989.
30. J.M. Prausnitz, "Molecular Thermodynamics for Chemical Process Design," BASF 125th Birthday Symposium, Ludwigshafen, Germany, September 1990.
31. J.M. Prausnitz, "Ziele und Methoden der Chemischen Verfahrenstechnik," Biannual Solvay Prize Symposium, Solvay Corporation, Solingen, Germany, September 1990.

Invited Talks

22. J.M. Prausnitz, "Synthetic Nature of Molecular Thermodynamics," Chemical Engineering Department, Princeton University, Princeton, NJ, April 1990.
23. J.M. Prausnitz, "Group Contributions for Thermodynamic Properties" and "Applications of Continuous Thermodynamics," Chemical Engineering Department, Massachusetts Institute of Technology, Cambridge, MA, April 1990.
24. J.M. Prausnitz, "Applications of Molecular Thermodynamics," Polymer section, Marshall Laboratory, DuPont, Philadelphia, PA, April 1990.

Work for Others



UNITED STATES OFFICE OF NAVAL RESEARCH

Superconductivity*

Vladimir Z. Kresin, Investigator

INTRODUCTION

This research is concerned with different aspects of superconductivity, such as the mechanisms of high- T_c , organic superconductivity, properties of the new oxides, and applications.

A unified approach to the description of high- T_c oxides has been developed. This approach allows us to understand many different unusual properties of these materials. Several predictions, such as an appearance of the two-gap structure, were verified experimentally.

The analysis of organic superconductors versus high- T_c cuprates has been carried out. The origin of the present limitations of T_c of organics has been studied.

1. Two-Gap Superconductivity (Publications 1, 4, 7, and 11)

V.Z. Kresin, S.A. Wolf,[†] and G. Deutscher[‡]

The short coherence length requires the introduction of two-gap structure in the high- T_c oxides, such as the $Y_1Ba_2Cu_3O_{7-x}$ compound.

The system is characterized by three coupling constants, describing intraplane and intrachain pairing interactions and transitions between the two subsystems. Superconductivity in the chains is not intrinsic and is induced by various charge-transfer channels: the intrinsic proximity effect and phonon-mediated transitions. The theory describes the effect of the oxygen ordering on T_c and the induced gap and allows us to describe a number of experiments ("plateau" effect, zero-bias anomaly, microwave losses, etc.).

[†]Permanent address: Naval Research Laboratory, Washington, D.C.

[‡]Permanent address: Department of Physics and Astronomy, Tel Aviv University, Tel Aviv, Israel.

*This work was supported by the U.S. Office of Naval Research under Contract No. N00014-89-F0015 through an agreement with the U.S. Department of Energy under Contract No. DE-AC03-76SF00098.

2. T_c and the Carrier Concentration. Spectroscopy of the High- T_c Oxides (Publications 2, 3, 5, and 13)

V.Z. Kresin and H. Morawitz[†]

The electron-phonon coupling is shown to depend on the carrier concentration n . As a result of this dependence, T_c reaches a maximum at some value of n . This maximum of T_c has been observed in the high- T_c oxides. At a higher n , there is a superconductor-normal metal transition. The calculated carrier concentration, which corresponds with T_c^{\max} , is in agreement with experimental data.

The appearance of a maximum of T_c and the superconductor-normal metal transition in the region of large n is due to a crossover between the electronic and phonon momenta. This nontrivial behavior of T_c has been observed in the new high- T_c oxides and is a direct consequence of the electron-phonon mechanism.

The dependence of the Sommerfeld constant on n is predicted to be nonmonotonic, and this prediction has been confirmed experimentally.

The superconducting transition affects the positron-annihilation lifetime in the high- T_c oxides. This effect is due to the unusual properties of the oxides in the normal state and, in particular, to the small Fermi energy. The value of the shift also depends on the interlayer distance.

[†]Permanent address: IBM Almaden Research Center, San Jose, CA.

3. Organic Superconductivity (Publications 9 and 10)

V.Z. Kresin and S.A. Wolf[†]

Remarkable progress in the field of organic superconductivity was made during the last ten years. This progress has demonstrated the great potential of these materials for future development. Based on our previous evaluation of the major parameters of the cuprate superconductors, an analysis of organic superconductors versus cuprate superconductors was carried out. The organics are found to have a short coherence length and, as a result, display two-gap structure. Many of the normal and superconducting parameters of the two classes of compounds are quite similar. The Fermi surface of the organic superconductors contains a large number of nesting sites. This is very favorable for the occurrence of the

charge-density-wave (CDW) transition in this material. This factor is important, and its elimination might lead to further increases in T_c of organic low-dimensional materials.

The effect of pair correlation on the properties of π -electron systems in aromatic molecules has also been studied. It is manifested in the simultaneous appearance of an energy gap or an even number of π -electrons and of anomalous diamagnetism. The pairing is caused by polarization of the σ -core.

†Permanent address: Naval Research Laboratory, Washington, D.C.

4. Microwave Properties of the High- T_c Oxides (Publications 6, 8, and 12)

V.Z. Kresin

Microwave properties of the high- T_c oxides are studied. The frequency and temperature dependences of the impedance are obtained. Short coherence length leads to large losses. The effects of impurities and multi-gap structures are discussed. The multi-gap structure leads to a peculiar temperature dependence of the losses. The impedance of the proximity system is calculated. The presence of the acoustic plasmon branch leads to intrinsic residual losses.

1990 PUBLICATIONS AND REPORTS

Refereed Journals

1. V.Z. Kresin and S.A. Wolf, "Major Normal and Superconducting Parameters of High T_c Oxides," *Phys. Rev. B* **41**, 4278 (1990).
2. V.Z. Kresin and H. Morawitz, "Carrier Concentration Dependence of T_c in the layered Copper Oxides," *Solid State Comm.* **74**, 1203 (1990).
3. V.Z. Kresin and H. Morawitz, "Plasmon Spectrum in Layered Conductors," *Phys. Lett. A* **145**, 368 (1990).
4. V.Z. Kresin and S.A. Wolf, "Multigap Structure in the Cuprates," *Phys. C* **169**, 476 (1990).
5. V.Z. Kresin and H. Morawitz, "Positron-Annihilation Lifetime in the High T_c Oxides," *J. Super.* **3**, 227 (1990).
6. V.Z. Kresin, "High T_c Superconductor in an a.c. Field," *J. Super.* **3**, 177 (1990).

Other Publications

7. S.A. Wolf and V.Z. Kresin, "Major Parameters in High T_c Oxides," *IEEE Trans. Magn.* (in press).
8. V.Z. Kresin, "Microwave Properties of the High T_c Oxides," *IEEE Trans. Magn.* (in press).

9. S.A. Wolf and V.Z. Kresin, "Organics vs Cuprates: Why is T_c Still so Low in the Organics," in *Organic Superconductivity*, V.Z. Kresin and W.A. Little, eds., Plenum, New York, 1990, p. 31.
10. V.Z. Kresin, "Pair Correlation in Organic Molecules," in *Organic Superconductivity*, V.Z. Kresin and W.A. Little, eds., Plenum, New York, 1990, p. 285.
11. S.A. Wolf and V.Z. Kresin, "A Unified Approach to the Description of High T_c Oxides: Major Normal and Superconducting Parameter," in *Advances in Superconductivity II*, T. Ishiguro and K. Kajimura, eds., Springer-Verlag, Tokyo, 1990, p. 447.
12. V.Z. Kresin, "Proximity Effect and High T_c Superconductivity," in *Advances in Superconductivity II*, T. Ishiguro and K. Kajimura, eds., Springer-Verlag, Tokyo, 1990, p. 969.
13. V.Z. Kresin, H. Morawitz, and S.A. Wolf, "Correlation of Normal and Superconducting Properties in the New High Oxides," in *Proc. Int. Seminar on High T_c* , Dubna, USSR, 1990, p. 188.
14. V.Z. Kresin and S.A. Wolf, "Normal and Superconducting Properties and Unified Approach to the Description of High T_c Oxides," in *Proc. Conference on High T_c* , Maryland, 1990, p. 353.

Invited Talks

15. V.Z. Kresin, "Theoretical Aspects of High T_c Superconductivity," Los Alamos National Laboratory, Los Alamos, NM, January 1990.
16. V.Z. Kresin, "Proximity Effect," Applied Superconductivity Convention, Long Beach, CA, January 1990.
17. V.Z. Kresin, "Carrier Concentration Dependence of T_c ," IBM Research Center, San Jose, CA, February 1990.
18. V.Z. Kresin, "Properties of High T_c Oxides," University of Illinois, Urbana, March 1990.
19. V.Z. Kresin, "High T_c Superconductor in an a.c. Field," Symposium on High T_c Superconductors in High Frequency Fields, Williamsburg, VA, March 1990.
20. V.Z. Kresin, "Origin of High T_c ," International Conference on Advances in Materials Science, Greenbelt, MD, April 1990.
21. V.Z. Kresin, "Properties of High T_c Films," International Conference on High T_c Films, Denver, CO, May 1990.
22. V.Z. Kresin, "Pair Correlation in Organic Systems," International Conference on Organic Superconductivity, South Lake Tahoe, CA, May 1990.
23. V.Z. Kresin, "Correlation of Normal and Superconducting Properties in the New High T_c Oxides," International Seminar on High T_c , Dubna, USSR, July 1990.
24. V.Z. Kresin, "High T_c Superconductivity," Kernforschungszentrum, Karlsruhe, Germany, July 1990.
25. V.Z. Kresin, "Microwave Properties of the New High T_c Superconductors," Applied Superconductivity Conference, Aspen, CO, September 1990.
26. V.Z. Kresin, "Mechanisms of High T_c ," University of Utah, Salt Lake City, UT, November 1990.

Appendices



APPENDIX A

DIVISION PERSONNEL

1990 Scientific Staff

Investigators	Postdoctoral and Other Scientists	Graduate Students	Guests, Affiliates
Neil Bartlett	R. Hagiwara O. Tse C. Yom	W. Casteel	B. Shen H. Borrmann R. Jacubinas B. Schuler
Alexis Bell		D. Clarke K. Krishna R. Pittman	M. Sandoval G. Went
Robert Bergman		A. Baranger K. Bharucha M. Burn J. Duncan D. Glueck	J. Hartwig M. Hostetler R. Michelman R. Simpson P. Walsh R. Morris M. Nee R. Yrtis
Robert Connick	S. Lee		
Norman Edelstein	D. Ball J. Bucher	W. Kot	D. Piehler D. Chan D. Groenke Y. Hinatsu H. Leung
Richard Andersen	B. Campion	W. Lukens, Jr. P. Matsunaga	M. Smith M. Weydert J. Parry C. Sofield
Kenneth Raymond		T. Franczyk S. Franklin	L. Uhlir C. Deuschel-Corniol T. Dewey C. Gutierrez T. Karpishin S. Lee B. Lulay-Bryan M. Neu D. Sanna L. Tunstad H. Tsukube D. Watts D. Whisenhunt, Jr. D. White J. Xu

Investigators	Postdoctoral and Other Scientists	Graduate Students	Guests, Affiliates	
Andrew Streitwieser, Jr.		T. Boussie	C. Jenson	M. Bremer H. Gonzalez H. Wang
D. Templeton				L. Templeton
Harvey Gould	A. Belkacem C. Carlberg J. Schweppe			L. Blumenfeld G. Segre
Eugene Commins		S. Ross		
Charles Harris		R. Jordan J. King	W. Merry, Jr. E. Peterson	S. Gadd R. Hoff D. Padowitz M. Paige D. Russell K. Schultz B. Schwartz N. Tro J. Zhang
Harold Johnston		J. Burley P. Hunter B. Kim	C. Miller K. Patten, Jr. W. Sisk	
Yuan Lee	A. Kung	J. Allman B. Balko J. Chesko P. Chu E. Cromwell H. Davis	T. Miao J. Myers J. Price A. Suits M. Vrakking J. Zhang	D. Anex M. Cote M. Covinsky M. Crofton D. Gosalvez H. Li D. Liu G. Niedner-Schatteb K. Prather A. Stolow D. Stranges
William Lester, Jr.		A. Kaufman X. Mao	R. Owen	J. Andrews D. Bressanini N. Chan W. Glauser B. Hammond S. Huang D. Leff J. Odutola Z. Sun L. Terray C. Tsai
V. Kresin				N. Brooks

Investigators	Postdoctoral and Other Scientists	Graduate Students		Guests, Affiliates
William Miller	D. Colbert M. Shapiro D. Yeager	Y. Chang L. Gaucher	S. Keshavamurthy	S. Auerbach R. Hernandez J. Zhang
C. Bradley Moore	E.R. Lovejoy	H. Beal T. Butenhoff Y. Choi	S. Kim R. Van Zee	B. Do J. Harrison K. Lin T. Lowe
Daniel Neumark		R. Metz		R. Continetti D. Cyr
Norman Phillips				
Kenneth Pitzer	A. Anderko R. Anstiss S. Sterner			
John Prausnitz	H. Hooper	E. Anderson J. Baker L. Chou	J. De Pablo H. Hooper A. Sassi	D. Dee D. Freed S. Han A. Shaw
Michael Prior				R. Bruch D. Dewitt R. Herrmann R. Holt R. Hutton K. Randall
Richard Saykally		K. Busarow R. Cohen	N. Pugliano J. Scherer	
David Shirley	P. Heimann Z. Hussain L. Wang	J. Allman M. Blackwell Z. Huang E. Hudson W. Huff L. Medhurst	B. Niu B. Petersen A. Schach Von Wittenau L. Wang L. Wang M. Ziegeweid	J. Holloway E. Moler G. Remmers J. Walker
K. Peter Vollhardt	J. Gotteland E. West	R. Faust A. Kahn	R. Myrabo M. West	

Support Staff

Division Administrative Staff

Division Administrators: L. Maio, M. Montgomery*

Administration

L. Aubert
J. Edgar*
J. Leonard*
T. Lynem*

Personnel/Financial

K. deRaadt*
M. Graham
S. Nasman*

M. Smith*
S. Waters*

Purchasing

D. Pope*
S. Stewart*

Technical Editor

R. Albert

Travel

S. Quarello

Administrative/Secretarial Staff

R. Arcol
M. Atkinson
C. Becker
L. Denney
C. Gliebe
A. Harrington

J. Lilly
B. Moriguchi-Iwai
V. Narasimhan

M. Noyd
S. Schmitt
P. Southard

K. Steele
E. Weightman
K. Wong

*Materials Sciences Division effective 10/1/90.

APPENDIX B

DIVISION COMMITTEES

DIVISIONAL COUNCIL

R. Bergman
L. De Jonghe*
M. Denn*
H. Johnston
R. Ritchie*
G. Somorjai*
G. Thomas*
K. Westmacott*
A. Zettl*

DIVISIONAL RESEARCH STAFF COMMITTEE

R. Bergman
N. Edelstein
R. Muller
R. Ritchie*
K. Westmacott*

ADMINISTRATIVE STAFF COMMITTEE

M. Alper*
L. Maio
M. Montgomery*

SAFETY COMMITTEE

R. Ellis*
J. Haley
L. Maio
D. Meschi*
R. Muller
D. Owen*
P. Ruegg*
G. Shalimoff
K. Westmacott*

*Materials Sciences Division effective 10/1/90.

APPENDIX C

LIST OF DIVISIONAL SEMINARS

Chemical Dynamics Seminars

<u>Date</u>	<u>Speaker and Affiliation</u>	<u>Seminar Title</u>
2-2-90	P. Phillips, Department of Chemistry, Massachusetts Institute of Technology, Cambridge, MA	Absence of Localization in Statistically Disordered Solids
2-7-90	R.J. Bartlett, Quantum Theory Project, Departments of Chemistry and Physics, University of Florida, Gainesville	Molecules, Known and Unknown, Probed by Novel Electronic Structure Methods
2-15-90	S. Nagakura, The Graduate University for Advanced Studies, Yokohama, Japan	Magnetic Quenching of Fluorescence in Gaseous CS ₂ and NO
2-28-90	M. Thiemens, Department of Chemistry, University of California at San Diego, La Jolla, CA	New Isotope Effects and Application to Chemical-Physics, Atmospheric Chemistry and the Evolution of the Solar System
3-15-90	H. Koeppel, Institut für Physikalische Chemie der Universität Heidelberg, Germany	Multimode Molecular Dynamics Beyond the Born-Oppenheimer Approximation
3-16-90	V.L. Tal'roze, Institute of Energy Problems of Physical Chemistry, USSR Academy of Sciences, Moscow	The Chemical Physics of Atmospheric and Energy Problems
4-11-90	W. Klemperer, Department of Chemistry, Harvard University, Cambridge, MA	van der Waals Molecules
5-10-90	W.L. Vos, van der Waals Laboratory, Universiteit van Amsterdam, The Netherlands	Phase Behaviour of Binary Mixtures at High Pressures
5-11-90	H. Petek, Institute for Molecular Science, Okazaki, Japan	Non-Adiabatic and Adiabatic Isomerization Channels in cis-stilbene. A Dynamical and Spectroscopic Study
5-16-90	S.C. Farantos, Department of Chemistry, University of Crete and Institute of Electronic Structure and Laser, Iraklion, Crete, Greece	Chemical Dynamics and Phase Space Structure: A Periodic Orbit Approach
6-21-90	K. Muller-Dethlefs, Institute for Physical and Theoretical Chemistry, Technical University Munich, Garching, Germany	High-Resolution Zero Kinetic Energy Photo-Electron Spectroscopy of Molecular Systems

<u>Date</u>	<u>Speaker and Affiliation</u>	<u>Seminar Title</u>
6-30-90	A. McElroy, JILA, University of Colorado, Boulder	Intramolecular Vibrational Relaxation for Hydrocarbons in $\nu_{\text{CH}=1}$
7-10-90	E. Riedle, Institute for Physical and Theoretical Chemistry, Technical University Munich, Garching, Germany	Rotationally Resolved UV-Spectra: Investigation of Intramolecular Couplings in C_6H_6 and Determination of the Structure of C_6H_6 — Rare BAS VDW's Clusters
7-16-90	J. Garvey, Chemistry Department, State University of New York, Buffalo	Chemistry in Clusters
7-20-90	G. Scoles, Chemistry Department, Princeton University, Princeton, NJ	Intramolecular Vibrational Relaxation via Very High Resolution IR Absorption Spectroscopy in Molecular Beams
10-15-90	A. Burshstein, Thermochemical Laboratory, Novosibirsk, USSR	Non-Adiabatic Electron Transfer: Frictional Effects in Chemical Reactions in Solution
11-9-90	R.D. Coalson, Department of Chemistry, University of Pittsburgh, Pittsburgh, PA	Theory of Optical Spectra in Condensed Media
11-12-90	E.E. Nikitin, Institute of Chemical Physics, Soviet Academy of Sciences, Moscow, USSR	Semiclassical Theory for the Scattering of Polarized Atoms
11-14-90	A. van der Avoird, Vakgroep Theoret. Chem., Faculteit Natuurwetenschappen, Toernooiveld, 6525 ED Nijmegen, The Netherlands	<i>Ab initio</i> Potential Surfaces and Many-Body Dynamics of Binary Complexes: ArH_2O and ArNH_3
11-19-90	H. Kroto, School of Chemistry and Molecular Sciences, The University of Sussex, England	A Postbuckminsterfullerene View of the Chemistry, Physics and Astrophysics of Carbon

Other Seminars Hosted

8-27-90	C.A. Taft, Centro Brasileiro de Pesquisas Fisicas, Rio de Janeiro	Molecular and Condensed Matter Research at the CBPF
9-24-90	J.C. Light, Department of Chemistry, University of Chicago, Chicago, IL	Discrete Variable Methods and Quantum Monte Carlo
10-1-90	P.J. Reynolds, Physics Division, Office of Naval Research, Arlington, VA	Acceleration Methods in Quantum Monte Carlo

APPENDIX D

INDEX OF INVESTIGATORS*

Andersen, Richard A.	47, 48, 57
Bartlett, Neil	39
Bell, Alexis T.	42
Bergman, Robert G.	46
Connick, Robert E.	50
Edelstein, Norman M.	57
Gould, Harvey	34
Harris, Charles B.	3
Johnston, Harold S.	1, 14
Kresin, Vladimir Z.	75
Lee, Yuan T.	2, 6, 29, 30
Lester, William A., Jr.	13
Miller, William H.	16
Moore, C. Bradley	17, 20, 46
Neumark, Daniel	23
Pitzer, Kenneth S.	24, 71
Prausnitz, John M.	24, 69
Prior, Michael H.	36
Raymond, Kenneth N.	57
Shirley, David A.	7, 8, 9, 27
Streitwieser, Andrew, Jr.	57
Vollhardt, K. Peter C.	51

*Boldface numbers indicate investigators' main programs.

LAWRENCE BERKELEY LABORATORY
UNIVERSITY OF CALIFORNIA
TECHNICAL INFORMATION DEPARTMENT
BERKELEY, CALIFORNIA 94720